Accelerated Implementation of Intelligent Compaction Technology for Embankment Subgrade Soils, Aggregate Base, and Asphalt Pavement Materials: US 84 Waynesboro, Mississippi

Final Report ER10-03
US84, Waynesboro, MS, Field Project
July 13 to 17, 2009

Prepared By

David J. White, Ph.D.
Pavana KR. Vennapusa, Ph.D.
Heath Gieselman
Bradley Fleming
Stephen Quist
Luke Johanson

Earthworks Engineering Research Center (EERC)
Department of Civil Construction and Environmental Engineering
Iowa State University
2711 South Loop Drive, Suite 4600
Ames, IA 50010-8664
Phone: 515-294-7910
www.eerc.iastate.edu

April 1, 2010

TABLE OF CONTENTS

LIST OF FIGURES

LIST OF TABLES

ACKNOWLEDGMENTS

LIST OF SYMBOLS

a	Theoretical vibration amplitude (eccentric moment divided by the drum mass)
$a*$	Actual measured vibration amplitude (double integral of acceleration data)
A_Ω	Acceleration at fundamental frequency
$A_{X\Omega}$	Acceleration at X-order harmonic
A'	Machine acceleration
AFC	Automatic feedback control
b	Machine internal loss coefficient used in MDP calculation
b_0	Intercept in a linear regression equation
b_1, b_2, b_3	Regression coefficients
B	Contact width of the drum
C	Semivariogram scale
C_0	Semivariogram nugget
$C+C_0$	Semivariogram sill
CBR	California bearing ratio (weighted average to compaction layer depth)
CBR_{300}	Weighted average CBR to a depth of 300 mm
CCV	Continuous compaction value
CMV	Compaction meter value
COV	Coefficient of variation (calculated as the ratio of mean and standard deviation)
DPI	Dynamic cone penetration index
d_0	Measured settlement under plate
D_{10}	Particle size corresponding to 10% passing
D_{30}	Particle size corresponding to 30% passing
D_{60}	Particle size corresponding to 60% passing
E	Elastic modulus
E_{LWD-Z3}	Elastic modulus determined from 300-mm plate Zorn light weight deflectometer
E_{FWD-D3}	Elastic modulus determined from 300-mm plate Dynatest falling weight deflectometer
E_{V1}	Initial modulus from 300-mm diameter static plate load test
E_{V2}	Reload modulus from 300-mm diameter static plate load test
f	Vibration frequency
F	Shape factor
F_s	Drum force
g	Acceleration of gravity
G_s	Specific gravity
GPS	Global positioning system
h	Separation distance
IC-MV	Intelligent compaction measurement value
k_s	Roller integrated stiffness
LL	Liquid limit
m	Machine internal loss coefficient used in MDP calculation
m_d	drum mass
$m_e r_e$	Eccentric moment of the unbalanced mass
MDP	Caterpillar Machine drive power
MDP_{40}	See description in text

MV	Measurement value
n	Number of test measurements
p	Number of regression parameters
P_g	Gross power needed to move the machine
PI	Plasticity index
PL	Plastic limit
Point-MV	In-situ point measurement value
r	Radius of the plate
R	Semivariogram range
R'	Radius of the roller drum
R^2	Coefficient of determination
RMV	Resonant meter value
v	Roller velocity
w	Moisture content determined from Humboldt nuclear gauge
w_{opt}	Optimum moisture content
W	Roller weight
z_d	Drum displacement
α	Slope angle (roller pitch from a sensor)
φ	Phase angle
μ	Statistical mean
σ	Statistical standard deviation
σ_0	Applied stress
η	Poisson's ratio
γ_d	Dry unit weight determined from Humboldt nuclear gauge (NG)
γ_{dmax}	Maximum dry unit weight
$\gamma(h)$	Semivariogram

INTRODUCTION

This report presents results from a field investigation conducted on the US84 highway project in Waynesboro, Mississippi. The machine configurations and roller-integrated measurement systems used on this project included: a Caterpillar CP56 padfoot roller equipped with machine drive power (MDP) and compaction meter value (CMV) measurement technologies, a Sakai SW880 dual vibratory smooth drum roller equipped with compaction control value (CCV) technology, and a Case/Ammann SV212 smooth drum vibratory roller equipped with roller-integrated stiffness (k_s) and automatic feedback control. All the machines were equipped with real time kinematic (RTK) global positioning system (GPS) and on-board display and documentation systems. The project involved constructing and testing nine test beds with untreated and cement treated granular base and subgrade materials. The IC measurement values (IC-MVs) were evaluated by conducting field testing in conjunction with a variety of in-situ testing devices measuring density, moisture content, California bearing ratio (CBR), and elastic modulus. An open house was conducted near the end of the field investigation to disseminate results from current and previous IC projects. The Mississippi department of transportation (MSDOT), contractor's personnel, and representatives from the IC roller manufacturers participated in the field testing phase of the project and the open house.

The goals of this field investigation were similar to previous demonstration projects and included the following:

- document the impact of AFC operations on compaction uniformity,
- document machine vibration amplitude influence on compaction efficiency,
- develop correlations between IC measurement values to traditional in-situ point measurements (point-MVs),
- study IC roller measurement influence depth,
- compare IC results to tradition compaction operations,
- study IC measurement values in production compaction operations, and
- evaluate IC measurement values in terms of alternative specification options

This report presents brief background information for the four IC-MVs evaluated in this study (MDP, CMV, CCV, and k_s), documents the results and analysis from the laboratory and field testing, and documents the field demonstration activities. Geostatistical methods were used to quantify and characterize spatial non-uniformity of the embankment subgrade and subbase materials using spatially referenced IC-MV data. Regression analysis was performed to evaluate correlations between IC-MVs and in-situ soil properties determined using point-MVs. Density and moisture content tests were performed using Humboldt nuclear gauge, modulus tests were obtained using Zorn light weight deflectometer (LWD) setup with 300 mm diameter plates, Dynatest falling weight deflectometer (FWD) setup with 300 mm diameter plate, and static plate load test (PLT) setup with 300 mm diameter plate.

Empirical correlations between IC-MVs and in-situ point-MVs are first evaluated independently for each test bed which were sometimes obtained over a narrow measurement range and then combined to develop site wide correlations capturing a wide measurement range. This report provides new information with respect to IC-MVs and in-situ point-MVs on cement treated

materials. The results and correlations provided in this report should be of significant interest to the pavement, geotechnical, and construction engineering community and are anticipated to serve as a good knowledge base for implementation of IC compaction monitoring technologies and various new in-situ testing methods into earthwork construction practice.

BACKGROUND

Caterpillar CP56 padfoot, Case SV212 vibratory smooth drum, and Sakai SW880 dual drum IC rollers were used on the project (Figure 1). A digital display unit employing proprietary software is mounted in the roller cabin for on-board visualization of roller position, IC-MVs, coverage information, amplitude/frequency settings, speed, etc. The rollers were outfitted with a real-time kinematic (RTK) global positioning system (GPS) to continuously record the roller position information. Some key features of the rollers are summarized in Table 1. Caterpillar CP56 roller recorded machine drive power (MDP_{40}) and compaction meter value (CMV), Case SV212 roller recorded roller-integrated stiffness (k_s), and Sakai SW880 roller recorded continuous compaction value (CCV). Brief descriptions of these IC-MVs are provided in the following discussion.

Figure 1. Caterpillar CP56 (top left) padfoot, Case SV212 smooth drum, and Sakai SW880 dual smooth drum IC rollers used on the project

2

Table 1. Key features of the IC rollers used on the project

Feature	Caterpillar CP56	Case SV212	Sakai SW880
Drum Type	Padfoot	Smooth drum	Dual smooth drum
Frequency (f)	30 Hz	0 to 35 Hz	42, 50, and 67 Hz
Amplitude (a) Settings	Static, 0.90 mm (low amplitude), and 1.80 mm (high amplitude)	Amplitude settings using percent eccentric moments (0 to 100%) [0 represents no vibration and 100% represents high amplitude]	0.3 mm (low), 0.6 mm (high)
IC-MV	MDP_{40} (shown as CCV in the output) and Geodynamik CMV	k_s (MN/m) (k_s system is developed by Ammann)	CCV
Display Software	AccuGrade®	Ammann Compaction Expert (ACE)®	Aithon MT-R®
GPS coordinates	UTM Zone Mississippi East (NAD83)	UTM Zone Mississippi East (NAD83)	UTM Zone Mississippi East (NAD83)
Output Documentation	Date/Time, Location (Northing/Easting/Elevation of left and right ends of the roller drum), Speed, CCV, CMV, RMV, Frequency, Amplitude (theoretical), Direction (forward/ backward), Vibration (On/Off)	Date/Time, Location (Latitude/Longitude/ Elevation), Machine length/width, Direction (forward/ backward), Vibration (On/Off), Stiffness (k_s), Amplitude (actual), Speed, Frequency	Date/Time, Location (Northing/Easting/ Elevation), CCV, Temperature, Frequency, Direction (forward/backward), Vibration (On/Off), GPS Quality
Data frequency	About every 0.2 m at the center of the drum (for a nominal $v = 4$ km/h)	About every 1 m at the center of the drum (for a nominal $v = 4$ km/h)	About every 0.3 m at the center of the drum (for a nominal $v = 4$ km/h)
Output Export File	*.csv	*.txt	*.txt
Automatic Feedback Control (AFC)	No	Yes	No

Machine Drive Power (MDP) Value

MDP technology relates mechanical performance of the roller during compaction to the properties of the compacted soil. Detailed background information on the MDP system is provided by White et al. (2005). Controlled field studies documented by White and Thompson (2008), Thompson and White (2008), and Vennapusa et al. (2009) verified that MDP values are empirically related to soil compaction characteristics (e.g., density, stiffness, and strength). MDP is calculated using Eq. 1.

$$MDP = P_g - Wv\left(Sin\alpha + \frac{A'}{g}\right) - (mv + b) \tag{1}$$

Where MDP = machine drive power (kJ/s), P_g = gross power needed to move the machine (kJ/s), W = roller weight (kN), A' = machine acceleration (m/s^2), g = acceleration of gravity (m/s^2), α = slope angle (roller pitch from a sensor), v = roller velocity (m/s), and m (kJ/m) and b (kJ/s) = machine internal loss coefficients specific to a particular machine (White et al. 2005). MDP is a relative value referencing the material properties of the calibration surface, which is generally a hard compacted surface (MDP = 0 kJ/s). Positive MDP values therefore indicate material that is less compact than the calibration surface, while negative MDP values indicate material that is more compacted than the calibration surface (i.e. less roller drum sinkage). The MDP values obtained from the machine were recalculated to range between 1 and 150 using Eq. 2 (referred to as MDP$_{40}$). In Eq. 3, the calibration surface with MDP = 0 kJ/s was scaled to MDP$_{40}$ = 150 and a soft surface with MDP = 54.23 kJ/s (40000 lb-ft/s) was scaled to MDP$_{40}$ = 1.

$$MDP_{40} = 150 - 2.77(MDP) \tag{2}$$

Compaction Meter Value (CMV) and Resonant Meter Value (RMV)

CMV is a dimensionless compaction parameter developed by Geodynamik that depends on roller dimensions, (i.e., drum diameter and weight) and roller operation parameters (e.g., frequency, amplitude, speed), and is determined using the dynamic roller response (Sandström 1994). It is calculated using Eq. 3, where C is a constant (300), $A_{2\Omega}$ = the acceleration of the first harmonic component of the vibration, A_{Ω} = the acceleration of the fundamental component of the vibration (Sandström and Pettersson 2004). Correlation studies relating CMV to soil dry unit weight, strength, and stiffness are documented in the literature (e.g., Floss et al. 1983, Samaras et al. 1991, Brandl and Adam 1997, Thompson and White 2008, White and Thompson 2008).

$$CMV = C \cdot \frac{A_{2\Omega}}{A_{\Omega}} \tag{3}$$

RMV provides an indication of the drum behavior (e.g. continuous contact, partial uplift, double jump, rocking motion, and chaotic motion) and is calculated using Eq. 4, where $A_{0.5\Omega}$ = subharmonic acceleration amplitude caused by jumping (the drum skips every other cycle). It is important to note that the drum behavior affects the CMV measurements (Brandl and Adam 1997) and therefore must be interpreted in conjunction with the RMV measurements (Vennapusa et al. 2010).

$$RMV = C \cdot \frac{A_{0.5\Omega}}{A_{\Omega}} \tag{4}$$

Roller-Integrated Stiffness (k_s) Measurement Value

The k_s measurement system was introduced by Ammann during late 1990's based on a lumped parameter two-degree-of-freedom spring dashpot system illustrated in Figure 2 (Anderegg and Kauffmann 2004). The spring dashpot model has been found effective in representing the drum-ground interaction behavior (Yoo and Selig 1980). The drum inertia force and eccentric force time histories are determined from drum acceleration data and eccentric position (neglecting frame inertia). The drum displacement (z_d) is determined by double integrating the measured peak drum accelerations. The roller-integrated stiffness (k_s) is determined using Eq. 5, where f is the excitation frequency, m_d is the drum mass, $m_e r_e$ is the eccentric moment of the unbalanced mass, φ is the phase angle, a is vibration amplitude. The k_s value represents a quasi-static stiffness value and is reportedly independent of the excitation frequency between 25 to 40 Hz (Anderegg and Kaufmann 2004).

$$k_s = 4\pi^2 f^2 \left[\frac{m_d + m_e r_e \cos\phi}{a} \right] \tag{5}$$
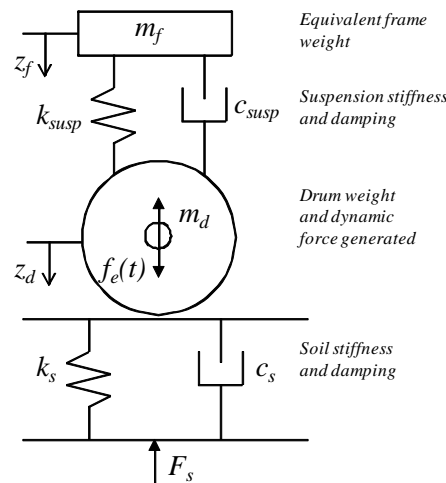
Figure 2. Lumped parameter two-degree-of-freedom spring dashpot model representing vibratory compactor and soil behavior (reproduced from Yoo and Selig 1980)

The k_s measurement system has the capability to perform compaction in a manual mode and in an automatic feedback control (AFC) mode. The AFC operations in the Case roller are controlled by the Ammann Compaction Expert (ACE) plus system. Three AFC operation settings are possible using the ACE plus system (Anderegg et al. 2006):

1. Low performance setting: Maximum applied force = 14 kN with vibration amplitude ($a*$) varying from 0.4 to 1.5 mm.
2. Medium performance setting: Maximum applied force = 20 kN with vibration amplitude ($a*$) varying from 1.0 to 2.0 mm.
3. High performance setting: Maximum applied force > 25 kN with vibration amplitude ($a*$) varying from 2.0 to 3.0 mm.

5

When operated in AFC mode, as sub-harmonic vibrations occur, the roller automatically adjusts the eccentric mass moment to adjust the vibration amplitude and excitation frequency (Anderegg et al. 2006). Correlation studies relating k_s to soil dry unit weight, strength, and stiffness are documented in the literature (Anderegg and Kaufmann 2004).

Roller-Integrated Compaction Control Value (CCV)

Sakai *Compaction Control Value* (CCV) is a vibratory-based technology which makes use of an accelerometer mounted to the roller drum to create a record of machine-ground interaction with the aid of GPS. The concept behind determination of CCV is that as the ground stiffness increases, the roller drum starts to enter into a "jumping" motion which results in vibration accelerations at various frequency components. This is illustrated in Figure 3.
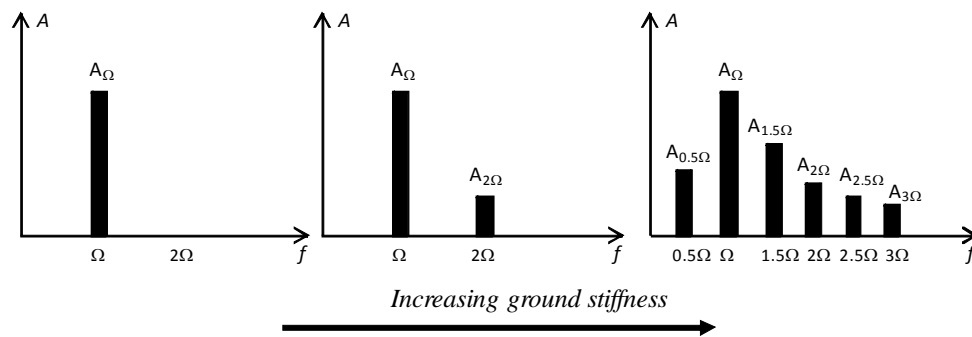
Figure 3. Changes in amplitude spectrum with increasing ground stiffness (modified from Scherocman et al. 2007)

The CCV is calculated using the acceleration data from first subharmonic (0.5Ω), fundamental (Ω), and higher-order harmonics (1.5Ω, 2Ω, 2.5Ω, 3Ω) as presented in Eq. 6.

$$\text{CCV} = \left[\frac{A_{0.5\Omega} + A_{1.5\Omega} + A_{2\Omega} + A_{2.5\Omega} + A_{3\Omega}}{A_{0.5\Omega} + A_{\Omega}} \right] \times 100 \qquad (6)$$

The vibration acceleration signal from the accelerometer is transformed through the Fast Fourier Transform (FFT) method and then filtered through band pass filters to detect the acceleration amplitude spectrum (Scherocman et al. 2007).

Overview of Project Earthwork Specifications

The MSDOT standard specifications for earthwork along with special provision No. 907-308-4M (Dated 08/14/2007) were implemented on the project. A typical pavement foundation layer section consisted of a 150 mm thick cement treated subgrade layer overlain by a 150 mm thick cement treated granular base material. The acceptance was based on achieving a target density and pay factors were provided in the special provision based on the achieved percent maximum density. Following were the QA and testing requirements:

- Each lot (750 m in length) is divided in to five sub lots with one density test taken at random in each sublot.
- For treated subgrade layers, the average of five density tests shall equal or exceed 96% of maximum density with no single density test below 94%.
- For treated base layers, the average of five density tests shall equal or exceed 97% of maximum density with no single density test below 95%. Pay factors were provided in the special provision based on the maximum achieved percent maximum density.

Following are some of the key construction related attributes of the specification and special provision documents:

- The soil to be treated should to be scarified and moisture-conditioned prior to spreading of the cement. All additional water required to bring the section to the required moisture content should to be added within one hour after the beginning of the mixing.
- The soil-cement mixture should be mixed using approved soil mixers (i.e., multiple pass mixers, single pass mixers, travelling plant mixers, and central plant mixers). A multiple pass mixing method using rotary-type mixer with multiple mixing passes (2 to 3) was employed on the project.
- The mixed material should to be shaped immediately after mixing. Initial compaction is should begin immediately, and machining and compacting should continue until the entire depth and width of the course is compacted to the required density within two hours of the time of beginning mixing.
- Compaction by vibration is not permitted after the cement has taken its initial set (i.e., one hour).
- After compaction, the surface should be reshaped to the required geometry and if necessary, shall be lightly scarified to remove imprints left by the compacting or shaping equipment. The surface should be sprinkled as necessary and thoroughly rolled with a pneumatic roller.
- Each treated layer should be covered with a bituminous curing seal as soon as possible (within 24 hours) after compaction. Placement of a subsequent layer above the treated layer was not permitted for at least seven calendar days. During this 7-day cure period, no traffic was permitted on the treated layer.

ANALYSIS METHODS

Regression Analysis

Simple linear and non-linear regression relationships between IC-MVs and in-situ point measurement values (Point MVs) were developed by spatially pairing the data obtained from the test beds. The analysis was performed by considering point-MVs as "true" independent variables and IC-MVs as dependent variables using the models shown in Eqs. 7 to 9, where b_0 = intercept and b_1, b_2 = regression parameters.

$$\text{Linear model: } IC-MV = b_0 + b_1 \cdot Point\,MV \tag{7}$$

Non-linear power model: $IC-MV = b_1(Point\ MV)^{b_2}$ (8)

Non-linear exponential model: $IC-MV = b_1\left(1-e^{(b_2 \times Point\ MV)}\right)$ (9)

Statistical significance of the independent variable was assessed based on *p*- and *t*-values. The selected criteria for identifying the significance of a parameter included: *p*-value < 0.05 = significant, < 0.10 = possibly significant, > 0.10 = not significant, and *t*-value < -2 or > +2 = significant. The best fit model is determined based on the strength of the regression relationships assessed by the coefficient of determination (i.e., R^2) values. For the analysis and discussion in this report, an R^2 value ≥ 0.5 is considered acceptable following the guidelines from European specifications. A statistical prediction interval approach for determining "target" values from the regression relationships would account for R^2 values in the relationships (see NCHRP 21-09, 2010). A regression relationship with lower R^2 values would result in higher target value and a regression relationship with higher R^2 value will result in lower target values.

Geostatistical Analysis

Spatially referenced IC measurement values provide an opportunity to quantify "non-uniformity" of compacted fill materials. Vennapusa et al. (2010) demonstrated the use of semivariogram analysis in combination with conventional statistical analysis to evaluate non-uniformity in QC/QA during earthwork construction. A semivariogram is a plot of the average squared differences between data values as a function of separation distance, and is a common tool used in geostatistical studies to describe spatial variation. A typical semivariogram plot is presented in Figure 4. The semivariogram γ(h) is defined as one-half of the average squared differences between data values that are separated at a distance h (Isaaks and Srivastava 1989). If this calculation is repeated for many different values of h (as the sample data will support) the result can be graphically presented as experimental semivariogram shown as circles in Figure 4. More details on experimental semivariogram calculation procedure are available elsewhere in the literature (e.g., Clark and Harper 2002, Isaaks and Srivastava 1989).

To obtain an algebraic expression for the relationship between separation distance and experimental semivariogram, a theoretical model is fit to the data. Some commonly used models include linear, spherical, exponential, and Gaussian models. A spherical model was used for data analysis in this report. Arithmetic expression of the spherical model and the spherical variogram are shown in Figure 4. Three parameters are used to construct a theoretical semivariogram: sill ($C+C_0$), range (R), and nugget (C_0). These parameters are briefly described in Figure 4. More discussion on the theoretical models can be found elsewhere in the literature (e.g., Clark and Harper 2002, Isaaks and Srivastava 1989). For the results presented in this section, the sill, range, and nugget values during theoretical model fitting were determined by checking the models for "goodness" using the modified Cressie goodness fit method (see Clark and Harper 2002) and cross-validation process (see Isaaks and Srivastava 1989). From a theoretical semivariogram model, a low "sill" and longer "range of influence" represent best conditions for uniformity, while the opposite represents an increasingly non-uniform condition.

Some of the results presented in this report revealed nested structures with short-range and long-range components in the experimental semivariograms. Nested structures have been observed in geological applications where different physical processes are responsible for spatial variations

8

at different scale (see Chiles and Delfiner 1999). For the cases with nested structures, nested spherical variograms combining two spherical models (with two sill values and two range values) are fit to the experimental semivariogram data.

Spherical Semivariogram

$\gamma(0) = 0$

$\gamma(h) = C_0 + C\left[\dfrac{3h}{2R} - \dfrac{h^3}{2R^3}\right] ----> 0 < h < R$

$\gamma(h) = C_0 + C ----> h > R$

Range, R: As the separation distance between pairs increase, the corresponding semivariogram value will also generally increase. Eventually, however, an increase in the distance no longer causes a corresponding increase in the semivariogram, i.e., where the semivariogram reaches a plateau. The distance at which the semivariogram reaches this plateau is called as range. Longer range values suggest greater spatial continuity or relatively larger (more spatially coherent) "hot spots".

Sill, $C+C_0$: The plateau that the semivariogram reaches at the range is called the sill. A semivariogram generally has a sill that is approximately equal to the variance of the data.

Nugget, C_0: Though the value of the semivariogram at h = 0 is strictly zero, several factors, such as sampling error and very short scale variability, may cause sample values separated by extremely short distances to be quite dissimilar. This causes a discontinuity at the origin of the semivariogram and is described as nugget effect. (Isaaks and Srivastava, 1989)

Figure 4. Description of a typical experimental and spherical semivariogram and its parameters

EXPERIMENTAL TESTING

Description of Test Beds

A total of nine test beds including two subgrade materials ("white sand" and "red sand"), one base material, and treated subgrade and base materials were studied. A summary of test beds with material conditions and tests performed is provided in Table 2. A summary of material index properties is provided in Table 3. Details regarding construction and testing of each test bed are provided in the discussion later and in test bed summary sheets in the Appendix. The following specific objectives were targeted for the different test beds evaluated in this study:

- Capture data over wide measurement range to develop IC-MV and different in-situ point-MV correlations – TBs 1, 2, 3, 4, 5, 6, 7, 8, and 9.
- Demonstrate the usefulness of using IC-MV maps for selection of QA test locations – TBs 2, 4, 5, and 8.
- Explore geostatistical methods to quantify and characterize spatial non-uniformity of embankment materials – TB1, 2, 3, 4, 5, 6, 8, and 9.
- Evaluate AFC mode operations in comparison with manual mode operations – TBs 7, 8, and 9.
- Compare IC-MVs on untreated and treated (shortly after compaction and after 2 days curing) subgrade and base layers – TBs 3 and 8 for base, and TBs 4, 5,6, and 9 for subgrade.

Table 2. Summary of test beds and in-situ testing

TB	Material	Date	Machine(s)	Pass	Theoretical Amplitude (mm) or setting, Speed (km/h)*	Notes/In-situ Test Measurements
1	Granular base [existing compacted layer]	07/13	S	1	0.30, 5	E_{LWD-Z3}, E_{FWD-D3}, γ_d, w, RC, E_{V1}, E_{V2}, CBR
			C	2-7	0.90, 4	
2	Cement Treated Granular base [5 day cure]	07/13	S	Map	0.30, 5	E_{LWD-Z3}, E_{FWD-D3}, γ_d, w, RC, E_{V1}, E_{V2}, CBR
3	Cement Treated Granular Base [same area as TB1]	07/14	C	5	0.90, 4	—
			C/A	Map	Ecc.= 15%, 4	E_{LWD-Z3}, E_{FWD-D3}, γ_d, w, RC, E_{V1}, E_{V2}, CBR
4	Granular Subgrade [existing compacted layer]	07/14	S	Map 1	0.60, 5	E_{LWD-Z3}, γ_d, w, RC, E_{V1}, E_{V2}, CBR
			C/A	Map 2	Ecc. = 15%, 4	
			C	Map 3	0.90, 4	
5	Cement Treated Granular Subgrade [portion of TB4: ISU compaction]	07/15	C	1-6	Lanes 1-3: 0.90, 4 Lanes 4-6: static, 4	E_{LWD-Z3}, E_{FWD-D3}, γ_d, w, RC, E_{V1}, E_{V2}, CBR
			C/A	Map	Ecc. = 15%, 4	
6	Cement Treated Granular Subgrade [portion of TB4: Contractor compaction]	07/15	C/A	Map	Ecc. = 15%, 4	—
7	Granular Subgrade [portion of subgrade with white sand pocket]	07/15	C/A	Map 1	Ecc. = 15%, 4	E_{LWD-Z3}, γ_d, w, RC, E_{V1}, E_{V2}, CBR
			C/A	Map 2	AFC (Medium), 4	
			C	Map 3	0.90, 4	
8	Cement Treated Granular Base [2 day cure on TB3]	07/16	C/A	Map 1	Ecc. = 10%, 4	E_{LWD-Z3}, E_{FWD-D3}, γ_d, w, RC, E_{V1}, E_{V2}, CBR
			C/A	Map 2	AFC (Low), 4	
9	Cement Treated Granular Subgrade [2 day cure on TB5]	07/17	C/A	Map 1	Ecc. = 15%, 4	E_{LWD-Z3}, E_{FWD-D3}, γ_d, w, RC, E_{V1}, E_{V2}, CBR
			C/A	Map 2	AFC (High), 4	

Notes: TB – test bed, * - nominal, C – Caterpillar, C/A – Case/Ammann, S - Sakai ; Ecc – Percent eccentric moment setting in Case/Ammann machine for amplitude adjustment, AFC – automatic feedback control mode. C – Caterpillar, C/A – Case/Ammann, S – Sakai, w – moisture content, γ_d – dry unit weight, RC – relative compaction, CBR – California bearing ratio determined from dynamic cone penetrometer (DCP) test, E_{LWD-Z3} – elastic modulus determined using 300 mm diameter plate Zorn light weight deflectometer (LWD), E_{V1} and E_{V2} – initial and reload moduli determined from static plate load test (PLT), E_{FWD-D3} – elastic modulus determined using 300 mm diameter plate Dynaest falling weight deflectometer (FWD) test.

Laboratory Testing

Laboratory testing was performed on two subgrade materials and one base material obtained from the project. Testing involved conducting grain size analysis and Atterberg limits tests to classify the materials in accordance with unified soil classification system (USCS) and American association of state highway and transportation officials (AASHTO) system. A summary of the material index properties is provided in Table 3. Grain size distribution curves of the three materials are presented in Figure 5. Standard Proctor tests were conducted on untreated materials by varying the moisture content of the material and the results are presented in Figure 6. Maximum dry unit weight (γ_{dmax}) and optimum moisture content (w_{opt}) results from Proctor tests are summarized in 3. Proctor tests were also conducted on treated subgrade and base material samples obtained from the test beds during construction.

Table 3. Summary of material index properties

Parameter	Subgrade (Red Sand)	Subgrade (White Sand)	Base
Standard Proctor Test Results (ASTM D698-00a)			
γ_{dmax} (kN/m^3)	19.04	16.27	18.02
w_{opt}	10.8	14.0	10.1
Grain-Size Analysis Results (ASTM D 422-63)			
Gravel Content (%) (> 4.75mm)	0	0	0
Sand Content (%) (4.75mm – 75μm)	63	92	84
Silt Content (%) (75μm – 2μm)	19	4	7
Clay Content (%) (< 2μm)	18	4	9
D_{10} (mm)	—	0.09	0.01
D_{30} (mm)	0.03	0.15	0.20
D_{60} (mm)	0.20	0.23	0.35
Coefficient of Uniformity, c_u	—	2.7	49.1
Coefficient of Curvature, c_c	—	1.1	17.0
Atterberg Limits Test Results (ASTM D4318-05)			
Liquid Limit, LL (%)		Non Plastic	
Plastic Limit, PL (%)			
AASHTO Classification (ASTM D3282-09)	A-4	A-3	A-2-4
USCS Classification (ASTM D2487-00)	SM	SP-SM	SM
Specific Gravity, G_s (Assumed)	2.70	2.70	2.70
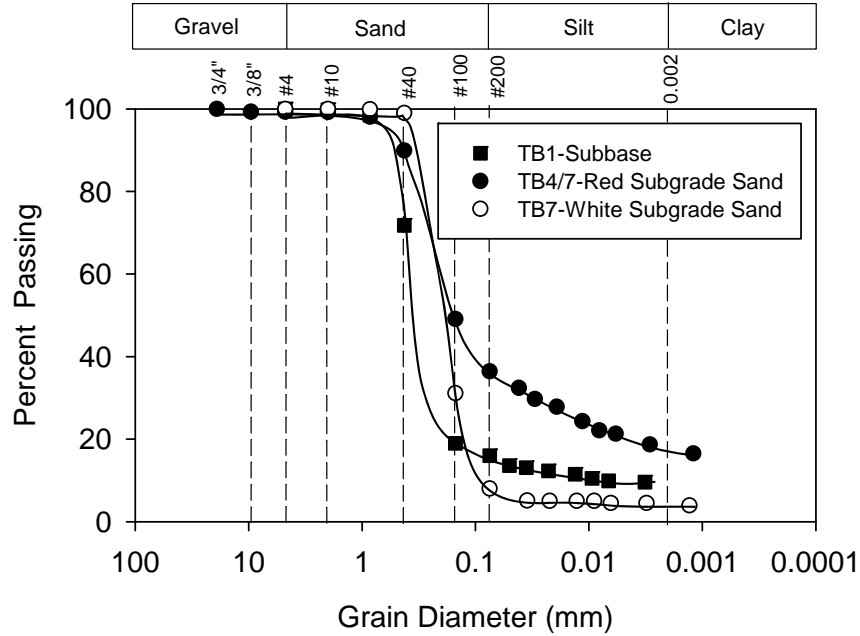
Figure 5. Grain-size distribution curves of base and subgrade materials
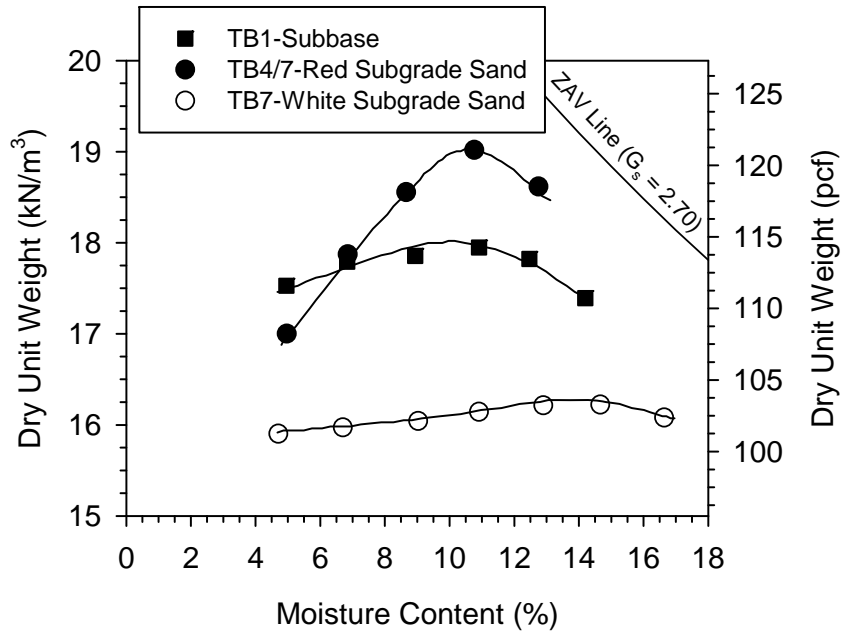
Figure 6. Laboratory standard Proctor moisture-density relationships for base and subgrade materials

To study the effect of compaction time delay on the density of the treated materials, samples were prepared in the laboratory and standard Proctor tests were conducted at various time intervals, i.e., at 0, 30, 60, 120, and 240 minutes after mixing. The treated "red sand" subgrade and base materials were prepared by adding 5.5% cement by dry weight of the soil, per project specifications. Results obtained from this study are presented in Figure 7 which indicates that the dry density of the treated materials reduce with increasing compaction delay time after

mixing. Similar results have been demonstrated by Arman and Saifan (1967) and indicated that a delay of two or more hours in compaction after mixing results in reduced durability, compressive strength, and density of the soil-cement mixture. Arman and Saifan (1967) recommended that compaction of soil-cement mixture should not be delayed beyond 0.80 times the initial setting time of the cement gel. Cowell and Irwin (1979) noted that delays beyond 3 hours may increase the required compactive effort to a level that may be beyond the capabilities of ordinary field compaction equipment. Specifications for the project indicated that the soil-cement mixture be compacted to required density within two hours after mixing (see earlier discussion under Overview of Earthwork Specifications section).
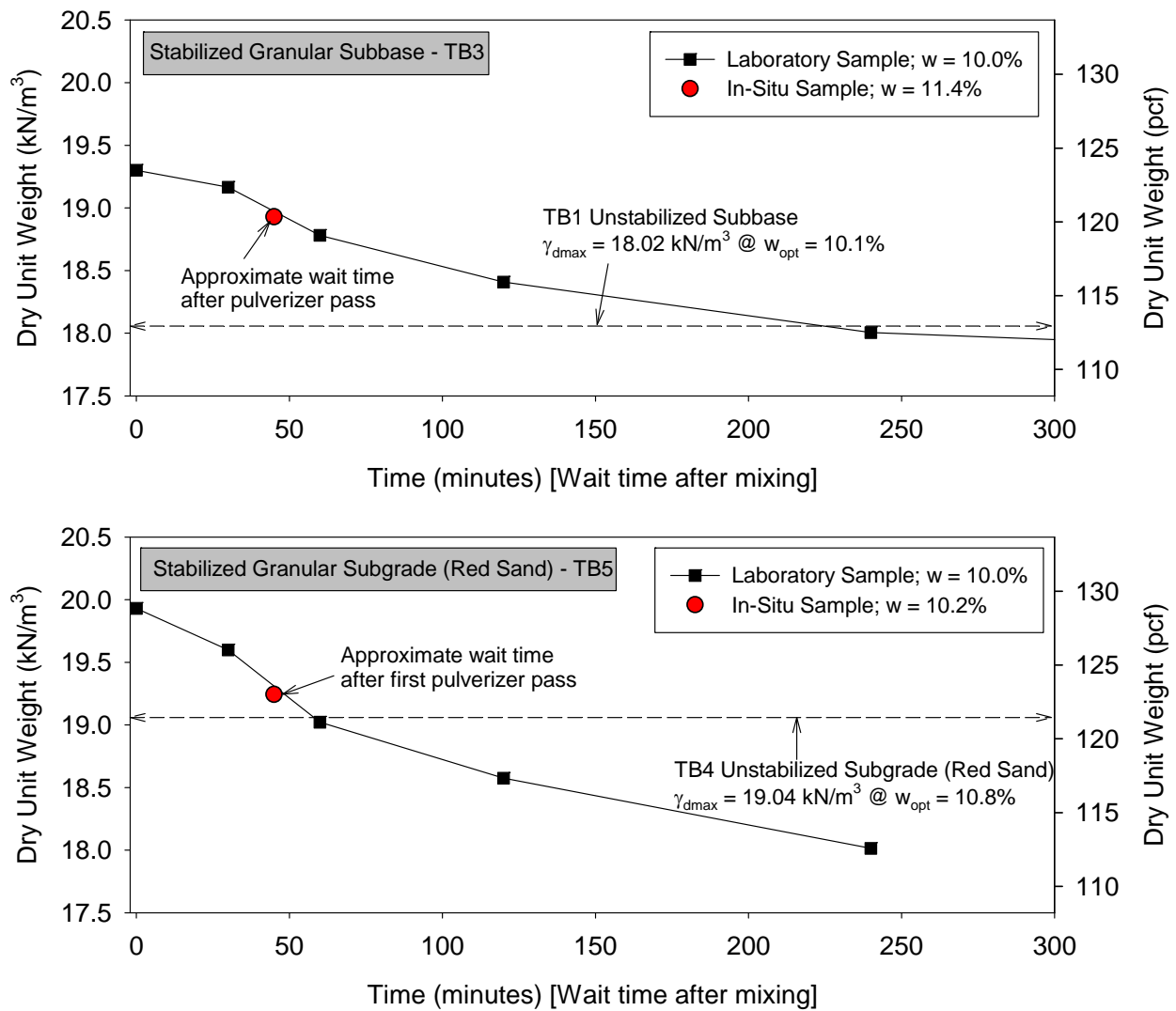
Figure 7. Effect of wait time (after mixing) on dry unit weight of treated base and subgrade materials

In-situ Testing Methods

Eight different in-situ testing methods were employed in this study to evaluate the in-situ soil engineering properties (Figure 8): (a) Zorn light weight deflectometer setup with 300 mm

13

plate diameter to determine elastic modulus (E_{LWD-Z3} for 300 mm plate diameter), (b) Dynamic Cone Penetrometer (DCP) to determine California bearing Ratio (CBR), (c) calibrated Humboldt nuclear gauge (NG)to measure moisture content (*w*) and dry unit weight (γ_d), (d) 300-mm diameter Dynatest falling weight deflectometer (FWD) to determine elastic modulus (E_{FWD-D3}), and (e) 300-mm plate diameter static plate load test (PLT) to determine initial (E_{V1}) and re-load modulus (E_{V2}). FWD tests were conducted by MSDOT personnel. All other in-situ tests were conducted by ISU research team.

LWD tests were performed following manufacturer recommendations (Zorn 2003) and the E_{LWD} values were determined using Eq. 10, where E = elastic modulus (MPa), d_0 = measured settlement (mm), η = Poisson's ratio (0.4), σ_0 = applied stress (MPa), r = radius of the plate (mm), F = shape factor depending on stress distribution (assumed as 8/3) (see Vennapusa and White 2009). The results are reported as E_{LWD-Z3} (Z represents Zorn LWD and 3 represents 300 mm diameter plate).

$$E = \frac{(1-\eta^2)\sigma_0 r}{d_0} \times F \qquad (10)$$

FWD testing was conducted by MSDOT personnel using a Dynatest trail mounted FWD by applying one seating drop using a nominal force of about 29 kN followed by three test drops each at a nominal force of about 29, 38, and 48 kN. The actual applied force was recorded using a load cell. A composite modulus value (E_{FWD-D3}) was calculated using the measured deflection at the center of the plate, corresponding applied contact force, and Eq. 1. Shape factor F = 8/3 was assumed in the calculations similar to LWD calculations.

Static PLT's were conducted by applying a static load on 300 mm diameter plate against a 6.2kN capacity reaction force. The applied load was measured using a 90-kN load cell and deformations were measured using three 50-mm linear voltage displacement transducers (LVDTs). The load and deformation readings were continuously recorded during the test using a data logger. The E_{V1} and E_{V2} values were determined from Eq. 10 using deflection values at 0.1 and 0.2 MPa applied contact stresses for subgrade materials and at 0.2 and 0.4 MPa contact stresses for base materials, as illustrated in Figure 9. Shape factor F = 8/3 and η = 0.4 were assumed in the calculations, similar to LWD and FWD calculations.

DCP tests were performed in accordance with ASTM D6951-03 to determine dynamic cone penetration index (DPI) and calculate CBR using Eq. 11. The DCP test results are presented in this report as CBR point values or CBR depth profiles. When the data is presented as point values, the data represents a weighted average CBR of the compaction layer depth or depth indicated in the subscript (e.g., CBR_{200} indicates weighted average CBR to a depth of 200 mm and CBR indicates weighted average CBR to the depth equal to the thickness of the compaction layer).

$$CBR = \frac{292}{DPI^{1.12}} \qquad (11)$$

Figure 8. In-situ testing methods used on the project: (a) Humboldt nuclear gauge, (b) dynamic cone penetrometer, (c) Zorn light weight deflectometer, (d) Dynatest falling weight deflectometer, (e) static plate load test
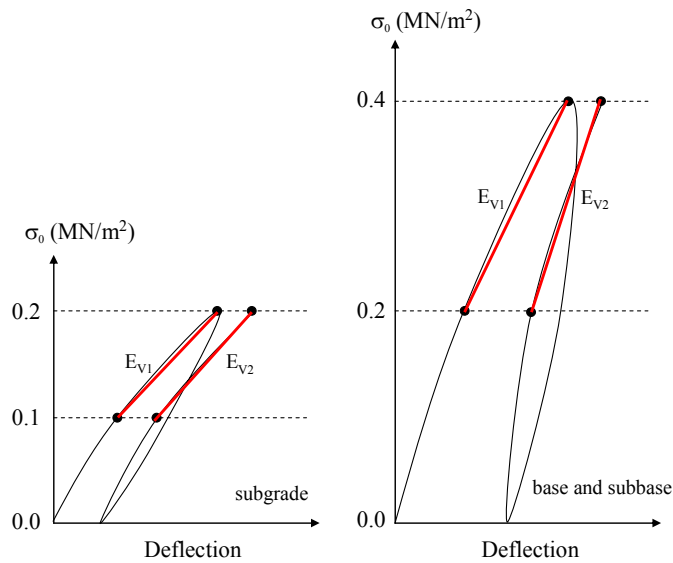
Figure 9. E_{V1} and E_{V2} determination procedure from static PLT for subgrade and base materials

EXPERIMENTAL TEST RESULTS

TB1 Granular Base Material (Untreated)

Test Bed Conditions, IC-MV Mapping, and Point-MV Testing

TB1 consisted of mapping the existing compacted granular base layer (untreated) with the Sakai smooth dual drum IC roller for one roller pass and Caterpillar padfoot IC roller for six roller passes (Figure 10). The area was mapped in four roller lanes. CCV IC-MVs were obtained from the Sakai roller using $a = 0.30$ mm, $f = 50$ Hz, and $v = 5$ km/h nominal settings. MDP_{40} and CMV IC-MVs were obtained from the Caterpillar roller using $a = 0.90$ mm, $f = 30$ Hz, and $v = 4$ km/h nominal settings. Point MVs (LWD, FWD, NG, PLT, and DCP) were performed at 6 randomly selected test locations following the Sakai roller pass.

Figure 10. TB1 granular base material after pass 1 with Sakai smooth drum roller (left) and pass 3 with Caterpillar padfoot roller (right)

Test Results and Analysis

IC-MV maps from the Sakai and Caterpillar roller passes are shown in Figure 11. In-situ point-MV test locations are shown on the CCV map in Figure 11. Figure 12 shows semivariograms, histogram, and box plots of the IC-MV data. A summary of the univariate and the spatial statistics of IC-MV and in-situ point-MV data are presented in Table 4.

The experimental semivariograms of the MDP_{40} values showed a nested spatial structure with short-range and long-range components. A nested spherical variogram was fit to the experimental semivariogram data. The CCV and CMV experimental semivariograms did not exhibit nested structures. Similar nested structures were observed for MDP_{40} measurements in an earlier field study (see NY field study report). The long-range spatial structure is attributed to the spatial variation in the underlying layer support conditions while the short-range spatial

structure is believed to be realted to soil properties closer to the surface. This long-range component was reduced considerably from pass 1 to 2 to 6 (Figure 12). The MDP_{40} semivariogram showed decreasing spatial non-uniformity with increasing passes which is evidenced by the decreasing sill value ($sill_1$ decreased from 82 to 20 and $sill_2$ decreased from 130 to 22 from pass 2 to 6; see Table 4). CMV semivariograms did not exhibit a significant change in the sill values (varied between 4 and 8) with increasing pass.

The box plots presented in Figure 12 present the range of the data observed for each pass. The bottom boundary of the box indicates the 25th percentile, the line within the box indicates the median, and the top boundary of the box indicates the 75th percentile of the IC-MV data. The error bars above and below the box indicate the 90th and 10th percentile, respectively. The circles outside the error bars are statistical outliers. On average, the MDP_{40} values decreased with increasing pass (pass 1 to 6 = 105.7 to 98.3), while the CMV measurements increased only slightly with increasing pass (pass 1 to 6 = 4.9 to 6.8). The decrease in MDP_{40} likely due to loosening of the material at the surface from padfoot indentations (see Figure 10).

Regression analysis results between CCV IC-MVs and in-situ point-MVs are presented in Figure 13. The relationships showed weak correlations with R^2 values ranging from 0 to 0.24. The correlations are weak because the range of measurements is narrow.
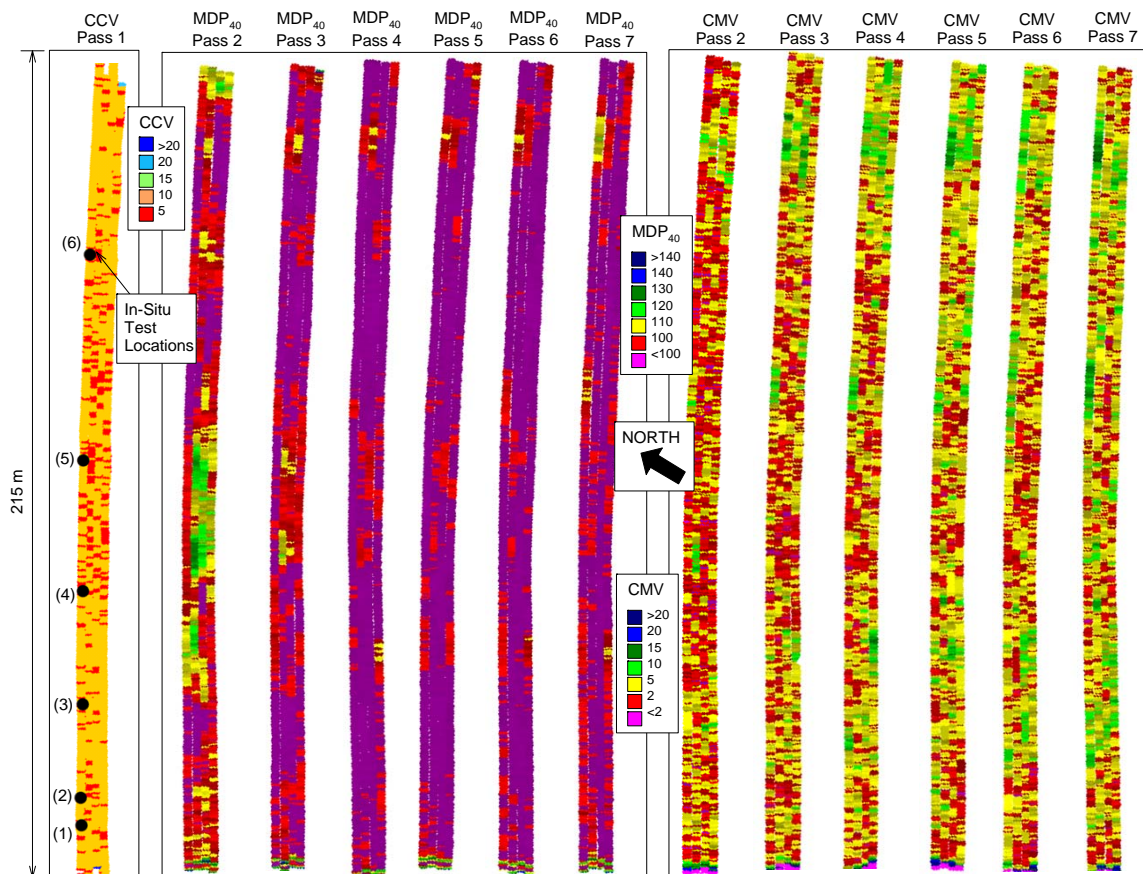
Figure 11. CCV, MDP$_{40}$, and CMV maps for passes 1 to 7 – TB1 granular base material
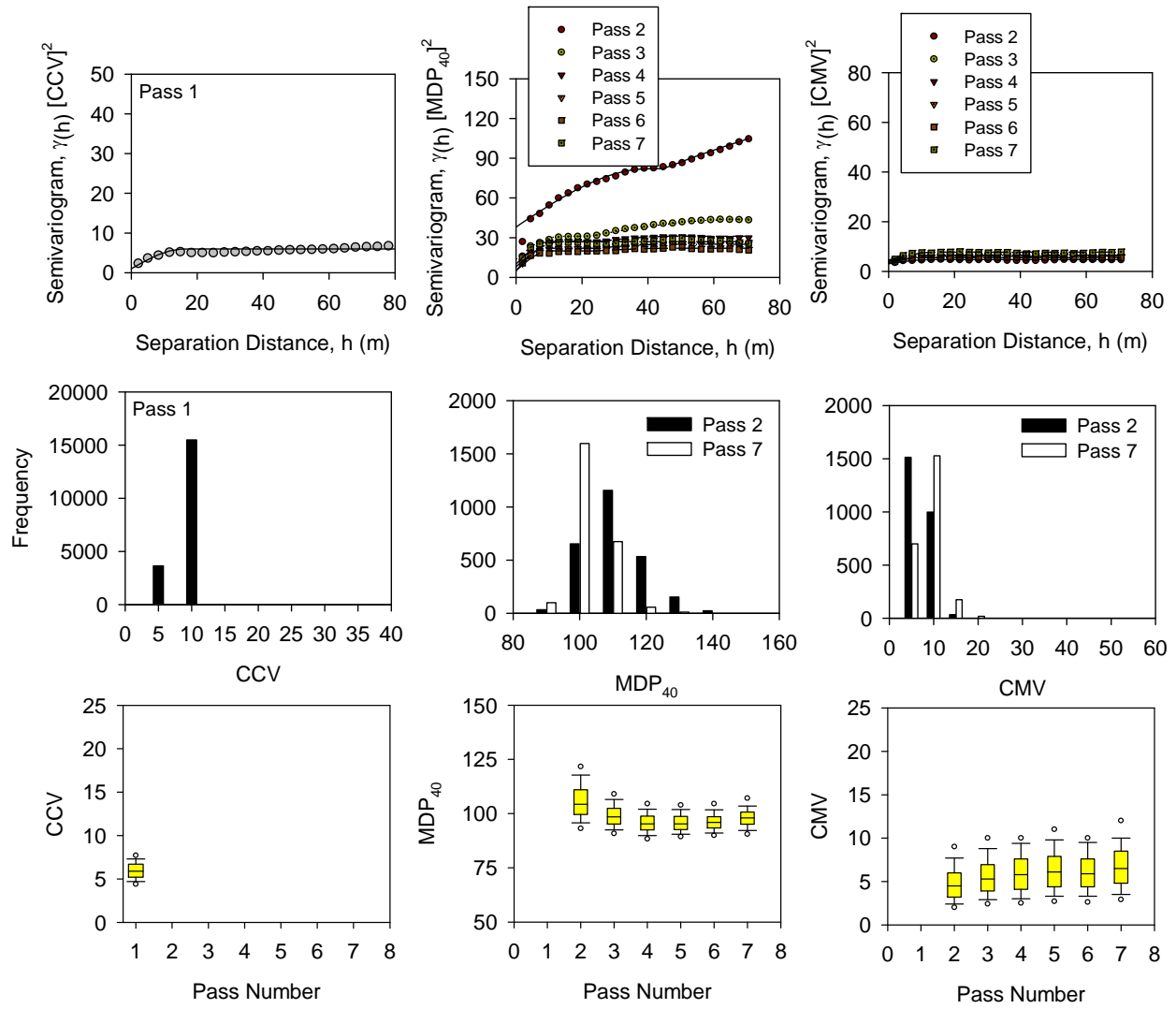
Figure 12. Semivariogram, histogram, and box plots (see description of box plots in text) of CCV, MDP$_{40}$, and CMV measurements - TB1 granular base material

Table 4. Summary of univariate and spatial statistics – TB1 granular base material

Pass	MV	n	Univariate Statistics			Spatial Statistics				
			μ	σ	COV (%)	Nugget	Sill$_1$	Range$_1$	Sill$_2$	Range$_2$
1	CCV	19211	6.1	2.9	47	1	6	16		—
2	MDP$_{40}$	2550	105.7	8.6	8	38	82	40	130	130
2	CMV	2550	4.9	2.2	45	3	5	12		—
3	MDP$_{40}$	2568	99.2	6.0	6	14	31	13	44	70
3	CMV	2568	5.6	2.4	43	4	6	15		—
4	MDP$_{40}$	2499	96.0	5.5	6	8	27	13	31	48
4	CMV	2499	6.0	2.5	41	4	7	11		—
5	MDP$_{40}$	2247	96.0	5.1	5	5	22	9	25	48
5	CMV	2247	6.3	2.6	41	4	7	11		—
6	MDP$_{40}$	2275	96.3	4.7	5	5	20	10	22	48
6	CMV	2275	6.1	2.4	39	4	4	11		—
7	MDP$_{40}$	2241	98.3	5.4	6	10	27	10		—
7	CMV	2241	6.8	2.8	41	5	8	14		—
2	γ_d (kN/m^3)	6	16.74	0.44	3					
2	RC (%)	6	92.9	0.02	3					
2	w (%)	6	8.5	1.5	18					
2	E$_{LWD-Z3}$ (MPa)	6	85	5	6	Not enough measurements				
2	E$_{V1}$ (MPa)	6	88	32	37					
2	E$_{V2}$ (MPa)	6	251	116	47					
2	E$_{FWD-D3}$ (MPa)	6	243	60	25					
2	CBR$_{200}$ (%)	6	46	7	16					

Note: CCV obtained at a = 0.30 mm, f = 55 Hz, and v = 4 km/h nominal settings; MDP$_{40}$ and CMV obtained at a = 0.90 mm, f = 30 Hz, and v = 4 km/h nominal settings.
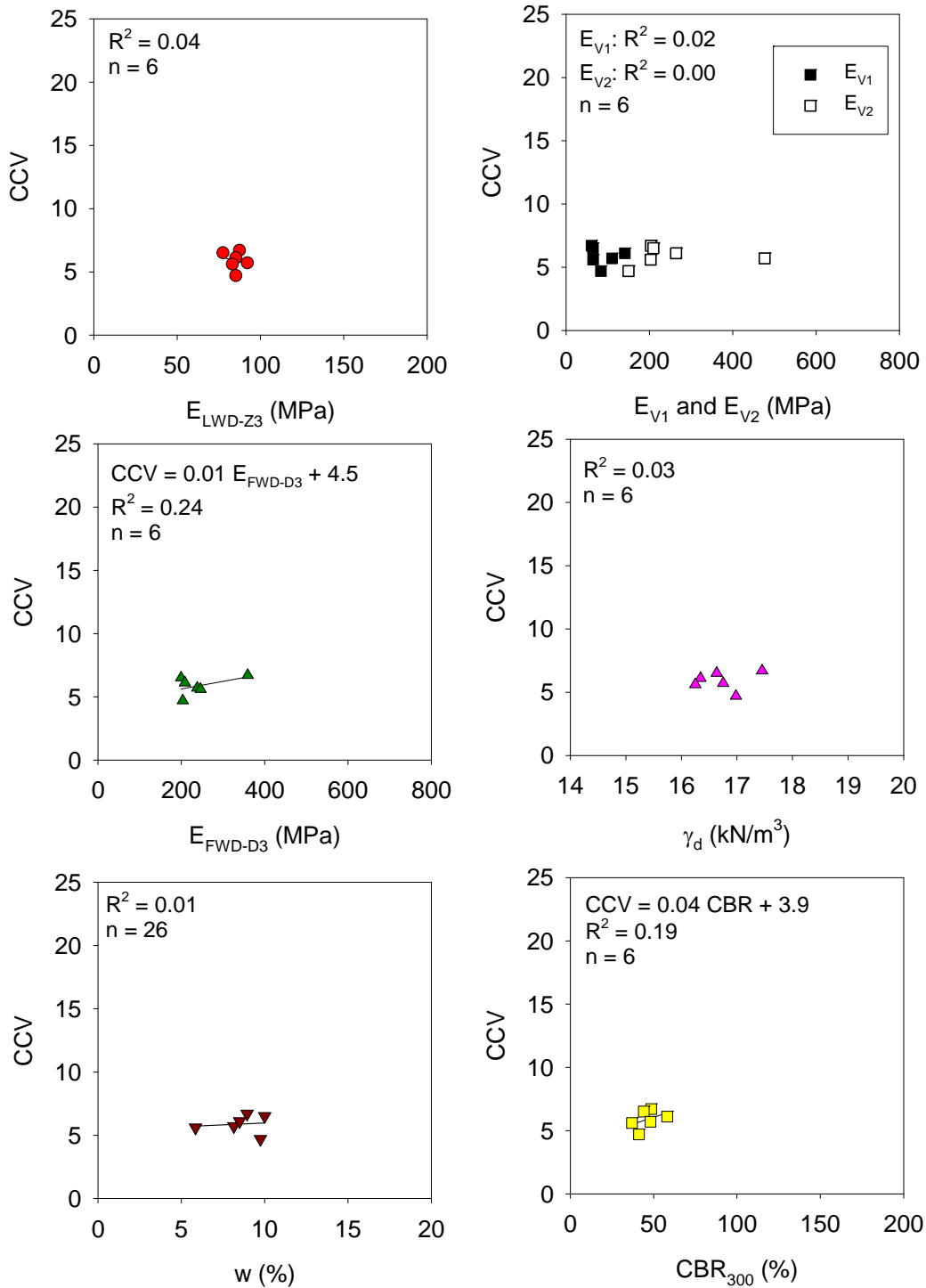
Figure 13. Regression analyses between CCV and in-situ point measurements - TB1 granular base material

Summary of Results

The test bed consisted of previously compacted granular base material (untreated) Measurements from TB1 involved obtaining IC-MV maps using Sakai and Caterpillar IC rollers,

and in-situ point-MVs (E_{LWD-Z3}, E_{V1}, E_{V2}, $E_{FWD-D3,}$ w, γ_d, and $CBR_{300,}$) at six randomly selected locations over a plan area of about 8 m x 215 m. Data analysis for this test bed comprised of geostatistical analysis of the spatially referenced IC-MV data and regression analysis between IC-MVs and in-situ point-MVs by spatially pairing the nearest point data. Following is a summary of key findings from these analyses:

- The MDP_{40} semivariograms showed a nested spatial structure with short-range and long-range components, while the CMV and CCV semivariograms did not. The reason for long-range structure is linked to possible spatial variation in the underlying support conditions while the short-range spatial structure is likely a result of soil properties close to the surface.
- The MDP_{40} semivariogram showed decreasing spatial non-uniformity with increasing pass. CMV semivariograms did not exhibit a significant change in the sill values with increasing passes.
- On average, MDP_{40} decreased (from 105.7 to 98.3) while CMV increased slightly (from 4.9 to 6.8) from pass 1 to 6. MDP_{40} values decreased due to material loosening at the surface from padfoot indentations.
- Regression analysis results between CCV IC-MVs and in-situ point-MVs showed weak correlations with R^2 values < 0.24, but the measurements were obtained only over a narrow range.

TB2 Treated Granular Base Material (5-day cure)

Test Bed Conditions, IC-MV Mapping, and Point-MV Testing

The test bed was located adjacent to TB1 and consisted of a 5-day cured 150 mm thick (nominal thickness) cement treated granular base layer (Figure 14). The test bed surface was coated with an asphalt binder to help retain moisture content in the treated base layer. The area was mapped in four roller lanes with the Sakai IC roller. CCV IC-MVs were obtained from the roller using a = 0.30 mm, f = 50 Hz, and v = 5 km/h nominal settings. Following the mapping pass, in-situ point-MVs (LWD, FWD, NG, PLT, and DCP) were performed at 17 to 20 test locations selected based on the IC-MV map over a wide range of CCV measurement values (CCV range = 4 to 25).

Figure 14. Picture of the test bed – TB2 treated base material

Test Results and Analysis

CCV map with DCP-CBR profiles at three selected locations are presented in Figure 15. In-situ point measurements (E_{LWD-Z3}, E_{V1}, E_{V2}, E_{FWD-D3}, RC, and *w*) at the DCP test locations are also provided in Figure 15. Figure 16 shows histogram and semivariogram plots of CCV IC-MV data. A summary of the univariate statistics of IC-MV and in-situ point-MV data are presented in Table 5.

As expected, the results indicate that the CCV IC-MVs and modulus/CBR point-MVs on the treated base layer (TB2) are greater than on the untreated base layer (TB1). The average CCV on TB2 is about 2.1 times greater than on TB1. The average E_{LWD-Z3}, E_{V1}, E_{V2}, E_{FWD-D3}, and CBR point-MVs are about 1.3, 2.6, 1.7, 1.8, and 1.8 times, respectively, greater on TB2 than on TB1. RC is however greater on TB1 (93%) than on TB2 (89%). The CCV semivariogram sill on TB2 (sill = 28) showed greater non-uniformity than on TB1 (sill = 6).

Regression analysis results between CCV IC-MVs and in-situ point-MVs are presented in Figure 17. The relationships showed weak correlations with R^2 values in the range of 0 to 0.41. However, positive trends are evident in CCV relationships with CBR and modulus point-MVs (i.e., E_{LWD-Z3}, E_{V1}, E_{V2}, and E_{FWD-D3}). No trend is observed in CCV relationships with density point-MVs. The primary reason for weak correlations despite a wide CCV measurement range is attributed to surface cracks observed following the vibratory roller pass (see Figure 18). The vibratory roller mapping pass was performed solely for research purposes, and is not recommended on treated layers as it can potentially break the cementitious bonds and cause a reduction in the strength/stiffness properties. Further, for such conditions it is recommended that the point MVs be performed before rolling.
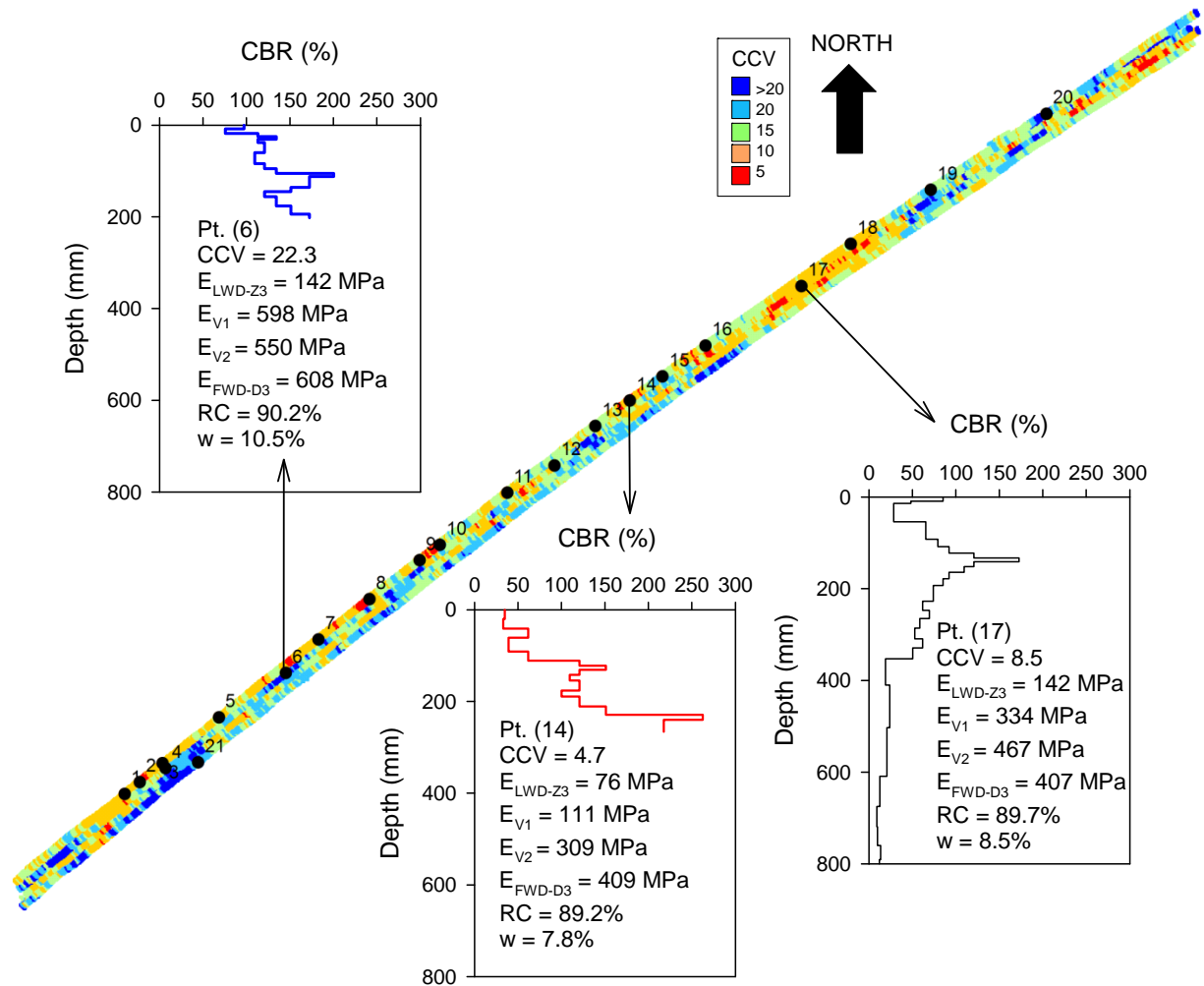
Figure 15. CCV map and CBR profiles at three select locations with low, medium, and high CCV values – TB2 treated base material (*a* = 0.30 mm, *f* = 55 Hz, *v* = 4 km/h nominal settings)
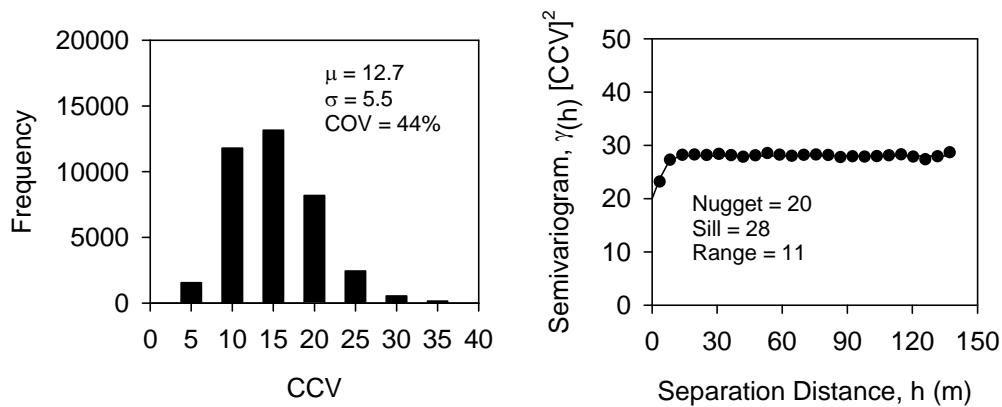
Figure 16. Histogram (left) and semivariogram (right) of CCV measurements – TB2 treated base material

Table 5. Summary of univariate statistics – TB2 treated base material

Pass	MV	n	μ	σ	COV (%)
1	CCV	37927	12.7	5.5	44
1	γ_d (kN/m^3)	20	16.77	0.32	2
1	RC (%)	20	88.6	0.02	2
1	w (%)	20	8.5	1.2	15
1	$E_{LWD\text{-}Z3}$ (MPa)	20	111	34	31
1	E_{V1} (MPa)	17	227	116	51
1	E_{V2} (MPa)	17	420	151	36
1	$E_{FWD\text{-}D3}$ (MPa)	21	433	115	26
1	CBR (%)	20	85	33	39
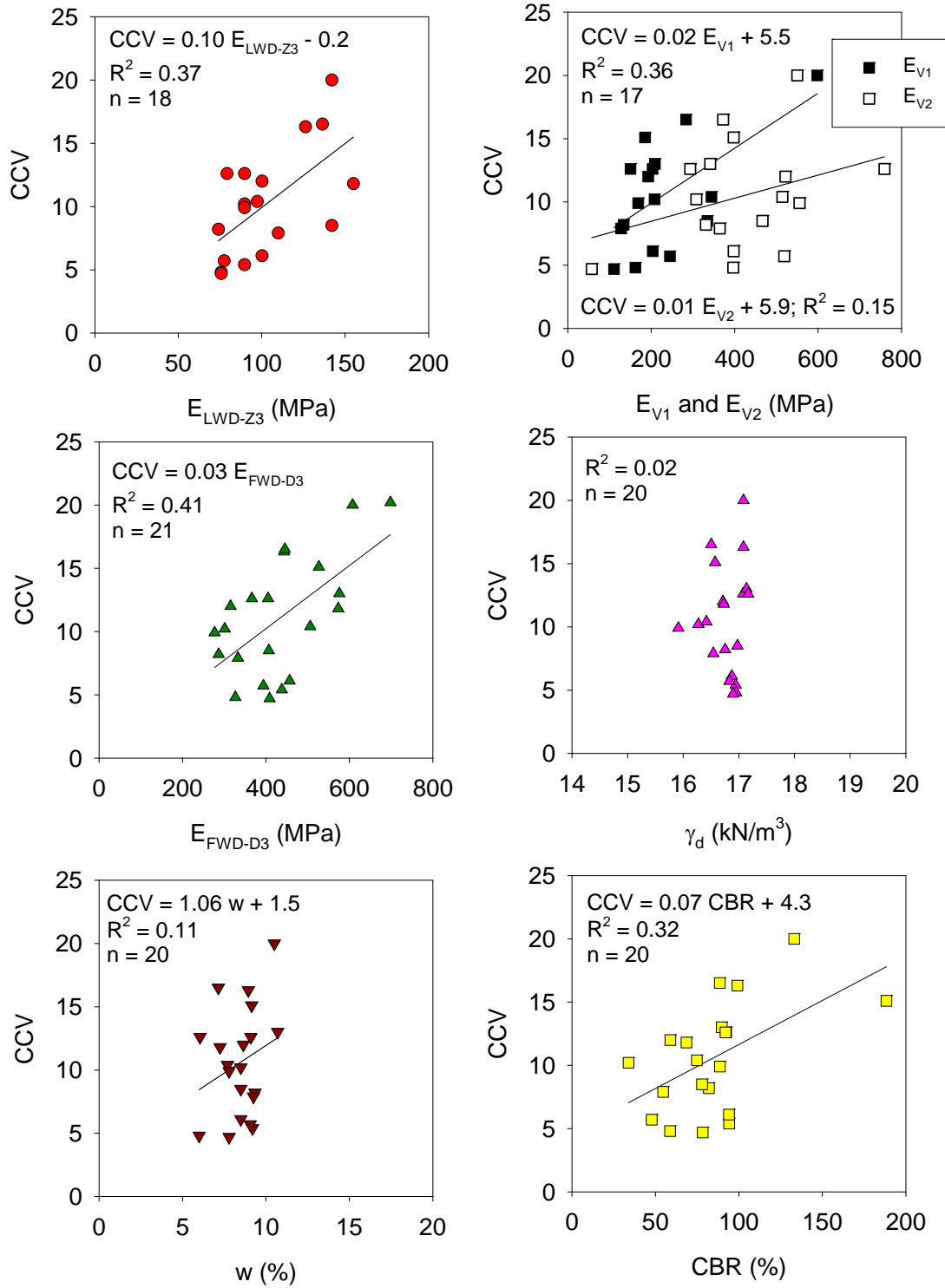
Figure 17. Regression analyses between CCV and in-situ point measurements – TB2 treated base material (5 day cure)

Figure 18. Cracks observed on the treated base material following the Sakai vibratory roller pass – TB2

Summary

The test bed consisted of a 5-day cured 150 mm thick cement-treated base layer. Measurements from TB2 involved IC-MV mapping using Sakai IC roller and obtaining in-situ point-MVs (E_{LWD-Z3}, E_{V1}, E_{V2}, E_{FWD-D3}, w, γ_d, and CBR) at 17 to 20 test locations selected based on the IC-MV map. Data analysis for this test bed comprised of geostatistical analysis of the spatially referenced IC-MV data and regression analysis between IC-MVs and in-situ point-MVs by spatially pairing the nearest point data. Following is a summary of key findings from these analyses:

- As expected, the CCV IC-MVs and modulus/CBR point-MVs on treated base layer (TB2) are greater than on the untreated base layer (TB1). The average CCV, E_{LWD-Z3}, E_{V1}, E_{V2}, E_{FWD-D3}, and CBR on TB2 are about 2.1, 1.3, 2.6, 1.7, 1.8, and 1.8 times, respectively, greater on TB2 than on TB1. RC is however greater on TB1 (93%) than on TB2 (89%).
- The CCV semivariogram sill on TB2 (sill = 28) showed greater non-uniformity than on TB1 (sill = 6).
- Regression analysis between CCV IC-MVs and in-situ point-MVs showed weak correlations with R^2 values in the range of 0 to 0.41. However, CCV relationships with CBR and modulus point-MVs (i.e., E_{LWD-Z3}, E_{V1}, E_{V2}, and E_{FWD-D3}) showed positive trends, while CCV relationship with density point-MVs did not. Cracks observed on the treated surface following vibratory rolling likely contributed to weak correlations.

TBs 3/8 Treated Base Material

Test Bed Construction

The test bed involved cement treatment of the TB1 granular base material with approximately 5.5% (of dry weight of soil) of cement. Photographs taken during the construction process are provided in Figure 19 to Figure 21. The construction sequence and time log from field observations are as follows:

26

a) scarified the base layer to about 150 mm depth and moisture-conditioning the base material to at target $w = 10\%$ [prior to 6:30 am],
b) spreaded stabilizer on the test bed [6:45 to 7:45 am],
c) preparing the soil-cement mixture using a rotary mixer (with two passes) [7:45 to 8:30 am],
d) compacted the area using a padfoot roller for one static pass and moisture-conditioning the soil-cement mixture with a water truck [8:30 to 9:15 am] (in-situ sample was obtained for laboratory Proctor test at 8:50 am),
e) compacted the area using padfoot roller for five to six passes [9:20 to 10:15 am],
f) compacted the area using vibratory smooth drum roller for two to four passes [10:00 to 10:45 am],
g) trimming the area to the desired elevation using a motor grader [10:30 to 11:00 am],
h) performed final compaction passes using a pneumatic rubber tire roller [10:45 to 11:55 am].
i) obtained IC-MV map using the Case/Ammann IC roller (one pass) [11:55 am to 12:40 pm]
j) obtained in-situ point-MVs (LWD, FWD, NG, PLT, and DCP) on the final compacted surface [12:24 to 1:20 pm]

The test bed was divided in to a 69 m long section (Section A) and a 130 m long section (Section B) (Figure 19). Section A was compacted using the Caterpillar padfoot IC roller using $a = 0.90$ mm, $f = 30$ Hz, and $v = 4$ km/h nominal settings, and the Case/Ammann smooth drum roller for using Ecc. = 15%, $f = 27$ Hz, and $v = 4.2$ km/h nominal settings, by the ISU research team. Roller measurements were continuously recorded during the Caterpillar IC roller passes. Case/Ammann smooth drum roller passes were not recorded due to data recording problems. All compaction operations on Section B were performed by the contractor. The area was compacted using a padfoot roller (in static mode) and a vibratory smooth drum roller.

IC-MV roller map (on Sections A and B) was obtained using the Case/Ammann smooth drum IC roller using Ecc. = 15%, $f = 27$ Hz, and $v = 4.2$ km/h nominal settings. Two days after treatment, the area was again mapped (referred to as TB8) using the Case/Ammann smooth drum IC roller in manual and AFC mode settings. For manual mode, the nominal settings used during mapping were Ecc. = 10%, $f = 27$Hz, and $v = 4.2$ km/h. For AFC mode, a low performance level with nominal $v = 4.2$ km/h was used for mapping. FWD point-MVs were obtained prior to mapping operations while other Point MVs (LWD, NG, PLT, and DCP) were obtained after the mapping operations. Tests were performed at 25 locations selected using the k_s IC-MV map.

Figure 19. TB3 treated base material compacted by ISU research team (section A) and contractor (section B)

Scarified and moisture-conditioned subbase

Placement of cement stabilizer on subbase

Soil-cement mixing process using puliverzier

Moisture-conditioning the soil-cement mixture

Compaction using Caterpillar padfoot IC roller

Moisture-conditioning after first pass

Figure 20. Pictures showing construction process on TB3 treated base

Compaction using Caterpillar padfoot roller

Compaction using Sakai smooth drum roller

Fine grading using motor grader

Final compaction passes using Caterpillar pneumatic tire roller

Figure 21. Pictures showing construction process on TB3 treated base

Test Results and Analysis

MDP_{40} and CMV IC-MV maps from compaction roller passes are presented in Figure 22. Box plots showing the range of data for each compaction pass is presented in Figure 23. Results indicate that on average MDP_{40} increased from about 112.4 to 115.3 from pass 1 to 5. No significant change in CMV was observed from pass 1 to 5 (average CMV = 6.2 to 6.8).

In-situ density measurements taken during compaction at various times after mixing are plotted in comparison with laboratory density relationship with time delay in Figure 24. Results indicate that on average the density measurements increased with increasing compaction effort but did not achieve the 95% RC required by the specifications.

k_s IC-MV, a^*, and f maps from TB3 (in manual mode) and TB8 (in manual and AFC modes) are presented in Figure 25. Histogram plots of k_s IC-MVs and in-situ point-MVs on TB3 and TB8 showing comparison between measurements obtained shortly after compaction and after 2-day cure are presented in Figure 26. Same results are presented as box plots in Figure 27. A summary of univariate statistics of k_s IC-MVs and in-situ point-MVs from TB3 and TB8 is provided in Table 6. Results indicate that on average the k_s IC-MV, E_{LWD-Z3}, E_{FWD-D3}, E_{V1}, E_{V2}, and CBR

30

measurement values increased by about 33%, 15%, 75%, 49%, 66%, and 320% after 2-day curing. Moisture content of the material decreased on average from about 10.5% to 7.1%. As a result of this decrease in moisture content, the average RC of the material increased slightly from about 91 to 92%.

Semivariograms of k_s IC-MVs obtained from TB3 in manual mode, and TB8 in manual and AFC modes are presented in Figure 28. Semivariogram plots for k_s IC-MVs indicate greater non-uniformity in k_s IC-MVs after two days of curing (TB8) compared to shortly after compaction (TB3). This is an important finding to note and has not been well documented in the literature. This increasing non-uniformity is attributed to various factors such as non-uniform application of cement, water content, mixing, compaction delay time, and compaction energy across the test bed area. Modulus (E_{LWD-Z3}, E_{V1}, E_{V2}, E_{FWD-D3}) and CBR point-MVs also indicated greater non-uniformity with higher COV values on TB8 compared to on TB3 (see Table 6). RC and density measurements did not show significant differences in COV between TB8 and TB3.

Correlations between k_s IC-MVs obtained in manual mode and in-situ point-MVs from TB3 and TB8 are presented in Figure 29 and Figure 30, respectively. Regressions on TB3 showed weak correlations with $R^2 < 0.13$ due to narrow range of measurements. k_s results on TB3 showed influence of moisture content with $R^2 = 0.37$. Regressions on TB8 between k_s IC-MVs and E_{FWD-D3} showed good correlations with $R^2 = 0.53$, while regressions with other point-MVs produced relatively weak correlations ($R^2 < 0.41$). Note that the E_{FWD-D3} measurements were obtained prior to roller mapping passes, while all other point-MVs were obtained after mapping passes. Similar to observations on TB2, surface cracks were observed on TB8 following vibratory roller passes which likely affected the point MVs and therefore the correlations.

Figure 28 compares k_s IC-MV, a^*, and f maps obtained in manual and AFC modes on TB8. The k_s measurements varied from 30 to 90 MN/m and the a^* measurements varied from 0.3 to 1.0 mm. The f measurements remained relatively constant at about 29 Hz. Analysis of k_s and a^* results indicated that the drum vibration amplitude was reduced with increase in k_s. Comparison between k_s and a^* for different response distances (i.e., 0, 1, 2, and 3 m) indicated that the response distance for altering the amplitude was in the range of 1 to 2 m (for variation in $v = 4.1$ to 4.5 km/h) (note that the roller data was reported approximately every 1 m).
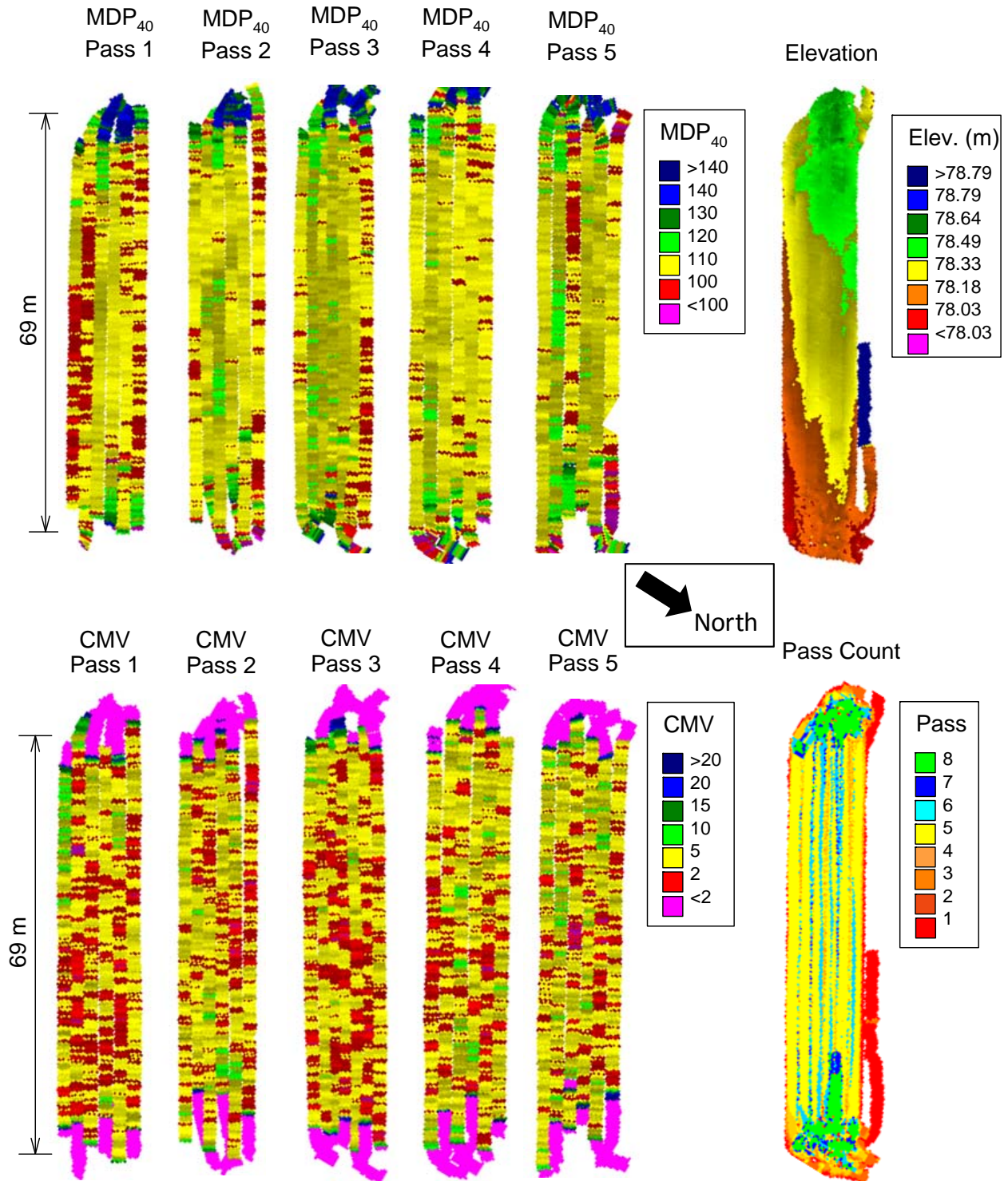
Figure 22. MDP$_{40}$ and CMV maps for passes 1 to 5, and elevation and number of roller passes maps – TB3 (section A) treated base material (a = 0.90 mm, f = 30 Hz, and v = 4 km/h nominal settings)
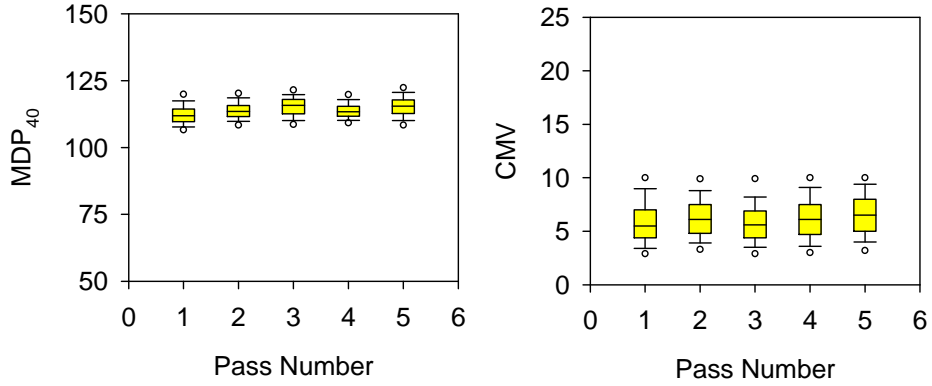
Figure 23. Box plots of MDP$_{40}$ and CMV measurements – TB3 treated base material (a = 0.90 mm, f = 30 Hz, and v = 4 km/h nominal settings)
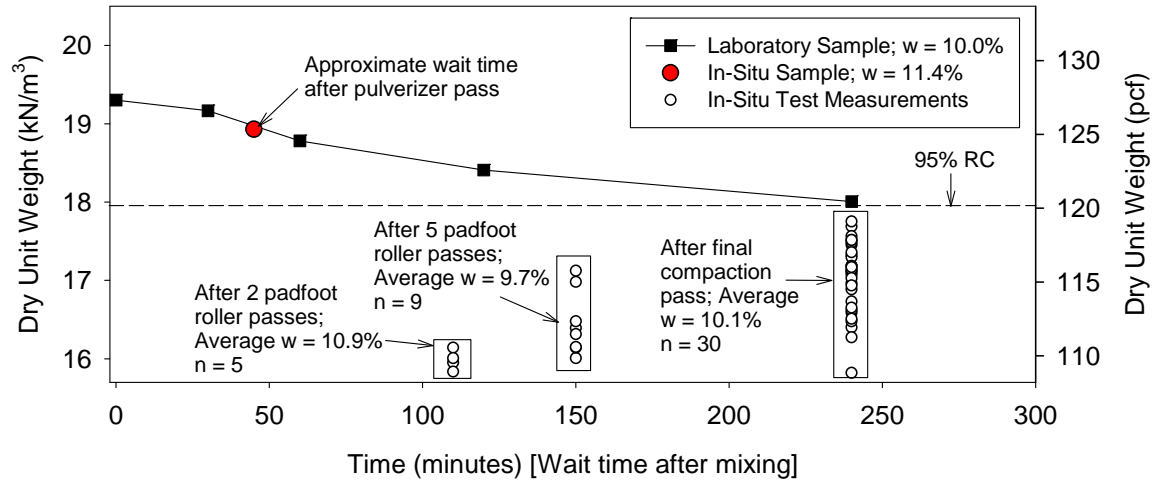
Figure 24. In-situ density test measurements during compaction in comparison with laboratory density measurements – TB3 treated base material
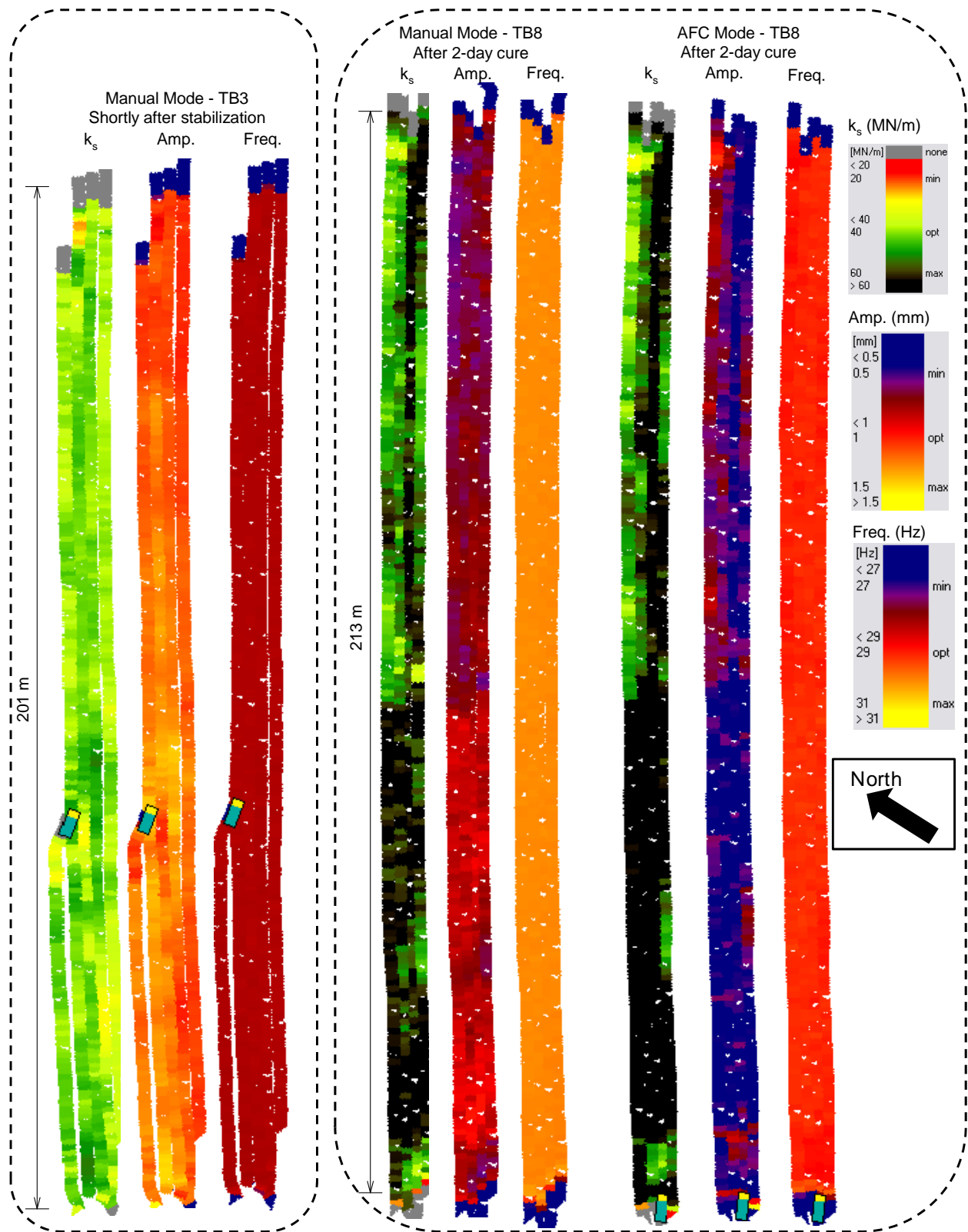
Figure 25. Comparison of k$_s$, a^*, and f maps obtained shortly after compaction (TB3) and after 2-day cure in manual and AFC modes (TB8)

34
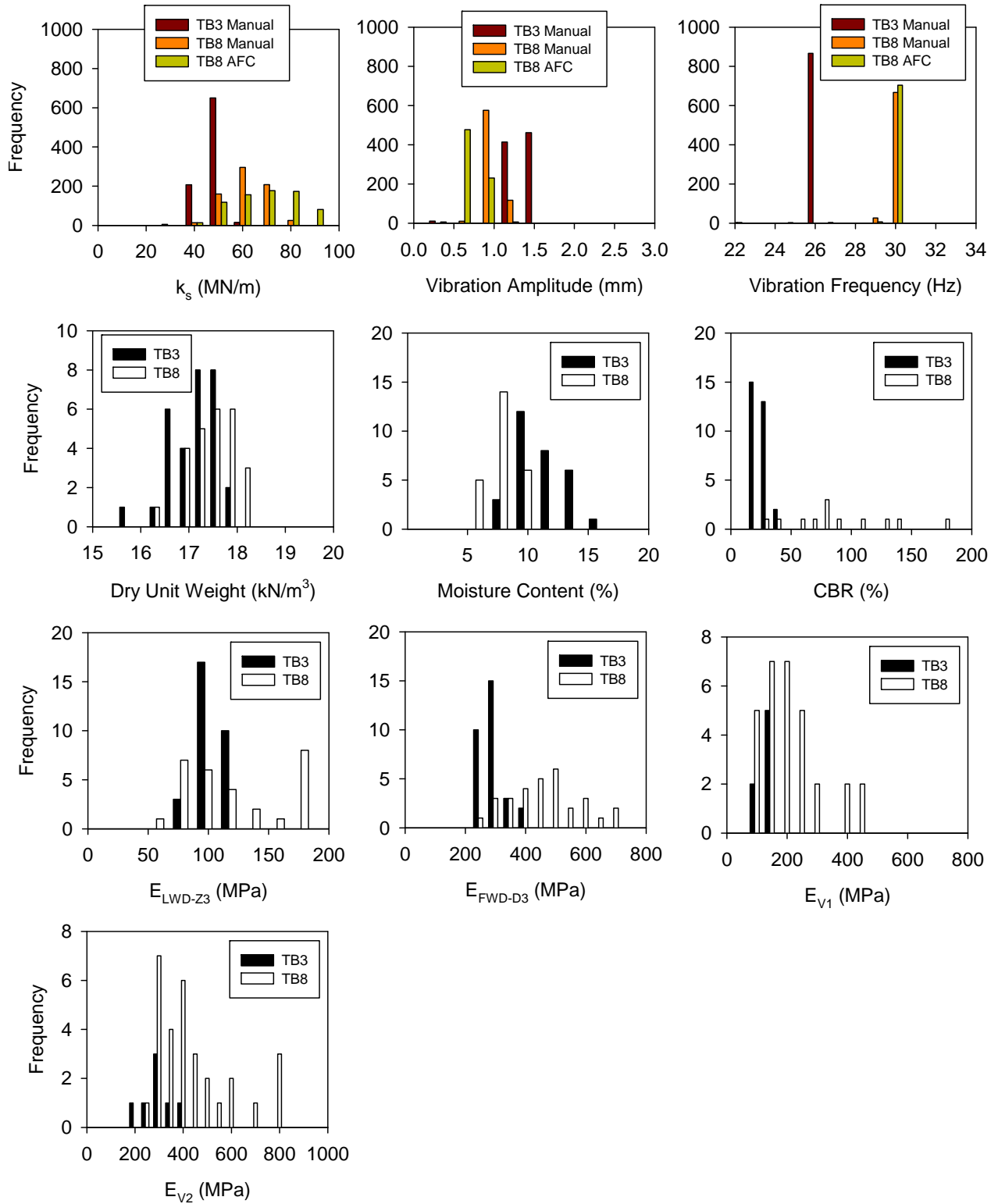
Figure 26. Histogram plots comparing measurements obtained shortly after compaction (TB3) and after 2-days curing (TB8)
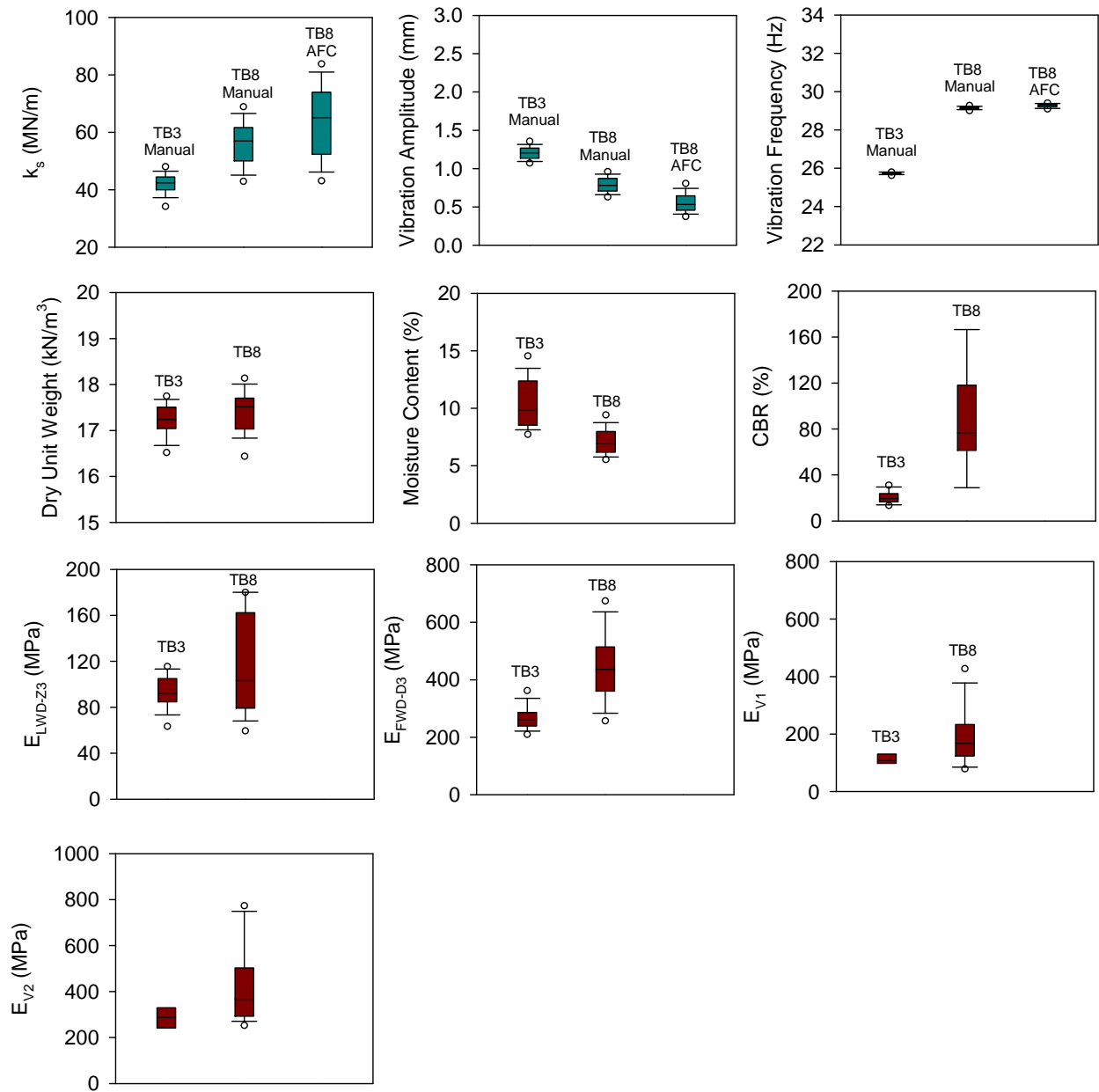
Figure 27. Box plots comparing measurements obtained shortly after compaction (TB3) and after 2-days curing (TB8)

Table 6. Summary of univariate statistics – TBs 3/8 treated base material

TB	MV	n	μ	σ	COV (%)
			Univariate Statistics		
TB3	k_s (MN/m)	890	42	6	14
	$a*$ (mm)	890	1.19	0.16	13
	f (Hz)	890	26	2	8
	γ_d (kN/m^3)	20	17.23	0.33	2
	RC (%)	20	91.1	1.7	2
	w (%)	20	10.5	2.1	20
	E_{LWD-Z3} (MPa)	19	90	15	16
	E_{V1} (MPa)	7	109	26	24
	E_{V2} (MPa)	7	284	54	19
	E_{FWD-D3} (MPa)	20	267	40	15
	CBR (%)	20	21	5	25
TB8	k_s (MN/m) [manual]	704	56	8	15
	$a*$ (mm) [manual]	704	0.79	0.11	13
	f (Hz) [manual]	704	29	1	3
	k_s (MN/m) [AFC]	720	64	13	20
	$a*$ (mm) [AFC]	720	0.56	0.14	25
	f (Hz) [AFC]	720	29	1	3
	γ_d (kN/m^3)	25	17.39	0.46	3
	RC (%)	25	91.9	2.4	3
	w (%)	25	7.1	1.1	16
	E_{LWD-Z3} (MPa)	25	104	33	32
	E_{V1} (MPa)	30	191	99	52
	E_{V2} (MPa)	30	422	157	37
	E_{FWD-D3} (MPa)	30	443	116	26
	CBR (%)	12	88	43	50

Note: Nominal v = 4.2 km/h during roller operation
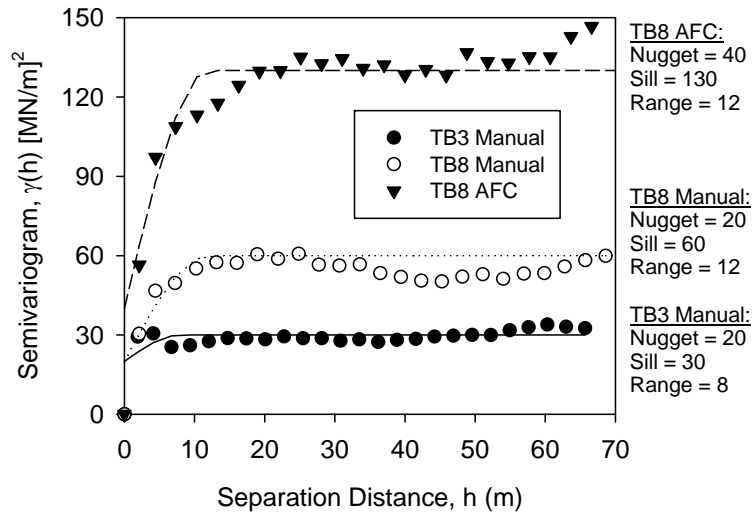
Figure 28. Semivariograms of k_s measurements obtained on TB3 in manual mode, TB8 in manual mode, and TB8 in AFC mode
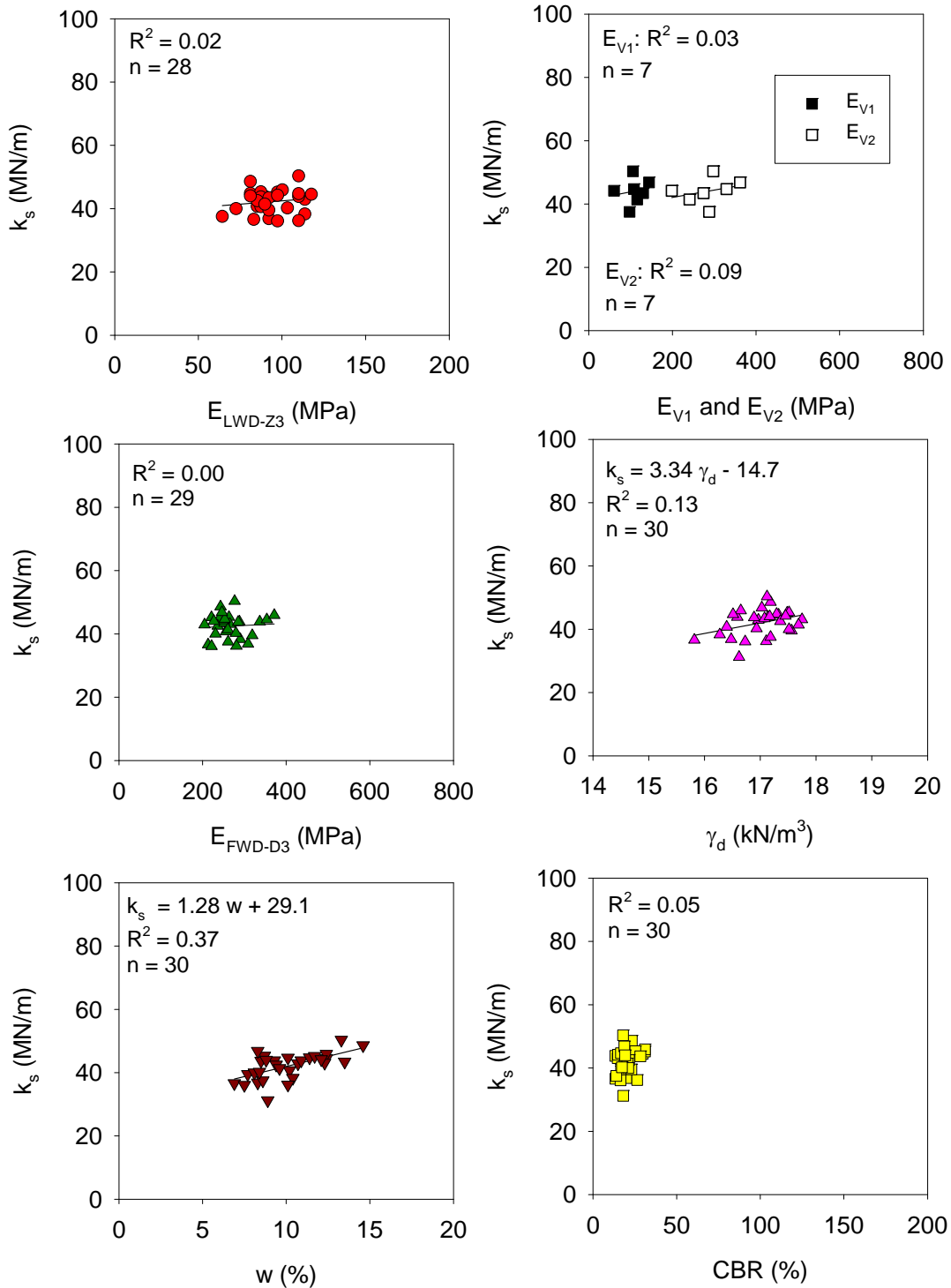
Figure 29. Regression analyses between k_s and in-situ point measurements – TB3 treated base material (shortly after compaction; manual mode)
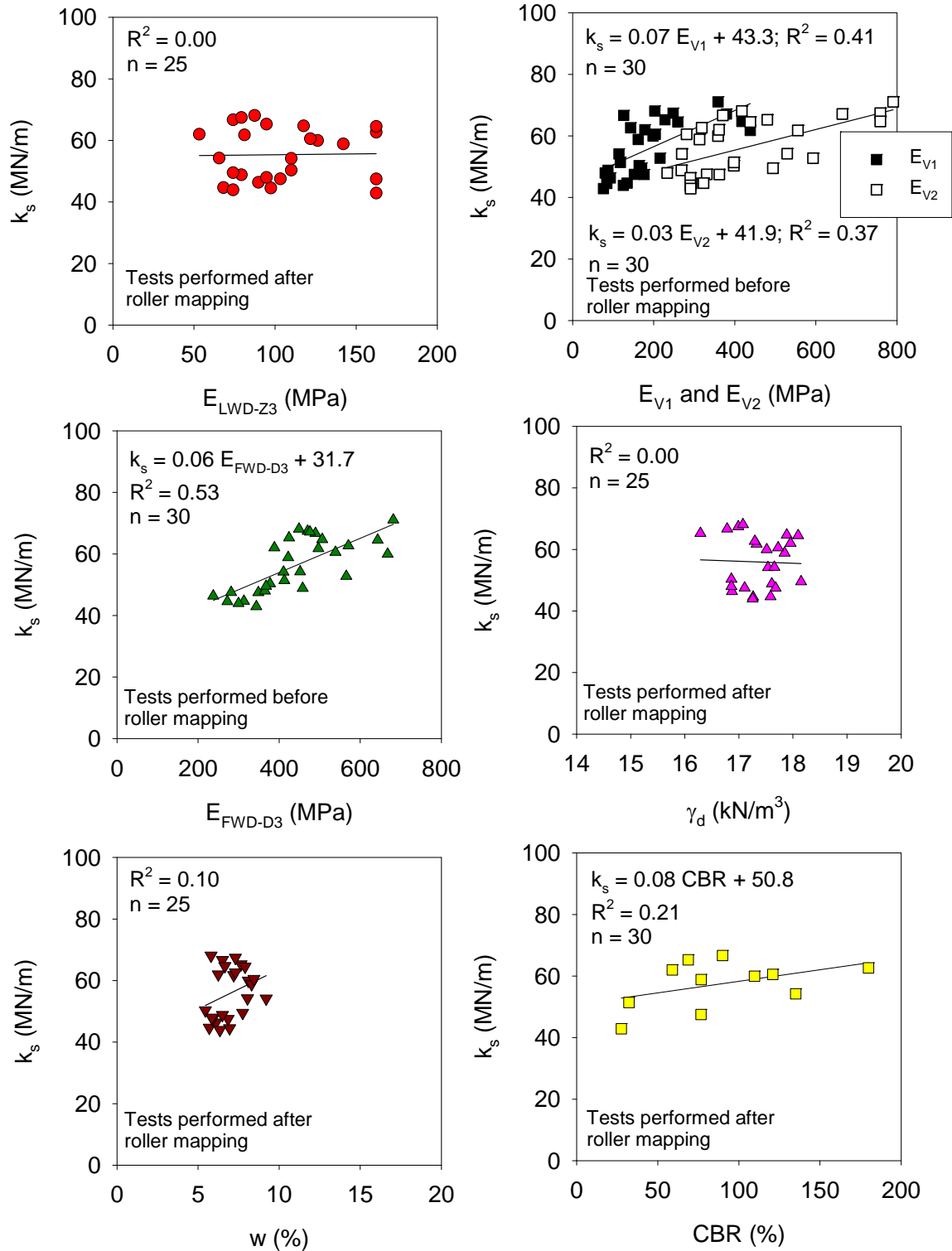
Figure 30. Regression analyses between k_s and in-situ point measurements – TB8 treated base material (after 2-day cure; manual mode)

Summary

　　TB3 consisted of construction of a 150 mm thick cement-treated base layer, obtaining MDP_{40} IC-MVs during compaction, k_s IC-MVs along with in-situ point-MVs (E_{LWD-Z3}, E_{V1}, E_{V2}, E_{FWD-D3}, w, γ_d, and CBR) shortly after treatment. TB8 involved obtaining k_s IC-MVs after 2 days of curing along with in-situ point-MVs (E_{LWD-Z3}, E_{V1}, E_{V2}, E_{FWD-D3}, w, γ_d, and CBR). Data analysis for TBs 3 and 8 comprised of geostatistical analysis of the spatially referenced k_s IC-MV data and regression analysis between IC-MVs and in-situ point-MVs by spatially pairing the nearest point data. Following is a summary of key findings from these analyses:

- During initial compaction on TB3 using Caterpillar padfoot IC roller, the average MDP_{40} increased from about 112.4 to 115.3, while no significant change in CMV was observed (average CMV = 6.2 to 6.8) from pass 1 to 5.
- As expected, the k_s IC-MVs and modulus/CBR point-MVs improved after 2 days of curing. Results indicated that on average the k_s IC-MV, E_{LWD-Z3}, E_{FWD-D3}, E_{V1}, E_{V2}, and CBR measurement values increased by about 33%, 15%, 75%, 49%, 66%, and 320% after 2 days of curing. Moisture content of the material decreased on average from about 10.5% to 7.1%. As a result of decrease in the moisture content, the average RC of the material increased slightly from about 91 to 92%.
- k_s IC-MVs and in-situ point-MVs showed greater non-uniformity on TB8 than on TB3. This is an important finding to note and has not been well documented in the literature. The reasons for this increased non-uniformity after curing is attributed to non-uniform application of cement, water, mixing, compaction delay time, and compaction energy across the test bed area. RC and density measurements did not show significant differences in terms of variability between TB8 and TB3.
- Regressions on TB3 between k_s IC-MVs and in-situ point-MVs on TB3 showed weak correlations with $R^2 < 0.13$ due to narrow range of measurements. k_s IC-MV results on TB3 showed influence of moisture content with $R^2 = 0.37$.
- Regressions on TB8 between ks IC-MVs and E_{FWD-D3} showed good correlations with $R^2 = 0.53$, while regressions with other point-MVs produced relatively weak correlations ($R^2 < 0.41$). The reason for better correlations with E_{FWD-D3} measurements is that the measurements were obtained prior to roller mapping passes, while all other point-MVs were obtained after mapping passes. Similar to observations on TB2, surface cracks were observed on TB8 following vibratory roller passes.
- AFC operations on TB8 indicated that the vibration amplitude was reduced with increase in k_s measurement values and the response distance for altering the amplitude was in the range of 1 to 2 m (for variation in $v = 4.1$ to 4. 5 km/h)

TB4 Granular Subgrade Material (Untreated)

Test bed conditions, IC-MV mapping, and Point-MV testing

The test bed consisted of a 530 m long section of existing compacted granular subgrade layer (untreated) (Figure 31). The area was mapped using Sakai smooth dual drum, Case/Ammann smooth drum, and Caterpillar padfoot IC rollers. Nominal machine settings used for mapping were as follows:

- Sakai: $a = 0.60$ mm, $f = 50$ Hz, $v = 5$ km/h
- Case/Ammann: Ecc. = 15%, $f = 27$Hz, $v = 4.2$ km/h
- Caterpillar: $a = 0.90$ mm, $f = 30$ Hz, $v = 4$ km/h

Following Sakai and Case/Ammann IC roller mapping passes, in-situ point-MVs (LWD, NG, PLT, and DCP) were performed at 39 test locations selected based on the IC-MV maps. Caterpillar padfoot IC roller mapping pass was performed following the in-situ point-MV testing.

Figure 31. TB4 compacted granular subgrade material

Test Results, Analysis, and Summary

IC-MV maps and DCP-CBR profiles at three selected locations are presented in Figure 32. Histogram plots of MDP_{40}, CMV, k_s, and CCV IC-MVs and corresponding semivariograms are presented in Figure 33. A summary of univariate and spatial statistics o f IC-MVs are provided in Table 7 and Table 8, respectively. A summary of univariate statistics of in-situ point-MVs are provided in Table 7. Correlations between IC-MVs and in-situ point-MVs are provided Figure 34 to Figure 37. Following are some key observations:

MDP_{40} measurements:

- On average, the MDP_{40} measurements on this test bed are about 1.4 times greater than on TB1 untreated granular base layer.
- MDP_{40} semivariograms indicate comparatively lower non-uniformity on this test bed (sill = 35) compared to on TB1untreated granular base ($sill_1 = 82$ and $sill_2 = 130$ for pass 1).
- Non-linear exponential relationships are observed in correlations between MDP_{40} and E_{LWD-Z3}, E_{V1}, E_{V2}, and CBR point-MVs. R^2 values for these relationships varied from 0.48 to 0.73. MDP_{40} values tend to reach an asymptotic value of 150, which is set as the maximum value in the AccuGrade software. Linear regression relationship is observed

42

between MDP_{40} and γ_d with relatively low R^2 value (0.32). No influence of w is observed in the relationships. It appears that the MDP measurement was not set to provide an adequate measurement range relative to the measurement range of plate load test modulus values.

CCV measurements:

- On average, the CCV measurements on this test bed are about 1.5 times greater than on TB1 untreated granular base layer.
- CCV semivariograms indicate comparatively higher non-uniformity on this test bed (sill = 20) compared to on TB1 untreated granular base (sill = 6).
- Linear regression relationships with right trends are observed in correlations between CCV and E_{LWD-Z3}, E_{V1}, E_{V2}, and CBR point-MVs. Relationship with E_{V1} showed R^2 = 0.66, while relationship with E_{LWD-Z3}, E_{V2}, and CBR showed R^2 values in the range of 0.21 to 0.31. No trend is observed in relationship with γ_d. No influence of w is observed in the relationships.

CMV measurements:

- On average, the CMV measurements on this test bed are about 3.6 times greater than on TB1 untreated granular base layer.
- CMV semivariograms indicate comparatively greater non-uniformity on this test bed (sill = 50) compared to on TB1 untreated granular base (sill = 5). This finding is similar to that of CCV semivariogram.
- Linear regression relationships are observed in correlations between CMV and E_{LWD-Z3}, E_{V1}, E_{V2}, γ_d, and CBR point-MVs. Relationships with E_{V1} and CBR showed $R^2 > 0.50$, while relationship with other point-MVs showed $R^2 < 0.20$. No influence of w is observed in the relationships.

k_s measurements:

- Linear regression relationships are observed in correlations between k_s and E_{LWD-Z3}, E_{V1}, E_{V2}, γ_d, and CBR point-MVs. Relationships with E_{V1} and E_{LWD-Z3} showed R^2 = 0.61 and 0.40, respectively, while relationship with other point-MVs showed $R^2 < 0.30$. No influence of w is observed in the relationships.
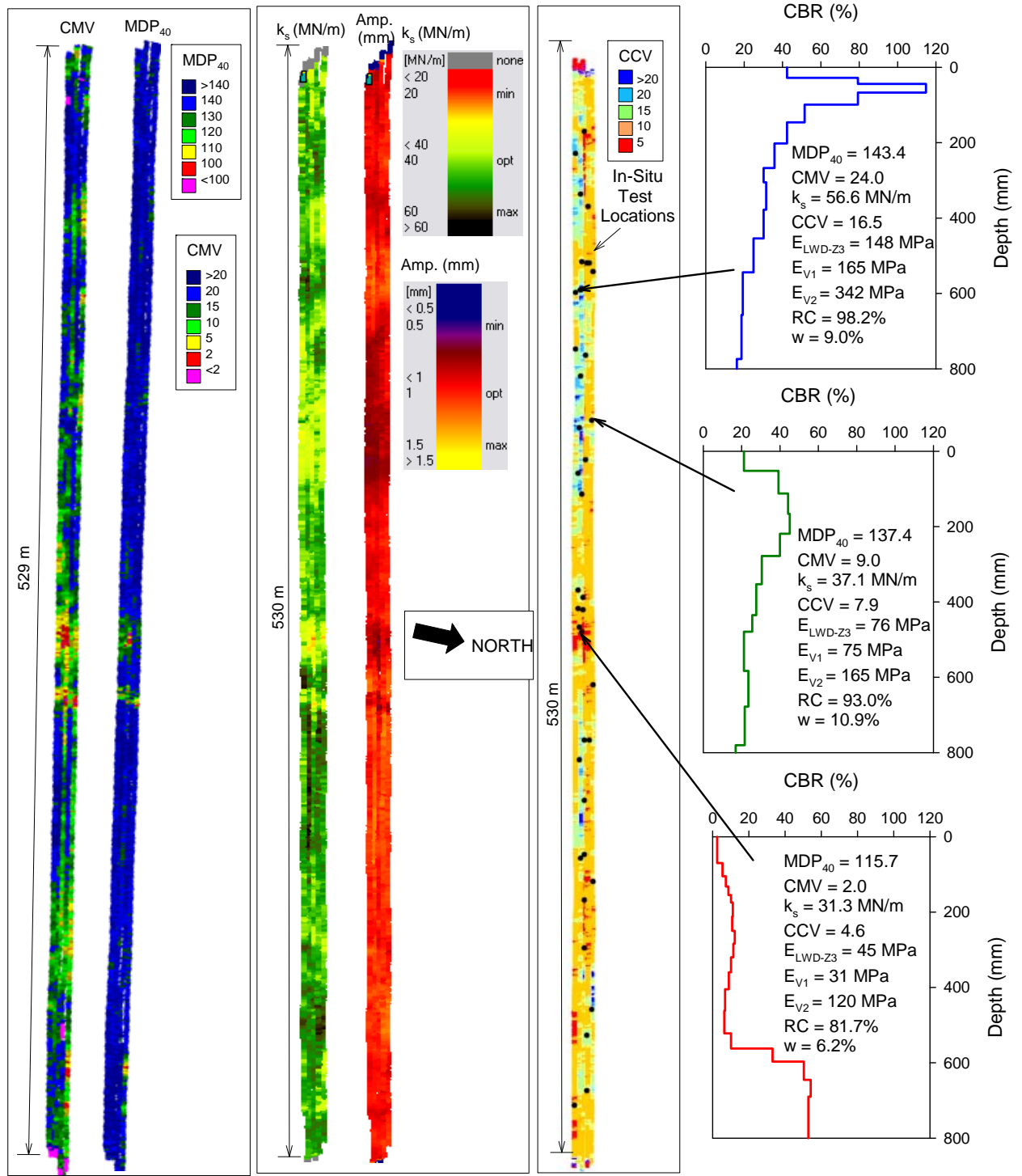
Figure 32. CMV, MDP$_{40}$, k$_s$ (and a^*), and CCV maps on TB4 compacted granular subgrade material along with DCP-CBR profiles at three selected locations
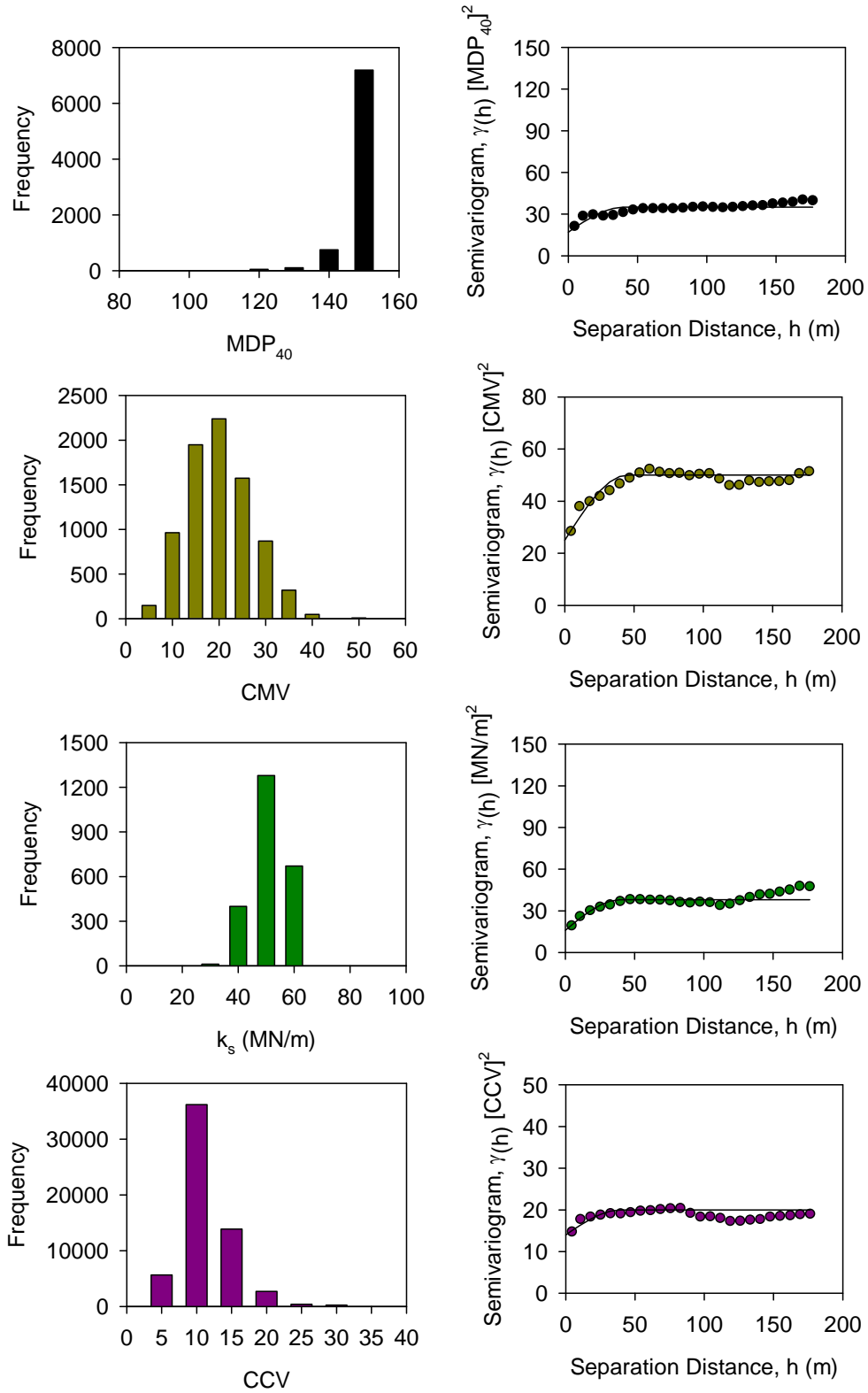
Figure 33. Histogram and semivariogram plots of CMV, MDP$_{40}$, k$_s$ and CCV measurements – TB4 compacted granular subgrade material

Table 7. Summary of univariate statistics – TB4 granular subgrade material

MV	n	μ	σ	COV (%)
CMV	8125	18.2	7.0	39
MDP_{40}	8125	144.8	5.8	4
k_s (MN/m)	2366	46.2	6.2	13
CCV	59405	9.0	4.4	49
γ_d (kN/m^3)	39	17.69	0.73	4
RC (%)	39	92.9	3.8	4
w (%)	39	9.1	1.8	20
E_{LWD-Z3} (MPa)	35	103	36	34
E_{V1} (MPa)	36	121	49	41
E_{V2} (MPa)	36	305	162	53
CBR_{200} (%)	39	66	42	63

Table 8. Summary of spatial statistics – TB4 granular subgrade material

MV	Nugget	Sill	Range
CMV	25	50	45
MDP_{40}	17	35	40
k_s	16	38	40
CCV	14	20	40
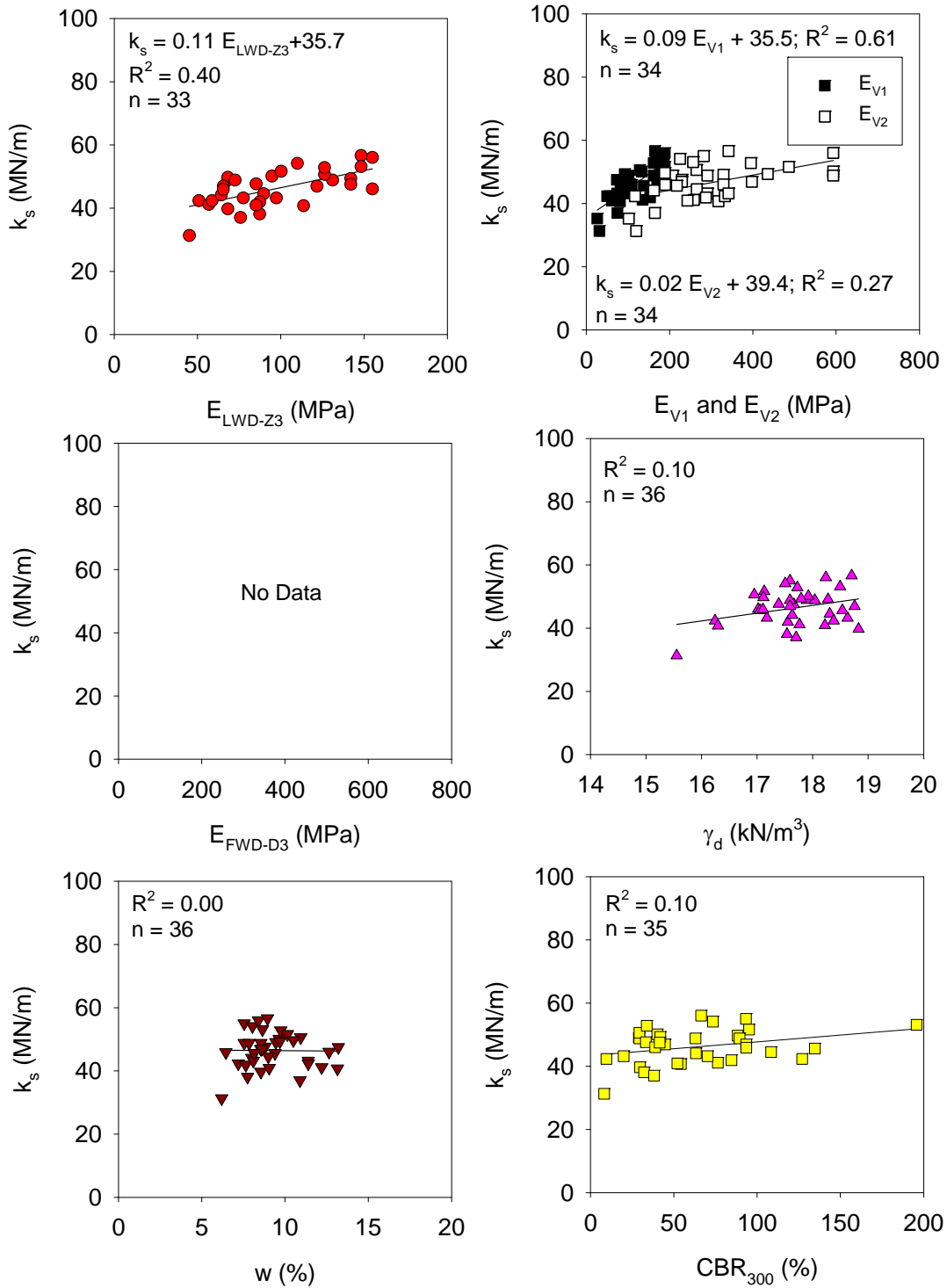
Figure 34. Regression analyses between k_s and in-situ point measurements – TB4 granular subgrade material
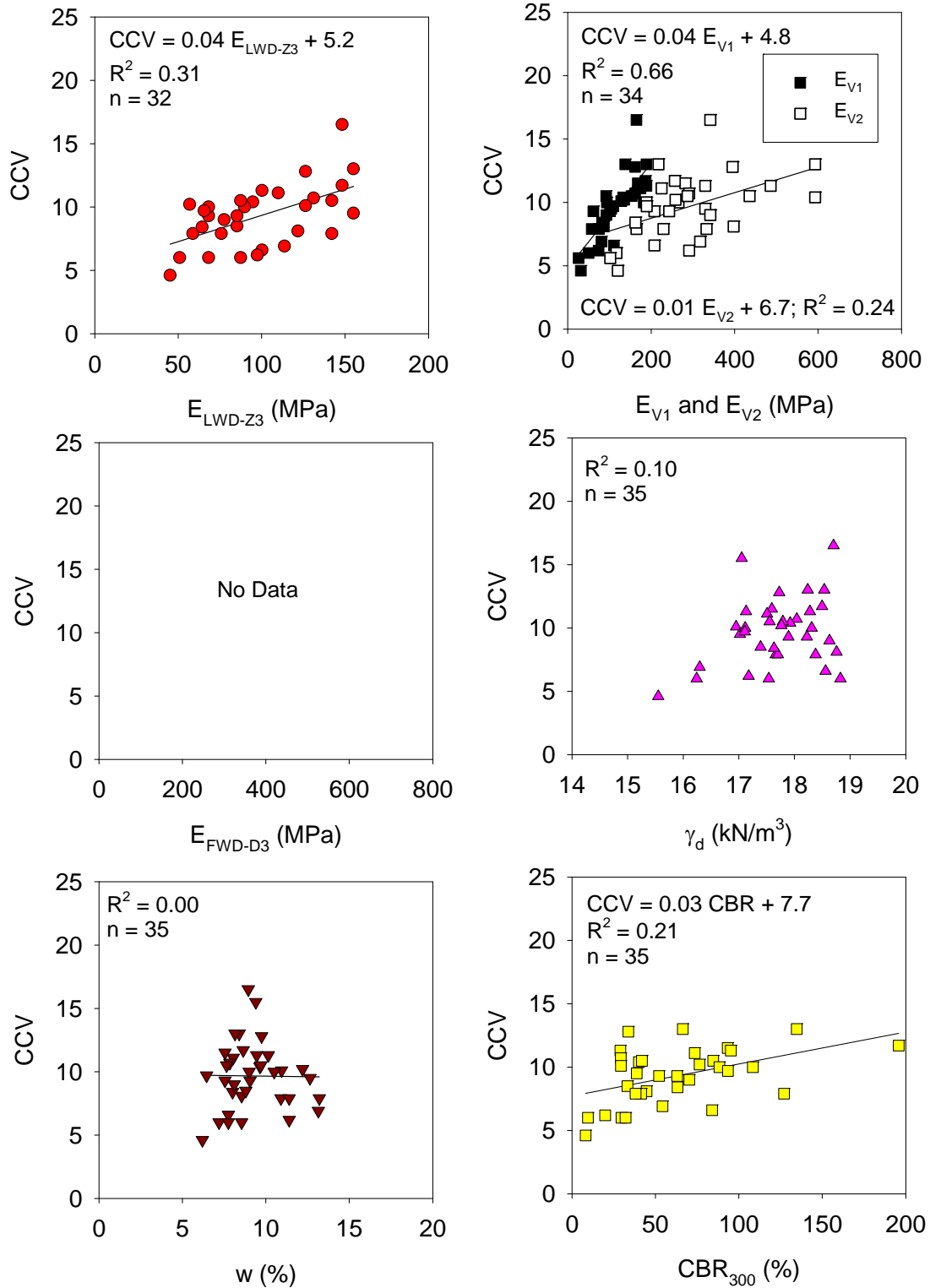
Figure 35. Regression analyses between CCV and in-situ point measurements – TB4 granular subgrade material

Figure 36. Regression analyses between MDP$_{40}$ and in-situ point measurements – TB4 granular subgrade material

Figure 37. Regression analyses between CMV and in-situ point measurements – TB4 granular subgrade material

TBs 5, 6, and 9 Treated Subgrade Material

Test Bed Construction and IC-MV Mapping

TBs 5 and 6 involved cement treatment of a portion of the TB4 granular subgrade material with 5.5% (of dry weight of soil) of cement. Photographs taken during the construction process are provided in Figure 38 and Figure 39. TB5 was compacted 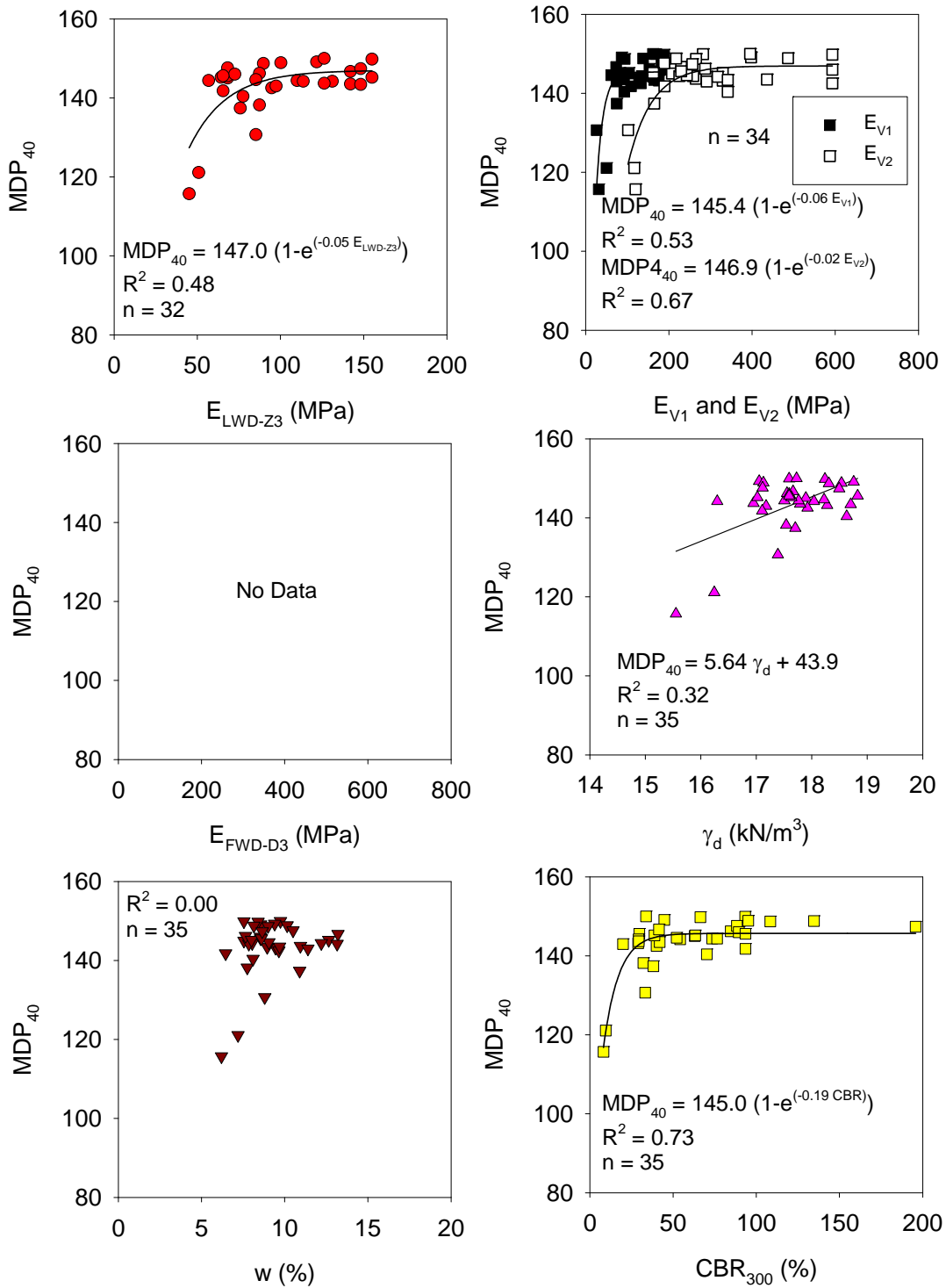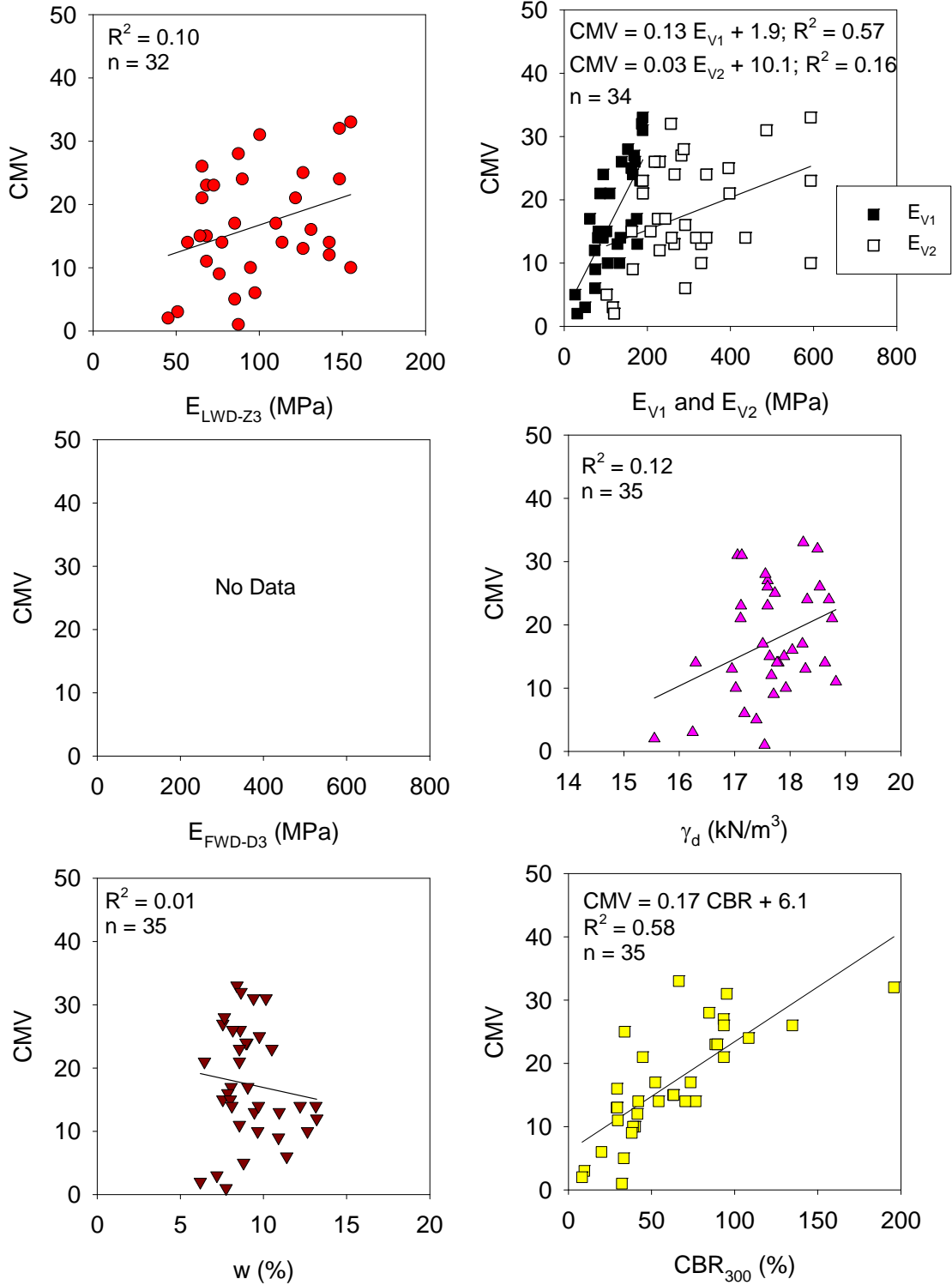by the ISU research team and the contractor, while TB6 was compacted solely by the contractor. The construction sequence followed in these test beds was similar to that of TB3 construction. Following is the construction sequence with time log from field observations on TB5:

a) scarified the subgrade layer to about 150 mm depth and moisture-conditioning he material to a target $w = 10\%$ [prior to 6:30 am],
b) spreaded stabilizer on the scarified test bed [6:45 to 7:45 am],
c) prepared the soil-cement mixture using a rotary mixer (with two passes) [7:45 to 8:15 am],
d) compacted the area using a padfoot roller for one static pass and moisture-conditioning the soil-cement mixture with a water truck [8:20 to 8:50 am] (in-situ sample was obtained for laboratory Proctor test at 8:30 am),
e) compacted the area using padfoot roller for 4 to 6 passes [8:55 to 10:15 am],
f) compacted the area using vibratory smooth drum roller for 4 passes [10:15 to 10:45 am],
g) trimmed the subgrade to desired elevation using motor grader [10:30 to 10:45 am],
h) in-situ density testing at 7 random test locations [10:30 to 11:00 am]
i) performed final compaction passes using pneumatic rubber tire roller [10:45 to 11:05 am].
j) performed in-situ point-MV testing at 7 random test locations [11:10 to 11:20 am]
k) obtained Case/Ammann IC roller map (one pass) [11:10 to 11:40 am]
l) performed in-situ point-MV testing (LWD, FWD, NG, PLT, and DCP) on the final compacted surface from 20 test locations selected based on the IC-MV map [1:15 to 2:25 pm]

On TB5, roller measurements were recorded during Caterpillar padfoot IC roller compaction. Three roller lanes on TB5 were compacted in static mode while the other three lanes were compacted in vibratory mode (low amplitude setting: $a = 0.90$ mm and $f = 30$ Hz). Case/Ammann IC-MV roller mapping was obtained using Ecc = 15%, $f = 27$ Hz, and $v = 4.2$ km/h nominal settings. Two days after treatment, the area was again mapped (referred to as TB9) using the Case/Ammann IC roller in manual and AFC mode settings. For manual mode, the nominal settings used during mapping were Ecc. = 15%, $f = 27$Hz, and $v = 4.2$ km/h. For AFC mode, a high performance level with nominal $v = 4.2$ km/h was used for mapping. Point MVs (FWD, LWD, NG, PLT, and DCP) were obtained after the mapping operations. Tests were performed at 20 test locations (same locations as TBs 5 and 6).

51

Placement of cement stabilizer on moisture-conditioned subgrade

Soil-cement mixing using rotary mixer

Compaction using Caterpillar padfoot IC roller

Moisture-conditioning after first compaction pass with padfoot roller

Compaction using Sakai smooth drum roller

Trimming process using motor grader

Figure 38. Pictures showing construction process on TBs 5/6 treated subgrade

Compaction using Caterpillar padfoot roller

Final compaction using Caterpillar pneumatic rubber tire roller

Final compacted stabilized subgrade – TBs 5/6

Figure 39. Pictures showing construction process and final compacted surface on TBs 5/6 treated subgrade

Test Results and Analysis

MDP_{40} and CMV IC-MV maps from compaction roller passes are presented in Figure 40. Box plots showing the range of data for each compaction pass is presented in Figure 41. Results indicate that on average MDP_{40} in static mode increased from about 115.8 to 130.5 while in vibratory low amplitude setting increased from about 111.6 to 122.4, from pass 1 to 5. No significant change in CMV was observed from pass 1 to 5 (average CMV = 4.9 to 5.5).

In-situ density measurements taken during compaction at various times after mixing are plotted in comparison with laboratory density relationship with time delay in Figure 42. Results indicate that on average the density measurements generally increased with increasing compaction effort but did not achieve the 95% RC required by the specifications.

k_s IC-MV, a^*, and f maps from TBs 5 and 6 (in manual mode), and TB8 (in manual and AFC modes) are presented in Figure 43. Histogram plots of k_s IC-MVs and in-situ point-MVs on TBs 5 and 6, and TB9 showing comparison between measurements obtained shortly after compaction and after 2-day cure are presented in Figure 44. Same results are presented as box plots in Figure 45. A summary of univariate statistics of k_s IC-MVs and in-situ point-MVs from TBs 5, 6, and 9

53

is provided in Table 9. Results indicate that on average the k_s IC-MV increased by about 18% after the 2-day curing period. CBR, E_{LWD-Z3}, E_{FWD-D3}, E_{V1}, and E_{V2} point-MVs showed a small increase or a decrease (-11% to +11%) on TB9 compared to TB5. Moisture content of the material increased on average from about 10.6% to 13.7%, and as a result the average RC of the material decreased slightly from 89 to 87%. Note that all in-situ point-MVs were obtained after roller mapping passes. Similar to observations on TBs 2 and 8, cracks were observed on TB9 following the vibratory roller passes which likely lowered the strength/stiffness at the surface of the treated subgrade layer.

Semivariograms of k_s IC-MVs obtained from TBs 5 and 6 in manual mode and from TB9 in manual and AFC modes are presented in Figure 46. Similar to findings from cement treated base layer test beds (TBs 3 and 8), semivariogram plots for k_s IC-MVs indicated greater non-uniformity in k_s IC-MVs after two days of curing (TB9) compared to shortly after compaction (TBs 5 and 6). As noted in TBs 3 and 8, this increased non-uniformity is likely caused because of various factors as non-uniform application of cement, water content, compaction delay time, and compaction energy across the test bed area.

Correlations between k_s IC-MVs obtained in manual mode and point-MVs from TB 5 and TB9 are presented in Figure 47 and Figure 48, respectively. Regressions on TB5 with E_{LWD-Z3}, E_{V1}, E_{FWD-D3}, and CBR showed good correlations with $R^2 > 0.50$, while with E_{V2}, γ_d and w showed weak correlations with $R^2 < 0.30$. Regressions on TB9 showed relatively weak correlations with all in-situ point-MVs ($R^2 < 0.5$), which is likely due to cracks observed on the treated surface following the mapping passes.

Figure 43 compares k_s IC-MV, a^*, and f maps obtained in manual and AFC modes on TB9. The k_s measurements varied from 17 to 60 MN/m, the a^* measurements varied from 0.5 to 3.0 mm, and the f measurements varied from 20 to 35 Hz. Analysis of k_s, a^*, and f results indicated that the vibration amplitude was decreased and the excitation frequency was increased with increase in k_s. Comparison between k_s and a^*, and k_s and f for different response distances (i.e., 0, 1, 2, and 3 m) indicated that the response distance for altering the amplitude and frequency was in the range of 1 to 2 m (for variation in $v = 4.1$ to 4.5 km/h) (note that the roller data was reported approximately every 1 m).

k_s IC-MV maps for TB4 subgrade material (untreated), TBs 5 and 6 treated subgrade material (shortly after treatment), and TB9 treated subgrade material (after 2-days curing), for the same spatial area is presented in Figure 49. Semivariograms of k_s IC-MVs for these test beds are presented in Figure 50, which indicates that the spatial non-uniformity was greater after 2-day curing on the treated subgrade layer compared to on subgrade layer before treatment and shortly after treatment.
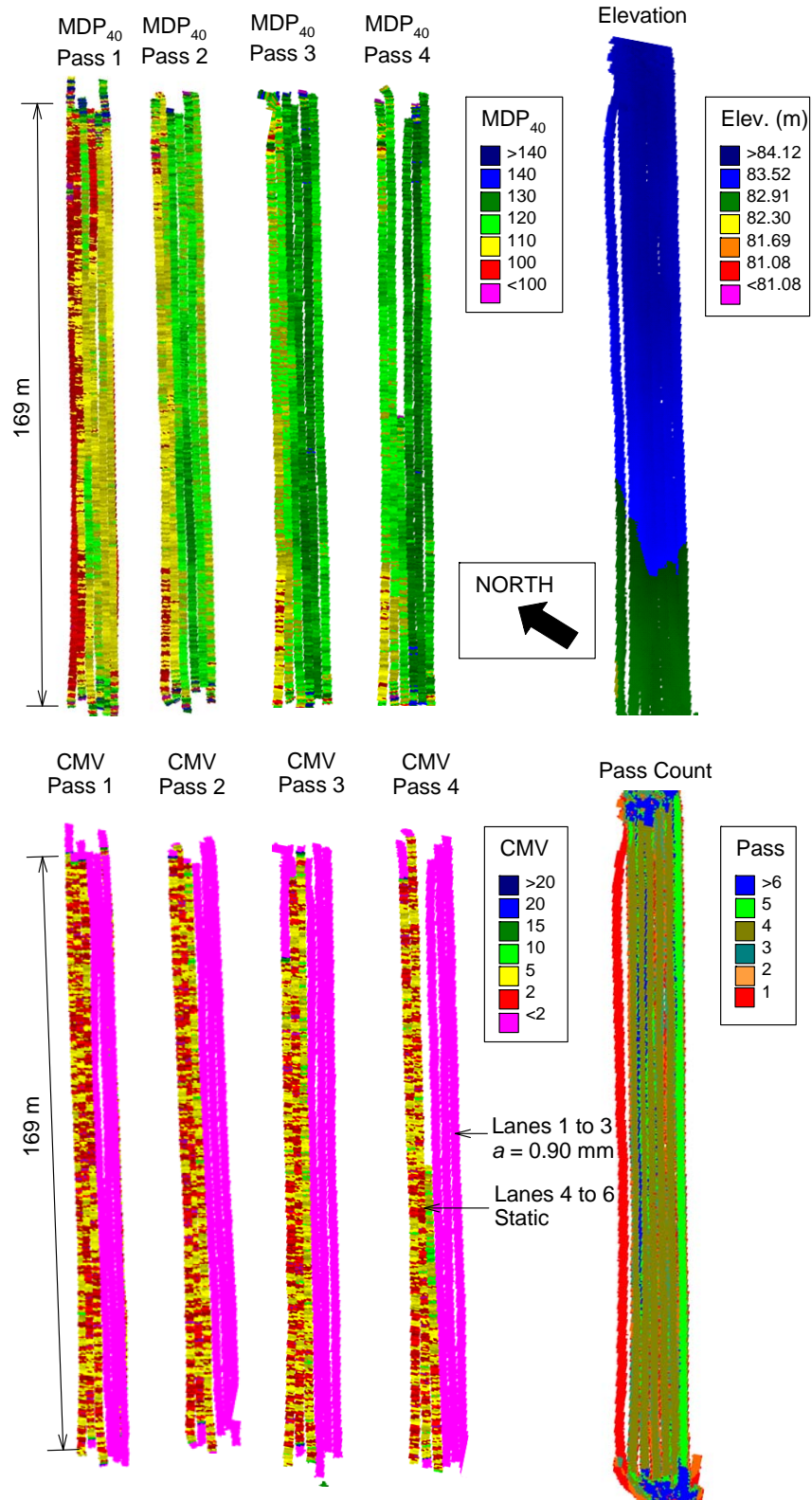
Figure 40. MDP₄₀ and CMV maps for passes 1 to 4, and elevation and number of roller passes maps – TB5 treated subgrade material (*a* = 0.90 mm, *f* = 30 Hz, and *v* = 4 km/h nominal settings)

55
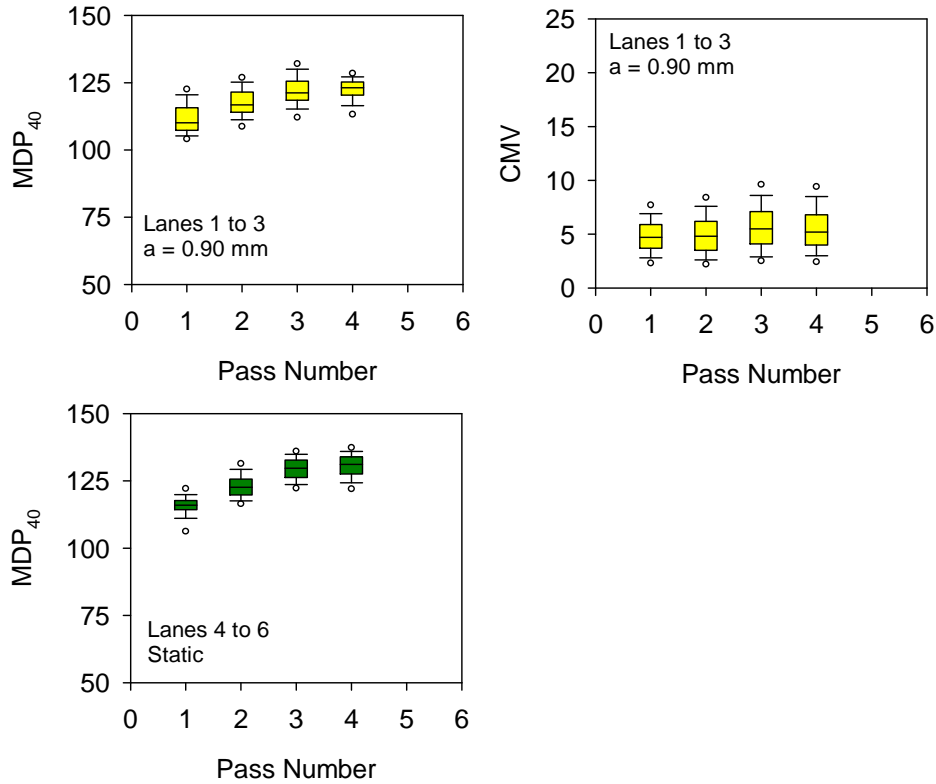
Figure 41. Boxplots of MDP$_{40}$ and CMV measurements for passes 1 to 4 – TB5 treated subgrade material
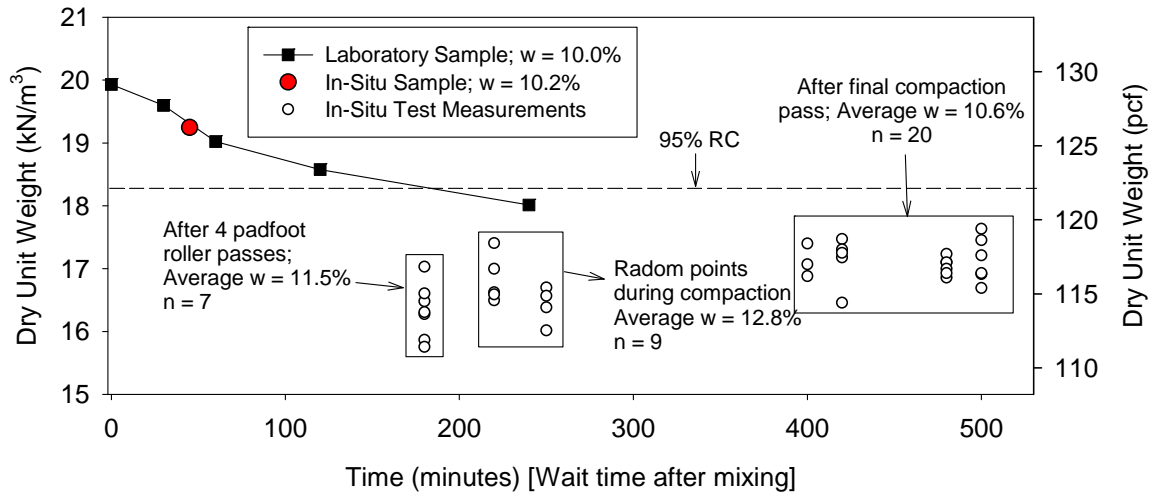
Figure 42. In-situ density test measurements during compaction in comparison with laboratory density measurements – TB5 treated subgrade material
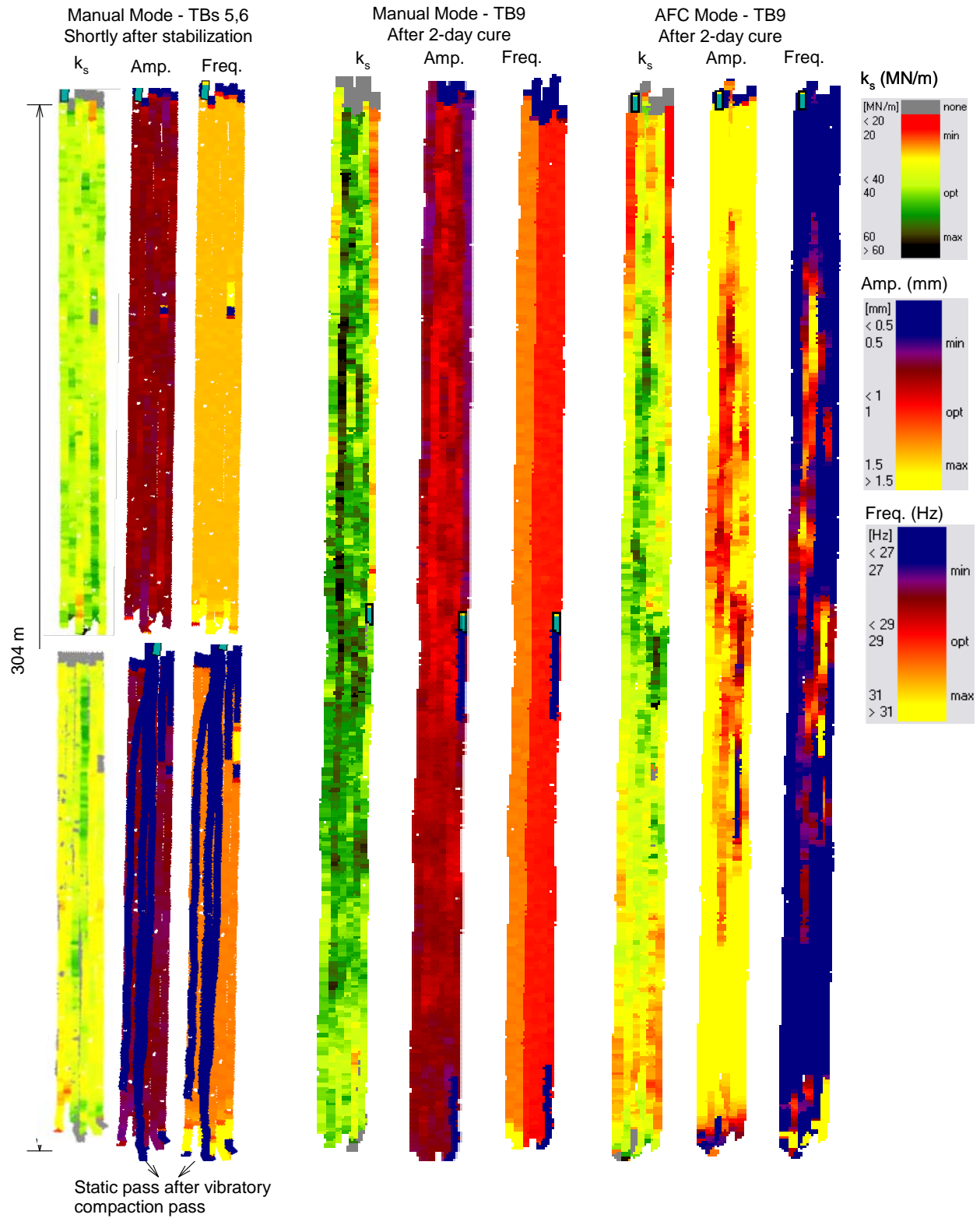
Figure 43. Comparison of k$_s$, a^*, and f maps obtained shortly after compaction (TB5/6) and after 2-day cure in manual and AFC modes (TB9)

Figure 44. Histogram plots comparing measurements obtained shortly after compaction (TB5/6) and after 2-days curing (TB9)

58
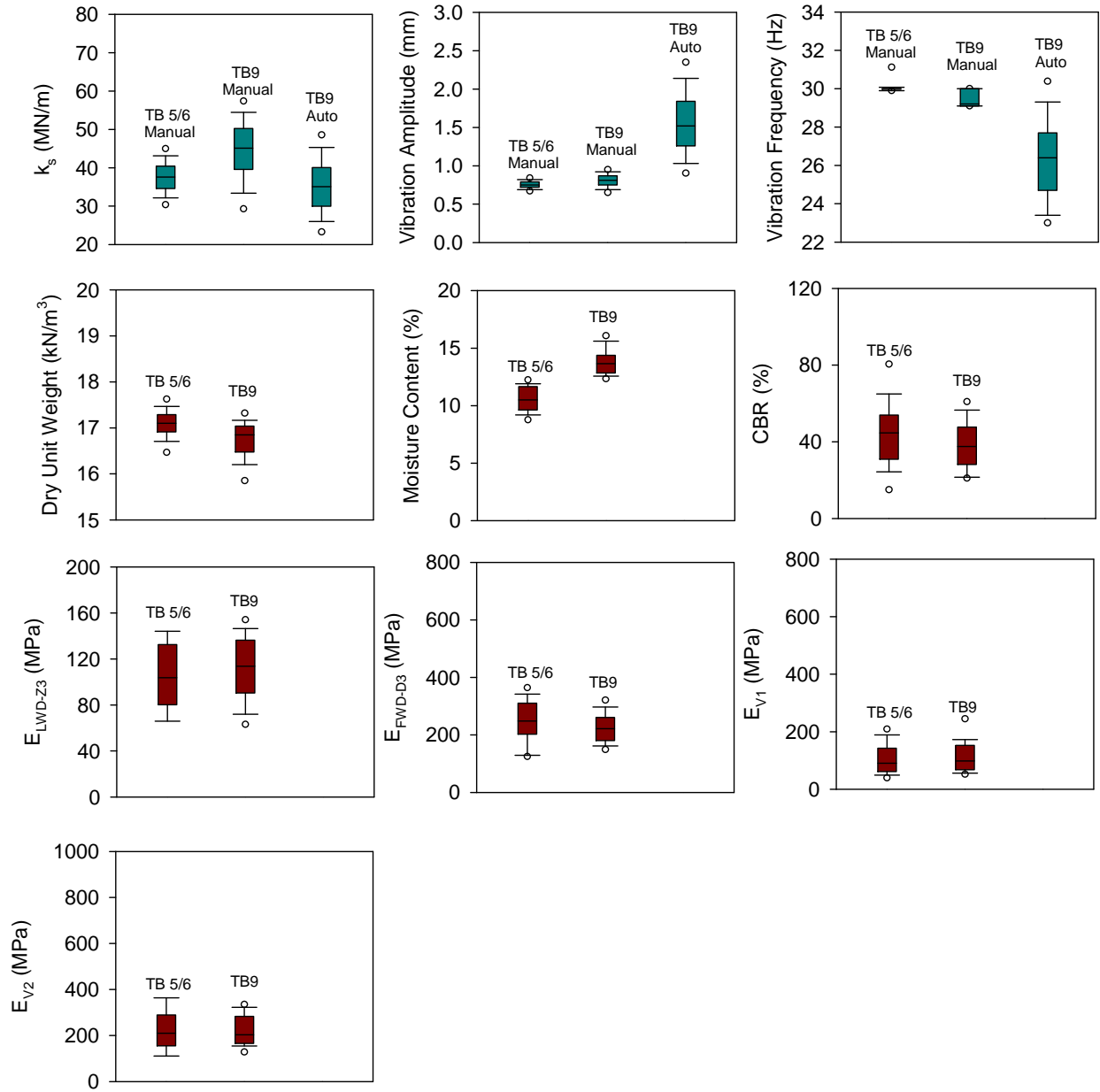
Figure 45. Box plots comparing measurements obtained shortly after compaction (TB5/6) and after 2-days curing (TB9)

Table 9. Summary of univariate statistics – TBs 5/9 treated base material

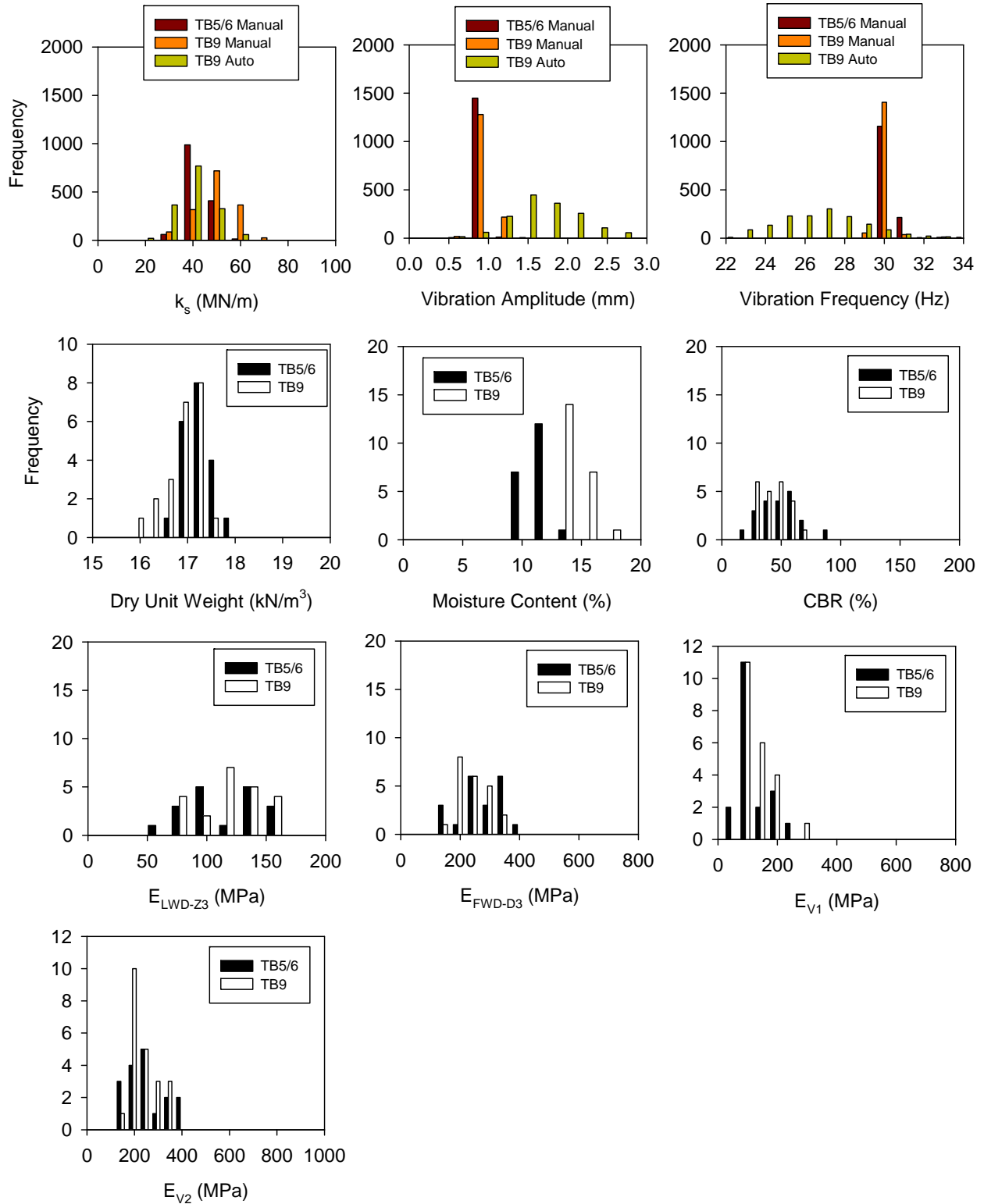| TB	MV	n	Univariate Statistics		
			μ	σ	COV (%)
TB5	k_s (MN/m)	1472	38	5	12
	$a*$ (mm)	1472	0.76	0.07	9
	f (Hz)	1472	30	1	3
	γ_d (kN/m^3)	20	17.10	0.28	2
	RC (%)	20	88.7	1.5	2
	w (%)	20	10.6	1.1	10
	E_{LWD-Z3} (MPa)	18	106	31	29
	E_{V1} (MPa)	19	102	50	49
	E_{V2} (MPa)	17	220	84	38
	E_{FWD-D3} (MPa)	20	249	73	29
	CBR (%)	20	44	16	37
TB9	k_s (MN/m) [manual]	1514	45	8	18
	$a*$ (mm) [manual]	1514	0.81	0.09	11
	f (Hz) [manual]	1514	29	1	2
	k_s (MN/m) [AFC]	1534	35	8	21
	$a*$ (mm) [AFC]	1534	1.56	0.44	28
	f (Hz) [AFC]	1534	26	2	9
	γ_d (kN/m^3)	20	16.85	0.30	2
	RC (%)	20	87.4	1.60	2
	w (%)	20	13.7	1.11	8
	E_{LWD-Z3} (MPa)	20	112	26	23
	E_{V1} (MPa)	20	113	54	48
	E_{V2} (MPa)	20	219	65	30
	E_{FWD-D3} (MPa)	20	223	50	23
	CBR (%)	20	39	12	31

Note: Nominal v = 4.2 km/h during roller operation
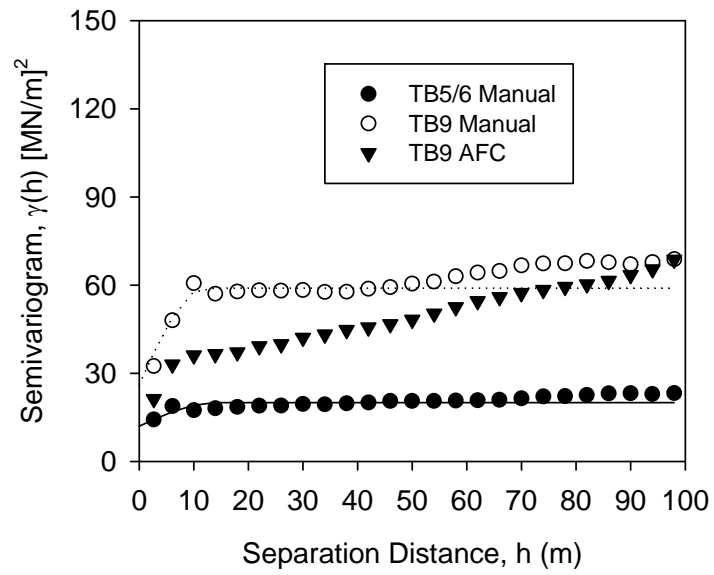
Figure 46. Semivariograms of k_s measurements obtained on TB5 in manual mode, TB9 in manual mode, and TB9 in AFC mode
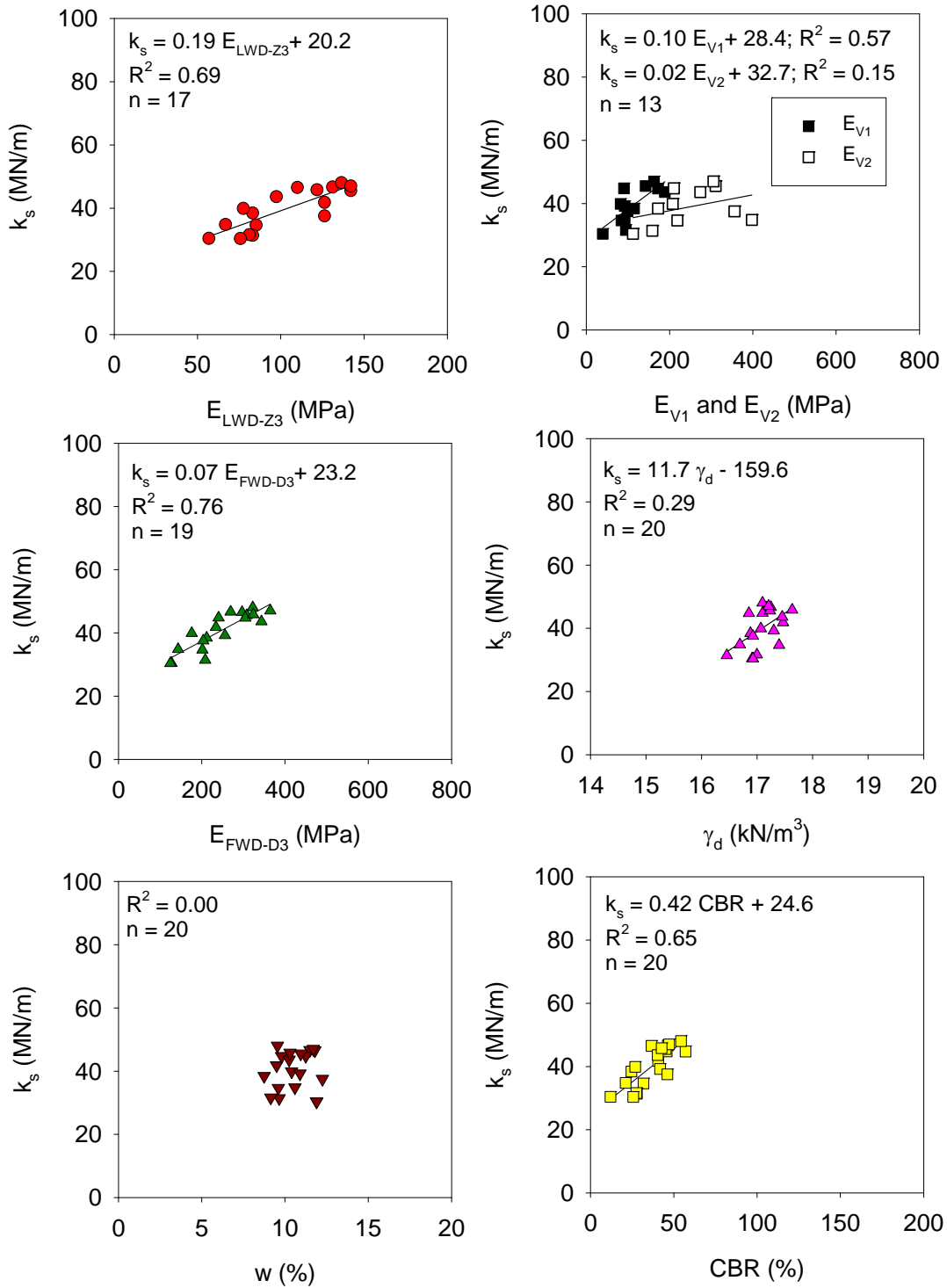
Figure 47. Regression analyses between k_s and in-situ point measurements – TB5 treated subgrade material (shortly after compaction; manual mode)
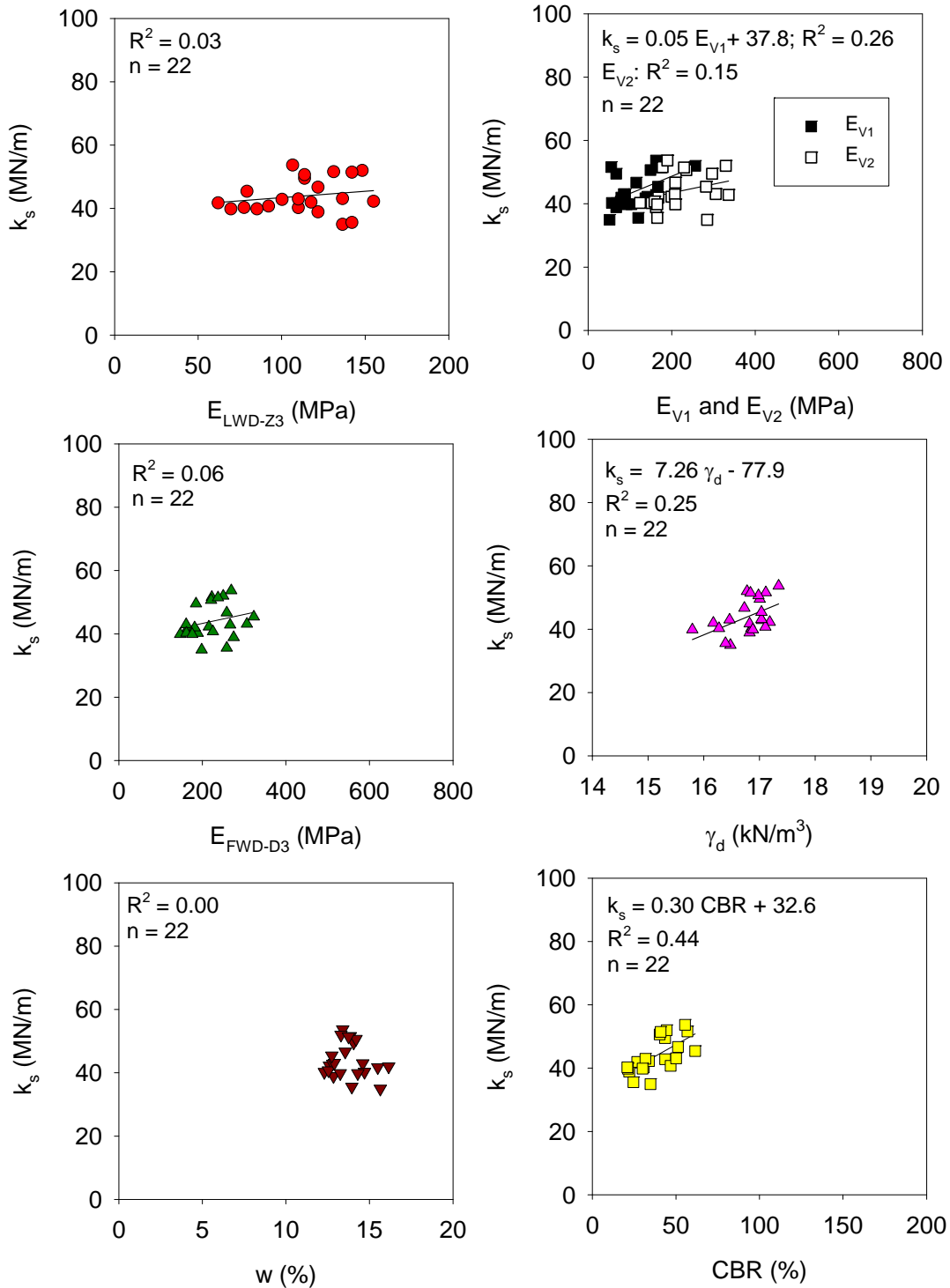
Figure 48. Regression analyses between k_s and in-situ point measurements – TB9 treated subgrade material (after 2-day cure; manual mode)
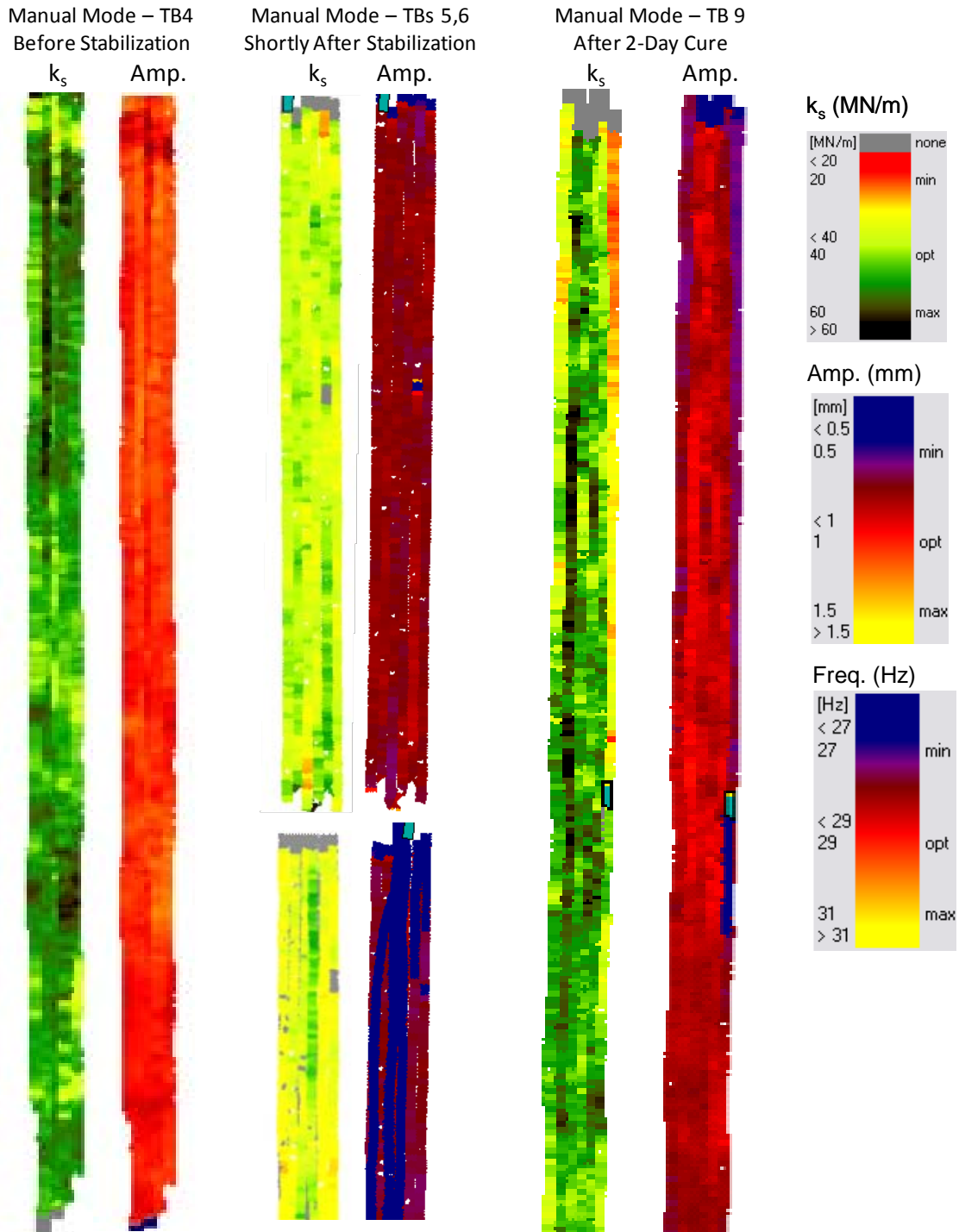
Figure 49. Comparison of ks and *a** maps obtained in manual mode on granular subgrade material before stabilization (TB4), shortly after stabilization (TB5/6), and 2-days after stabilization (TB9)

Figure 50. Comparison of semivariograms of k_s measurements obtained in manual mode on granular subgrade material before stabilization (TB4), shortly after stabilization (TB5/6), and 2-days after stabilization (TB9)

Summary

TBs 5 and 6 consisted of construction of a nominal 150 mm thick cement-treated base layer. TB5 was compacted by the ISU research team and the contractor, and TB6 was compacted solely by the contractor. MDP_{40} IC-MVs were obtained during padfoot roller compaction passes on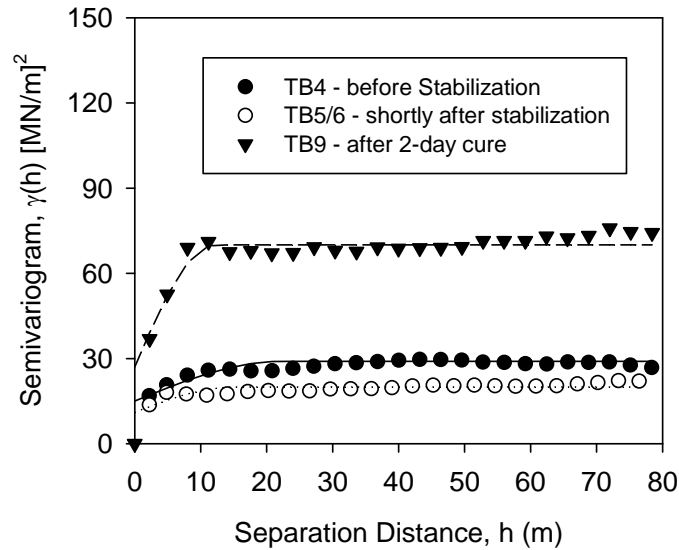 TB5, k_s IC-MVs along with in-situ point-MVs (E_{LWD-Z3}, E_{V1}, E_{V2}, E_{FWD-D3}, w, γ_d, and CBR) were obtained from TBs 5 and 6 shortly after treatment. TB9 involved obtaining k_s IC-MVs after 2 days of curing along with in-situ point-MVs (E_{LWD-Z3}, E_{V1}, E_{V2}, E_{FWD-D3}, w, γ_d, and CBR). Data analysis for TBs 5, 6, and 9 comprised of geostatistical analysis of the spatially referenced k_s IC-MV data and regression analysis between IC-MVs and in-situ point-MVs by spatially pairing the nearest point data. Following is a summary of key findings from these analyses:

- During initial compaction on TB5, results indicate that on average MDP_{40} in static mode increased from about 115.8 to 130.5, while in vibratory low amplitude setting increased from about 111.6 to 122.4, from pass 1 to 5. No significant change in CMV was observed from pass 1 to 5 (average CMV = 4.9 to 5.5).
- As expected, the k_s IC-MVs improved after 2 days of curing. Results indicated that on average the k_s IC-MV increased by about 18% after 2 days of curing.
- E_{LWD-Z3}, E_{FWD-D3}, E_{V1}, E_{V2}, and CBR point-MVs showed a small increase or a decrease (-11% to +11%) on TB9 compared to TB5. Note that the in-situ point-MVs were obtained after roller mapping passes, and the surface cracks observed after vibratory rolling is attributed to lowering the strength/stiffness of the treated subgrade layer. Moisture content of the material increased on average from about 10.6% to 13.7%, and as a result the average RC of the material decreased slightly from 89 to 87%.

65

- k_s IC-MVs showed greater non-uniformity on TB9 than on TBs 5 and 6. This is an important finding to note and has not been well documented in the literature. The reasons for this increased non-uniformity after curing are attributed to non-uniform application of cement, water content, mixing process, compaction delay time, and compaction energy across the test bed area.
- Regressions on TB5 with E_{LWD-Z3}, E_{V1}, E_{FWD-D3}, and CBR showed good correlations with $R^2 > 0.50$, while with E_{V2}, γ_d and w showed weak correlations with $R^2 < 0.30$. Regressions on TB9 showed relatively weak correlations with all in-situ point-MVs ($R^2 < 0.5$), which is likely due to cracks observed on the treated surface following the mapping passes.
- AFC operations on TB9 indicated that the vibration amplitude was reduced and the excitation frequency was increased with increase in k_s measurement values and the response distance for altering the amplitude and frequency was about 1 to 2 m (for variation in $v = 4.1$ to 4. 5 km/h)

TB7 Granular Subgrade Material (Untreated)

Test Bed Conditions, IC-MV Mapping, and Point-MV Testing

The test bed consisted of compacted existing granular subgrade material (untreated) over a length of about 110 m. The subgrade material was variable across the test bed with a portion containing white subgrade sand and a portion containing red subgrade sand (Figure 51). Laboratory gradation analysis results (Table 3) indicated that the white subgrade sand material (classified as SP-SM according to USCS) contained about 8% of fines while the red subgrade sand material (classified as SM according to USCS) contained about 37% fines passing the #200 sieve. The portion of the test bed with white sand was unstable under construction traffic (see Figure 51) due to relatively low shear strength in the material from lack of fines. The area was mapped in three roller lanes with Case/Ammann smooth drum roller for one pass each in manual mode (Ecc. = 15%, $f = 27$Hz, and $v = 4.2$ km/h) and in AFC mode (medium performance level, and $v = 3.2$ km/h) settings, and Caterpillar padfoot roller for one roller pass ($a = 0.90$ mm, $f = 30$ Hz, and $v = 4$ km/h). In-situ point-MVs (LWD, NG, PLT, and DCP) were obtained at 10 test locations along one roller lane.
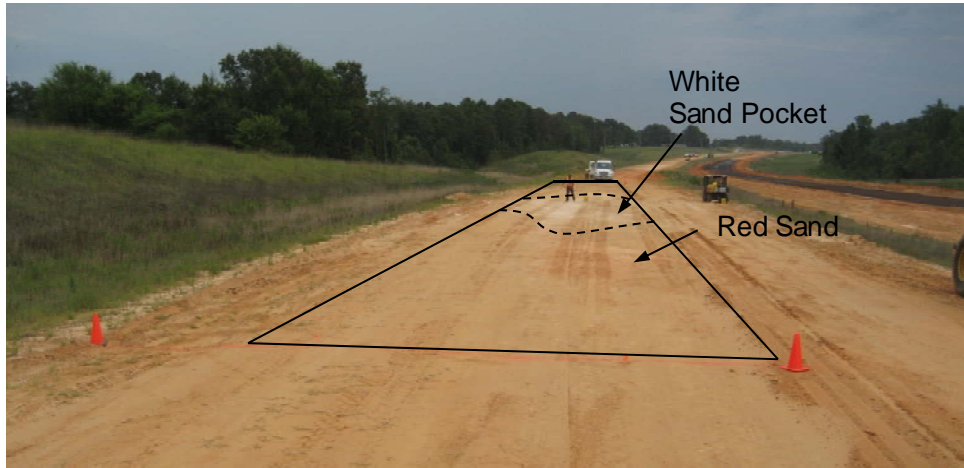
Figure 51. TB7 granular subgrade material (red sand subgrade with isolated white sand pocket)

Test Results and Analysis

IC-MV maps, linear plots along one roller lane, and DCP-CBR profiles at six selected locations along the test bed are presented in Figure 52. Comparison between MDP_{40}, CMV, and k_s IC-MVs and in-situ point-MVs are presented in Figure 53, Figure 54, and Figure 55, respectively. Results indicate that in-situ point-MVs and IC-MVs track well together with relatively soft conditions in the area with white subgrade sand material compared to the area with red subgrade sand material.

Correlations between MDP_{40}, CMV, and k_s IC-MVs and in-situ point-MVs are presented in Figure 56, Figure 57, and Figure 58, respectively. Due to the wide range of measurements, regression relationships showed good correlations with $R^2 > 0.70$ for this test bed.

Figure 59 shows comparison between k_s and *a** measurements obtained in manual and AFC modes in all three roller lanes. During AFC mode operation, the k_s measurements varied from 15 to 50 MN/m and the *a** measurements varied from 0.4 to 1.8 mm. The *f* measurements remained relatively constant at about 30 Hz. Analysis of k_s and a* measurements indicate that the *a** is reduced with increase in k_s. Comparison between k_s and *a** for different response distances (i.e., 0, 1, 2, and 3 m) indicated that the response distance for altering the amplitude and frequency was in the range of 1 to 2 m (for variation in *v* = 3.8 to 4.2 km/h) (note that the roller data was reported approximately every 1 m).
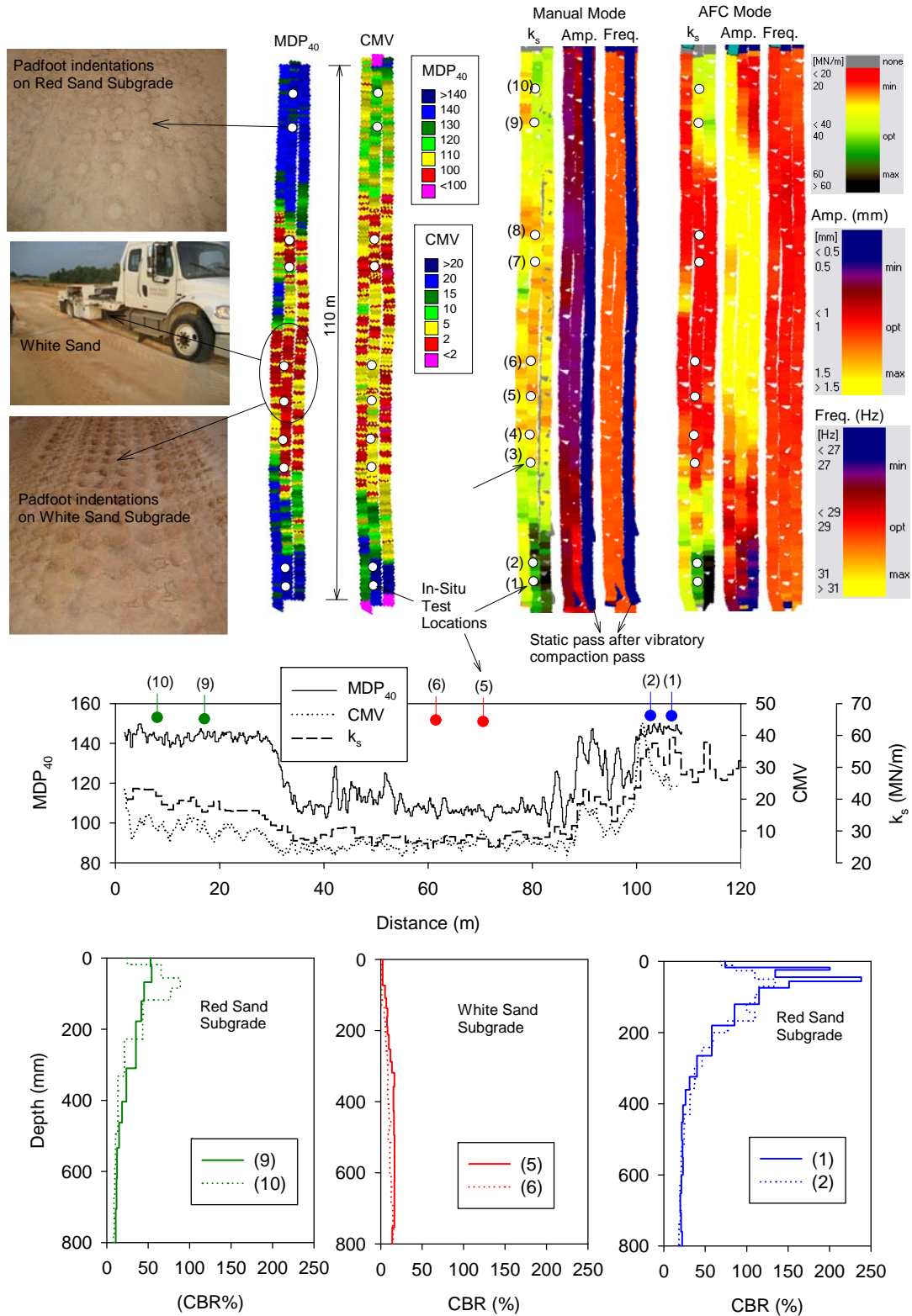
Figure 52. Roller spatial maps, MDP$_{40}$, CMV, and k$_s$ measurements along the middle lane, and DCP-CBR profiles at selected locations – TB7 granular subgrade material
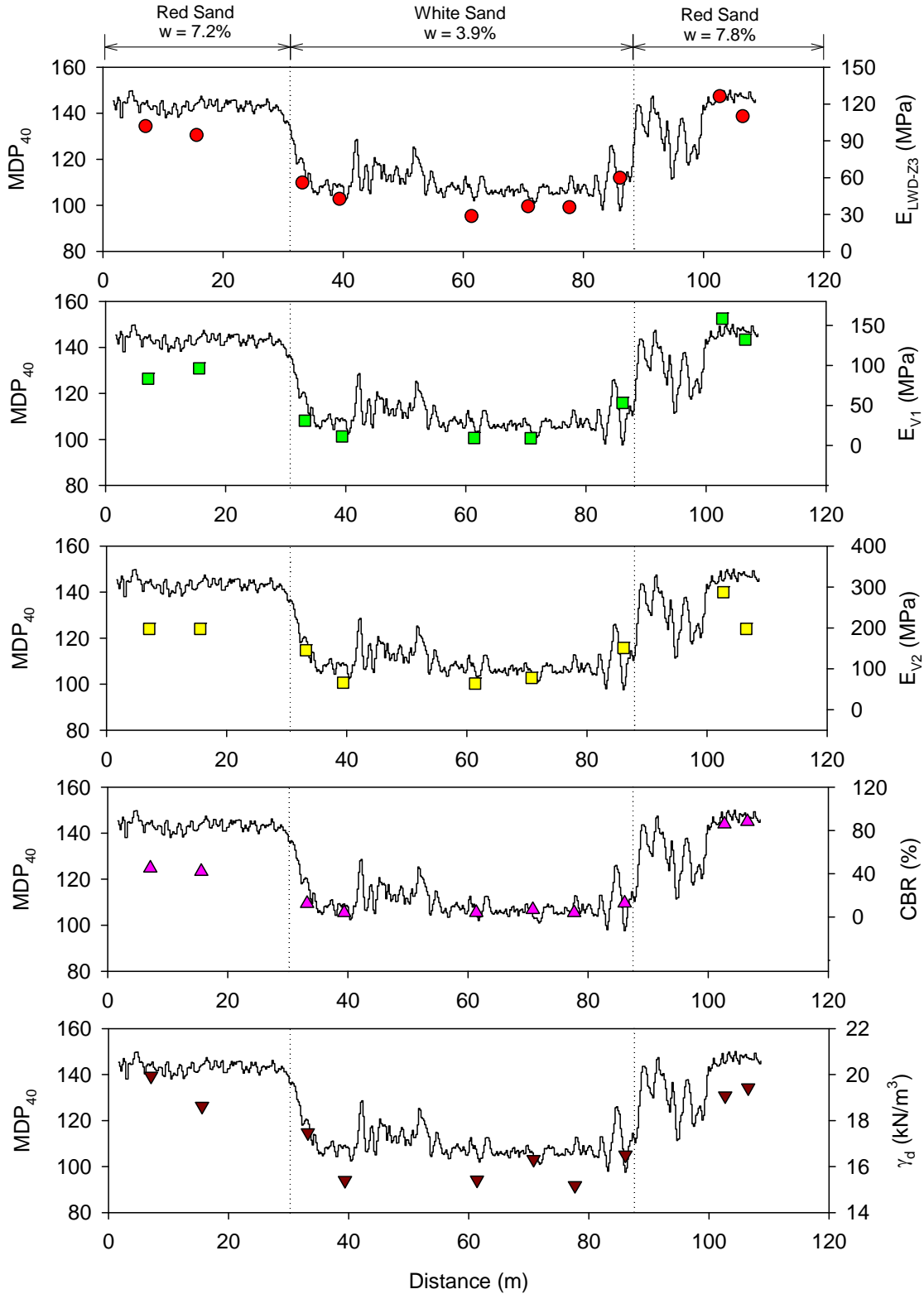
Figure 53. Comparison between MDP₄₀ and in-situ point measurements – TB7 granular subrade material

70
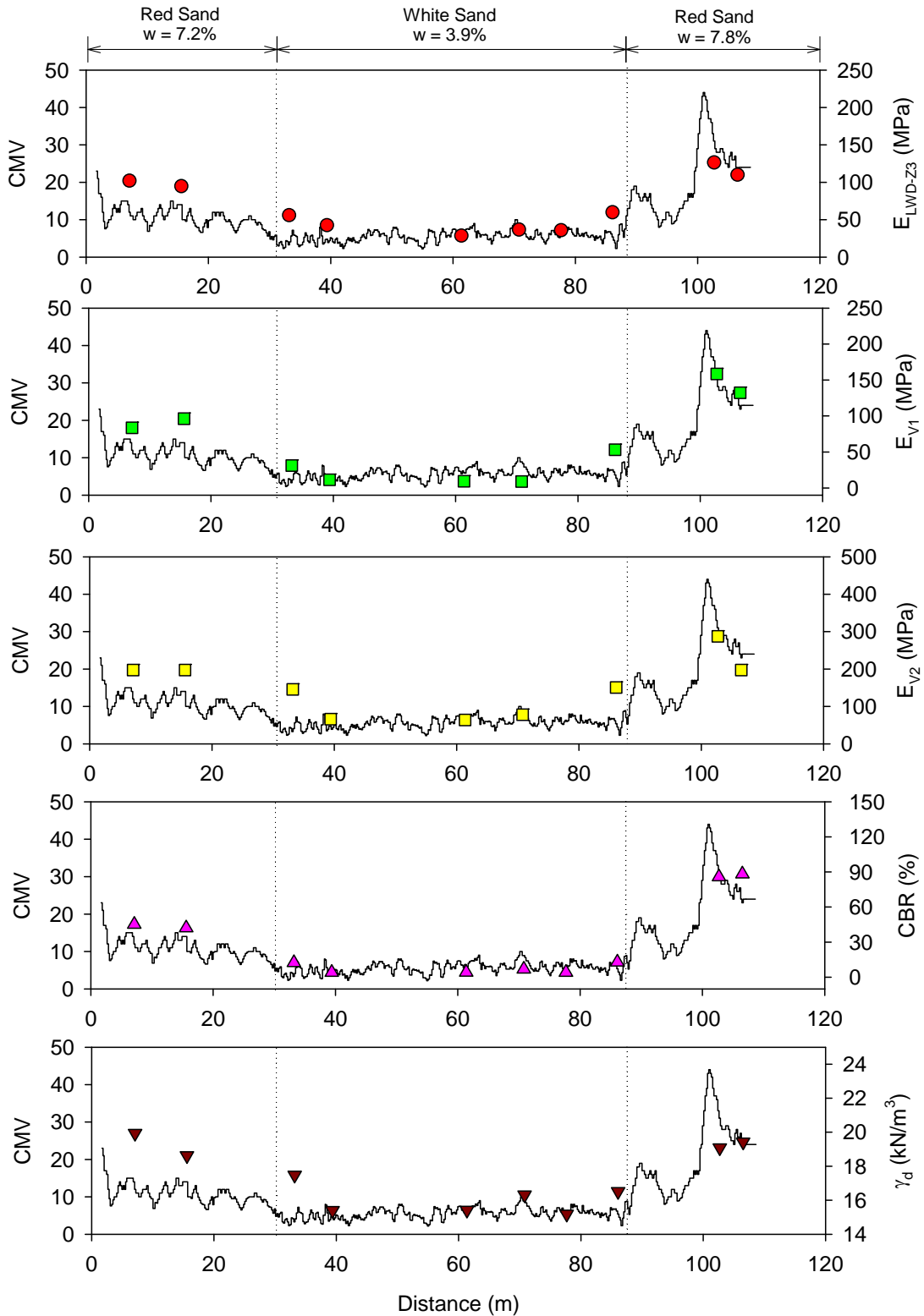
Figure 54. Comparison between CMV and in-situ point measurements – TB7 granular subrade material
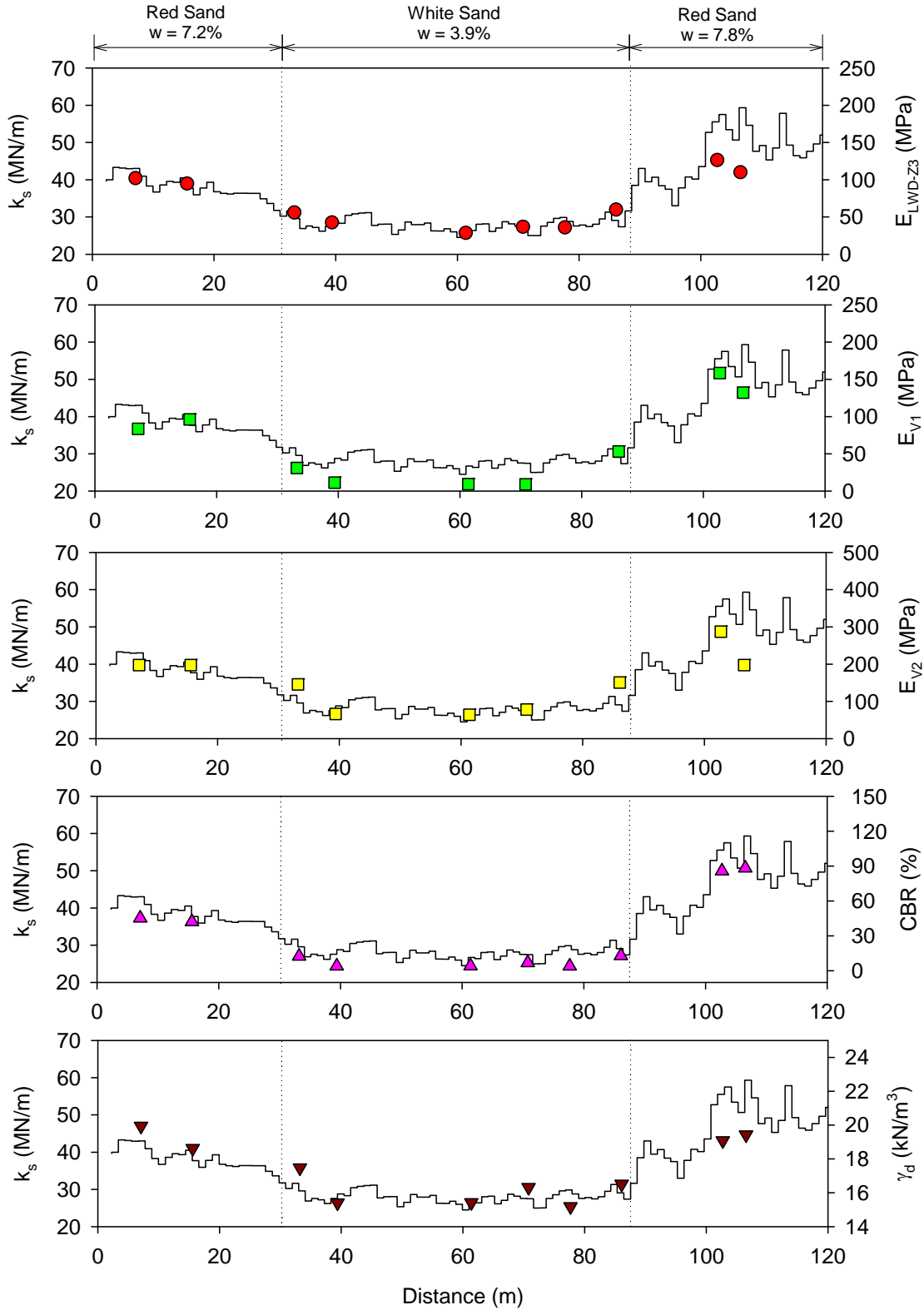
Figure 55. Comparison between k_s and in-situ point measurements – TB7 granular subrade material
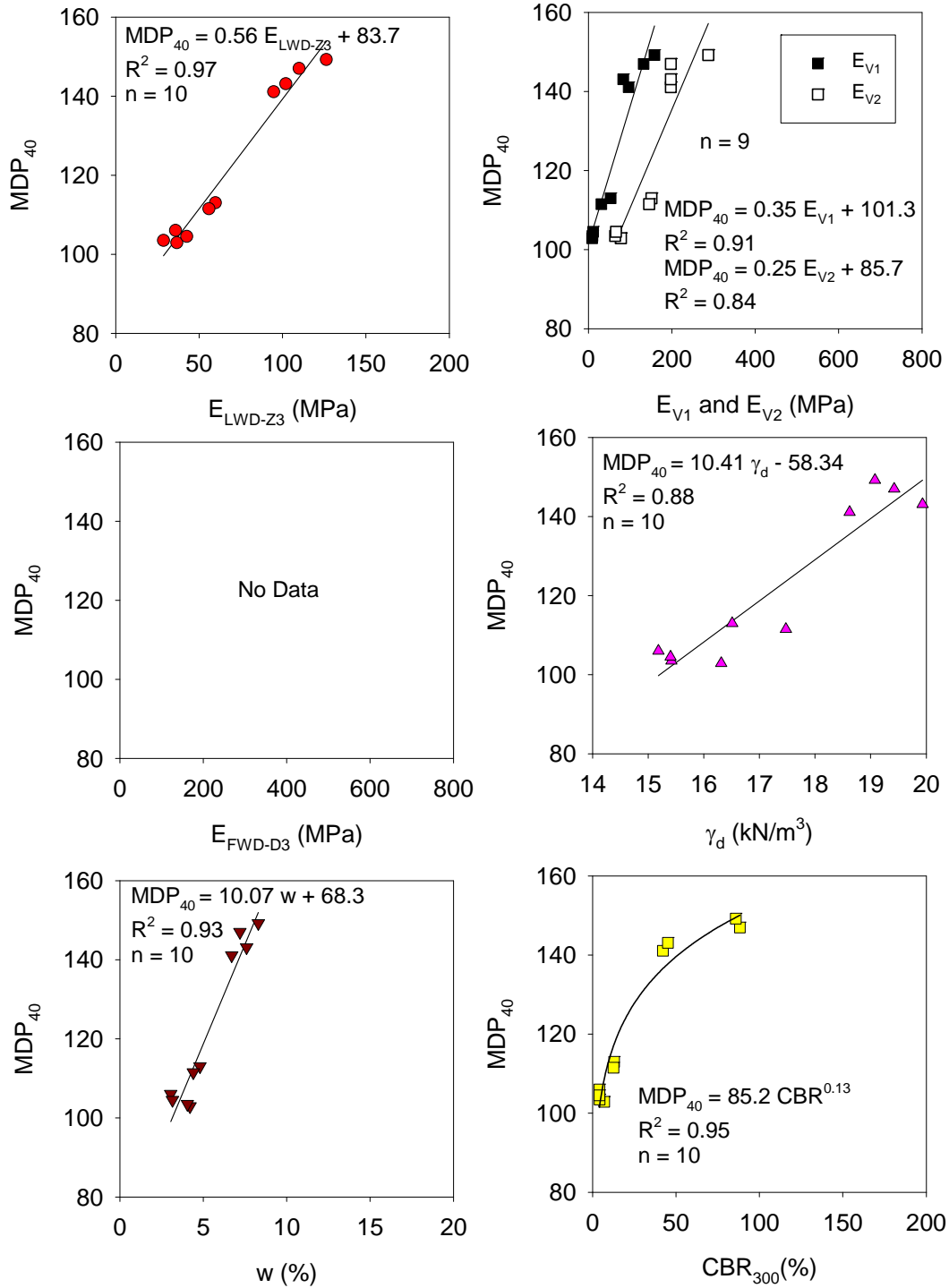
Figure 56. Regression analyses between MDP$_{40}$ and in-situ point measurements – TB7 granular subgrade material
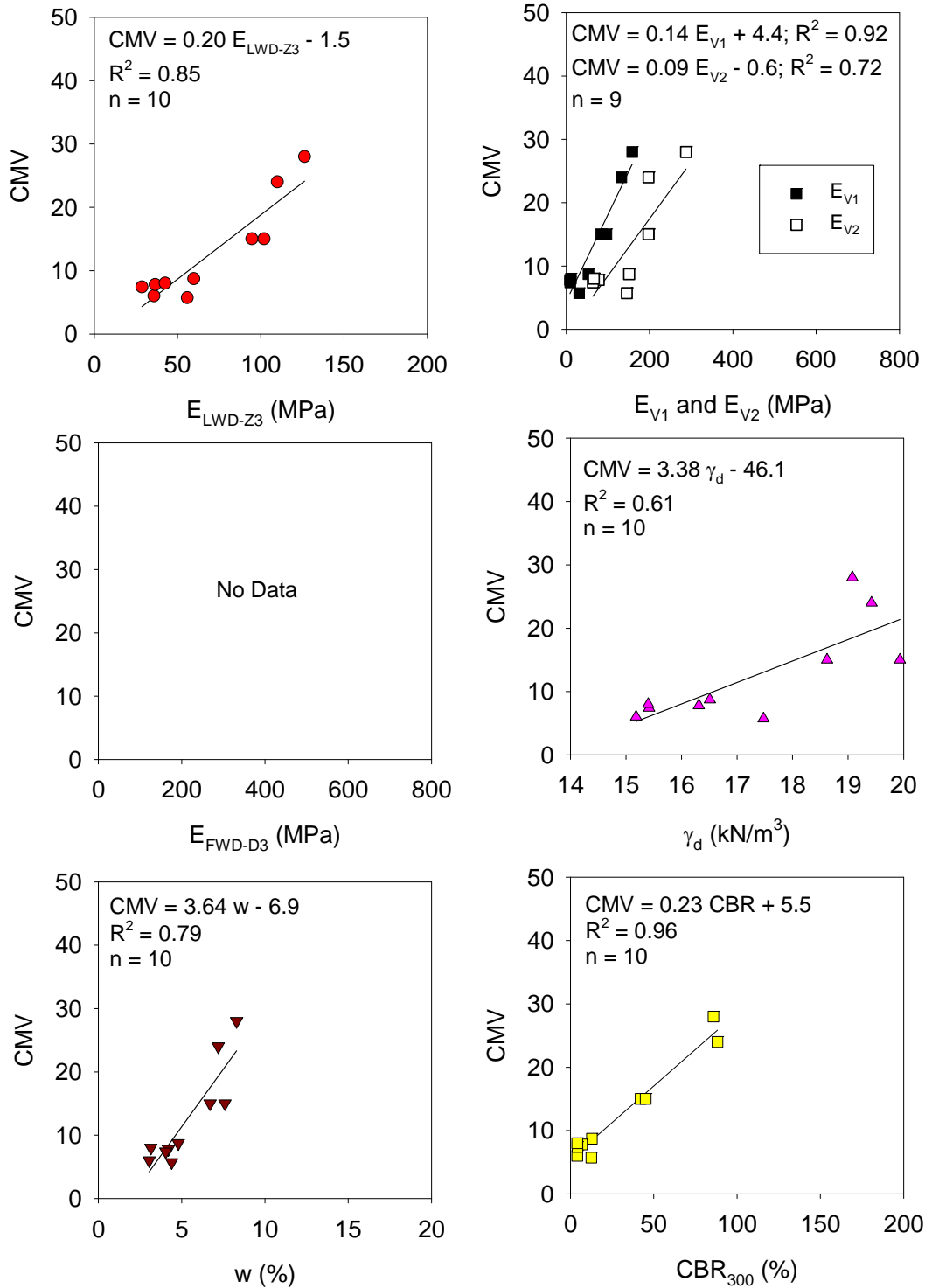
Figure 57. Regression analyses between CMV and in-situ point measurements – TB7 granular subgrade material
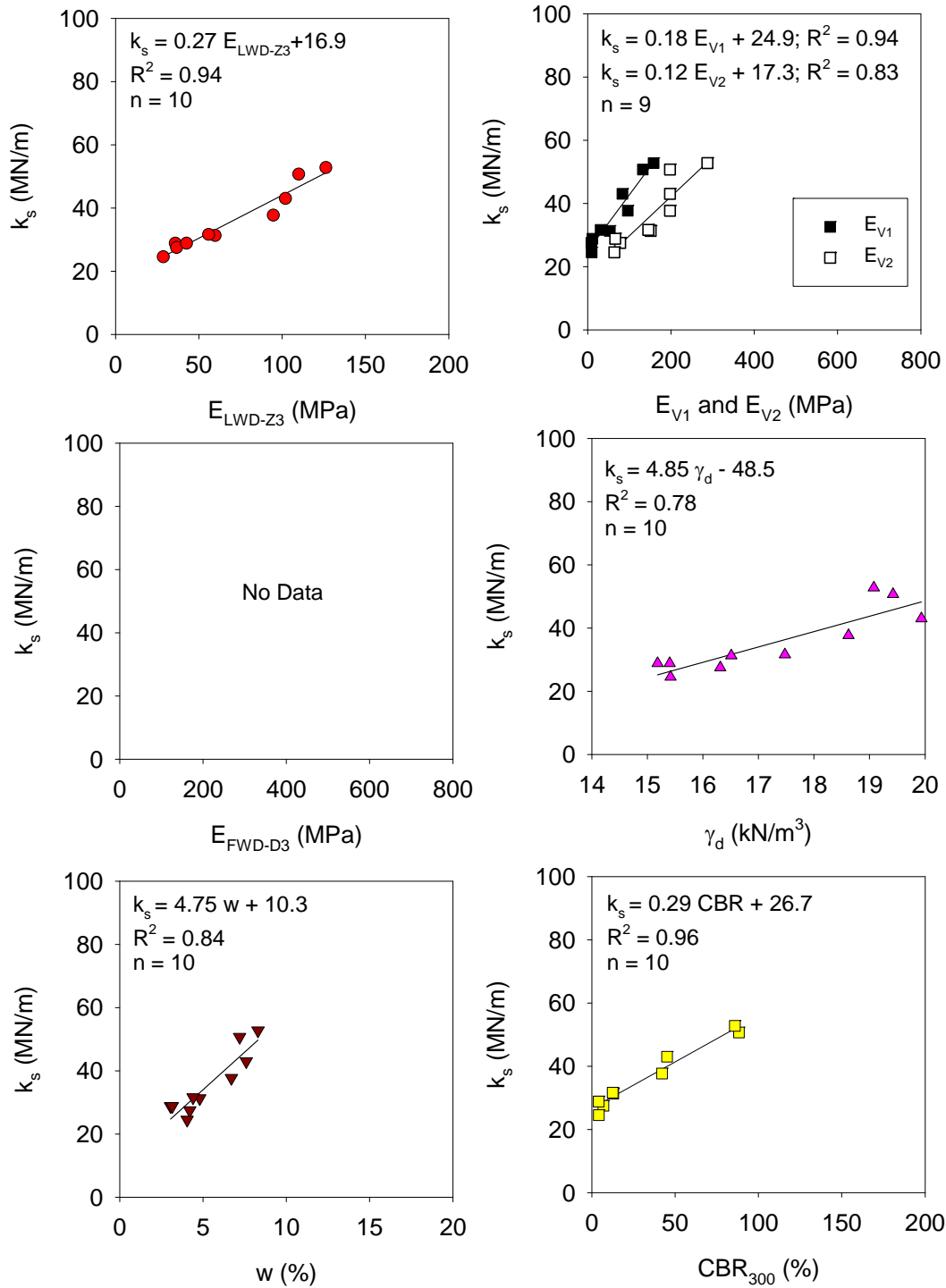
Figure 58. Regression analyses between k_s and in-situ point measurements – TB7 granular subgrade material
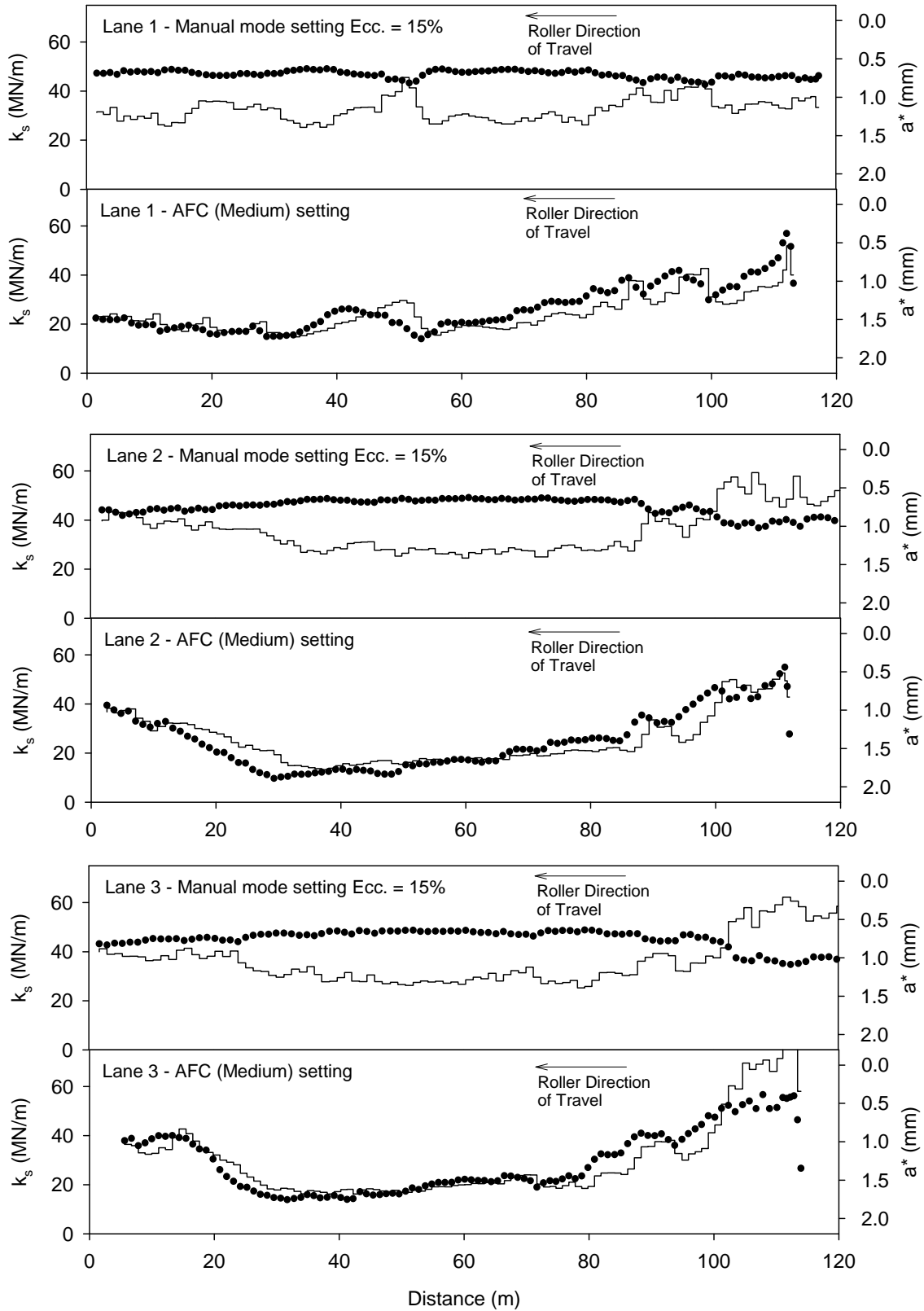
Figure 59. k_s (solid line) and a* (black circles) measurements in manual and AFC mode settings – TB7 granular subgrade material

Summary

The test bed consisted of compacted existing granular subgrade material (untreated) with variable material conditions (soft white subgrade sand and stiff red subgrade sand) over a length of about 110 m. The white subgrade sand material contained about 8% of fines while the red subgrade sand material contained about 37% fines passing the #200 sieve. MDP_{40}, CMV, and k_s IC-MV maps were obtained from this test bed in three roller lanes, and in-situ point-MVs were obtained along one roller lane from 10 test locations. Following are key findings from this test bed:

- Comparison of MDP_{40}, CMV, and k_s IC-MVs and in-situ point-MVs indicated that they both tracked well together by clearly distinguishing the soft (white subgrade sand) and stiff (red subgrade sand) conditions encountered on the test bed.
- Correlations between MDP_{40}, CMV, and k_s IC-MVs and in-situ point-MVs showed good correlations $R^2 > 0.70$.
- Analysis of k_s and $a*$ results from AFC mode operation indicated that the vibration amplitude was effectively decreased with increase in k_s, and that the response distance for altering the amplitude was in the range of 1 to 2 m (for variation in $v = 3.8$ to 4.2 km/h).

COMBINED REGRESSION ANALYSIS

Data presented above captured IC-MVs and corresponding in-situ point-MVs over a wide measurement range. The data from multiple test beds are combined in this section to develop site wide correlation results. As discussed above, some of the test bed results only represented a narrow range of measurement values. Combining results should provide a perspective of more general trends and associated variability. Note that for the relationships between IC-MVs and CBR, the weighted average CBR values were obtained for different depths for different test beds. For example, for TB2 with treated base layer the CBR was averaged over the compaction layer depth while for TB1 with untreated base layer the CBR was averaged over 300 mm depth (reported in the discussion as CBR_{300}).

Relationships between CCV and in-situ point-MVs based on the data obtained from TBs 1, 2, and 4 are presented in Figure 60. Correlation with E_{FWD-D3} showed the best relationship with $R^2 = 0.50$ compared to other point-MVs. Correlations with E_{V1} and E_{LWD-Z3} yielded $R^2 = 0.40$ and 0.31, respectively. Relationships with E_{V2} and CBR were relatively weak with $R^2 < 0.30$. No trend was observed in relationship with γ_d.

Relationships between MDP_{40} and various point-MVs based on the data obtained from TBs 4 and 7 are presented in Figure 61. Non-linear exponential relationships are observed in correlations between MDP_{40} and all in-situ point-MVs. R^2 values for relationships with E_{LWD-Z3}, E_{V1}, E_{V2}, and CBR_{300} point-MVs varied from 0.49 to 0.76. R^2 values for relationships with γ_d and w varied from 0.49 and 0.69, respectively. MDP_{40} values tend to reach an asymptotic value of 150, which is the maximum value set in the AccuGrade software. This observed non-linearity has practical implications as the MDP_{40} scaling used on the project (described in the background section of the report). For example, the MDP_{40} values are relatively insensitive (MDP_{40} ranged from about 140 and 150) to change in in E_{V1} from about 70 to 200 MPa while the MDP_{40} values

are very sensitive (MDP_{40} ranged from about 100 to 140) to change in E_{V1} from about 10 to 70 MPa. Similar findings are reported by White et al. (2009) from a field study in Minnesota. It appears that the MDP measurement was not set to provide an adequate measurement range relative to the measurement range of plate load test modulus values.

Relationships between CMV and various point-MVs based on data obtained from TBs 4 and 7 are presented in Figure 62. Correlation with E_{V1} showed the best relationship with $R^2 = 0.64$ compared to other point-MVs. Relationships with E_{V2} and E_{LWD-Z3} yielded relatively weak correlations with $R^2 = 0.24$. Relationship with γ_d was also relatively weak with $R^2 = 0.21$. No trend was observed in relationship with w.

Relationships between k_s and various point-MVs based on data obtained from TBs 3, 4, 5, 7, and 8 are presented in Figure 63. In-situ point-MVs obtained after vibratory roller passes on TBs 8 and 9 were deliberately ignored in the correlations analysis due to the effect of surface cracking observed on the treated surfaces following the roller passes. Correlation with E_{FWD-D3} showed the best relationship with $R^2 = 0.74$ compared to other point-MVs. Correlations with E_{V1}, E_{V2}, and E_{LWD-Z3} yielded $R^2 = 0.68$, 0.52, and 0.49, respectively. Relationship with γ_d was relatively weak with $R^2 = 0.30$. Some influence of w was noted with $R^2 = 0.22$.
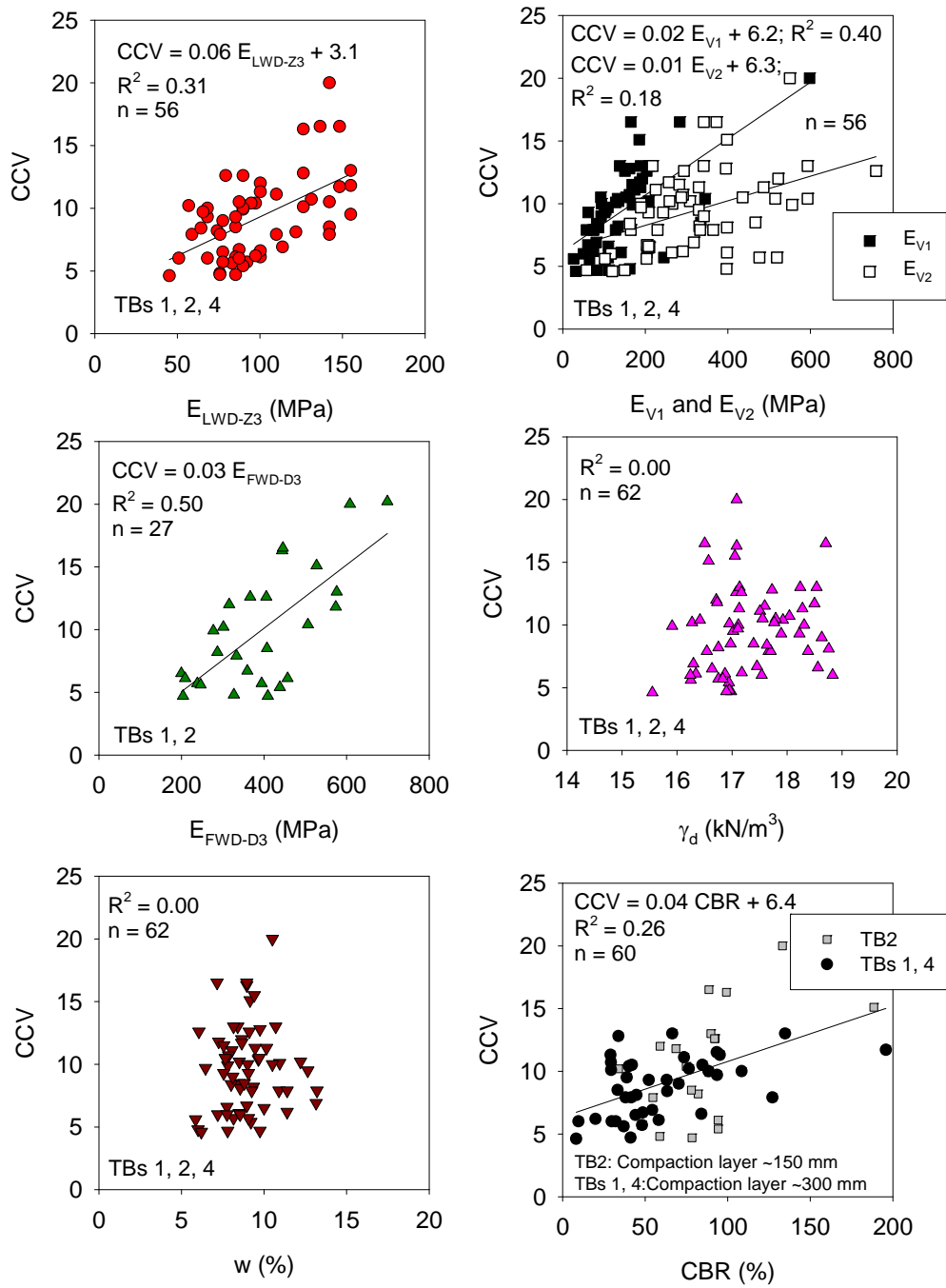
Figure 60. Regression analyses between CCV and in-situ point measurements – TBs 1, 2, and 4
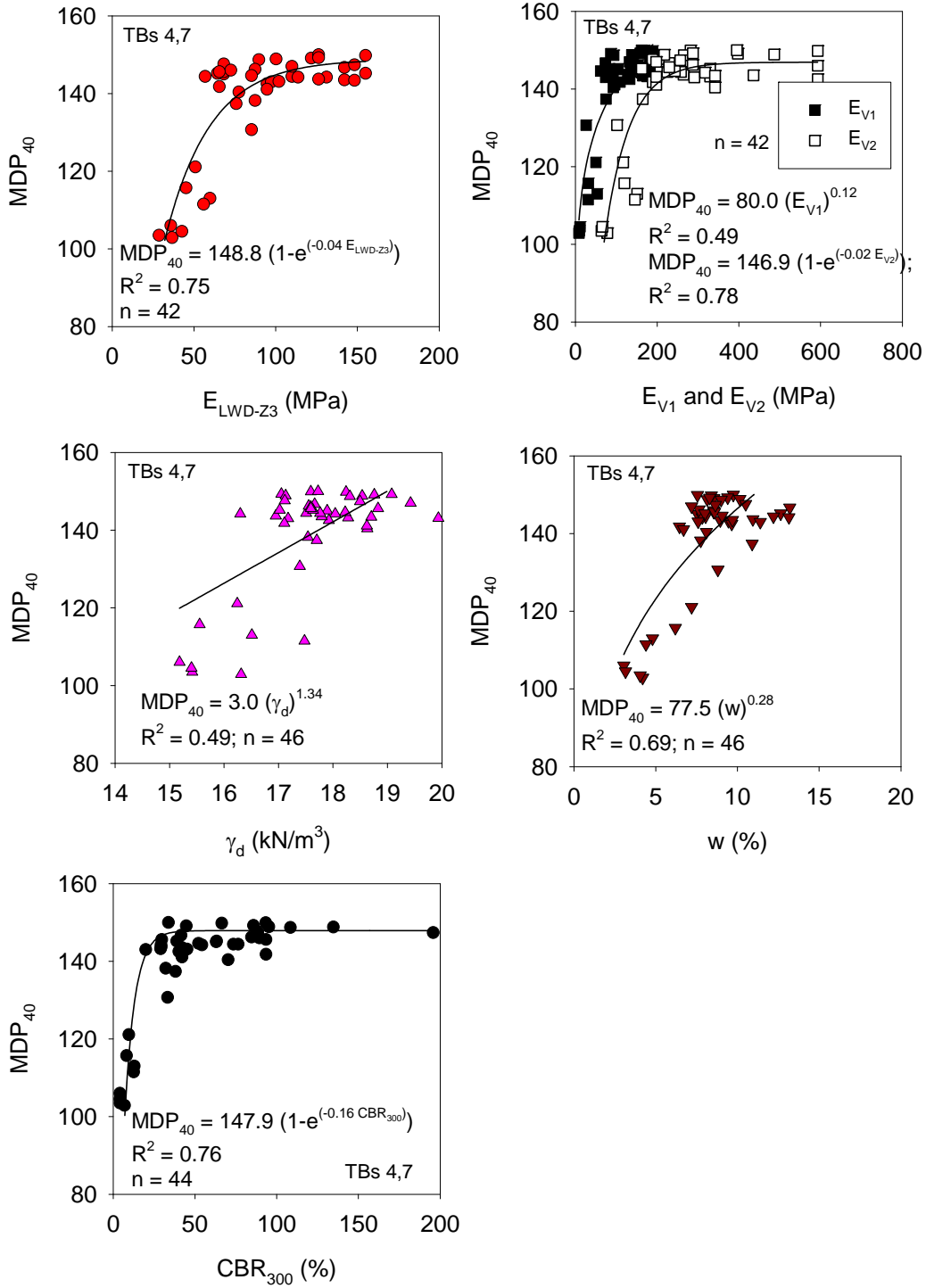
Figure 61. Regression analyses between MDP$_{40}$ and in-situ point measurements – TBs 4 and 7
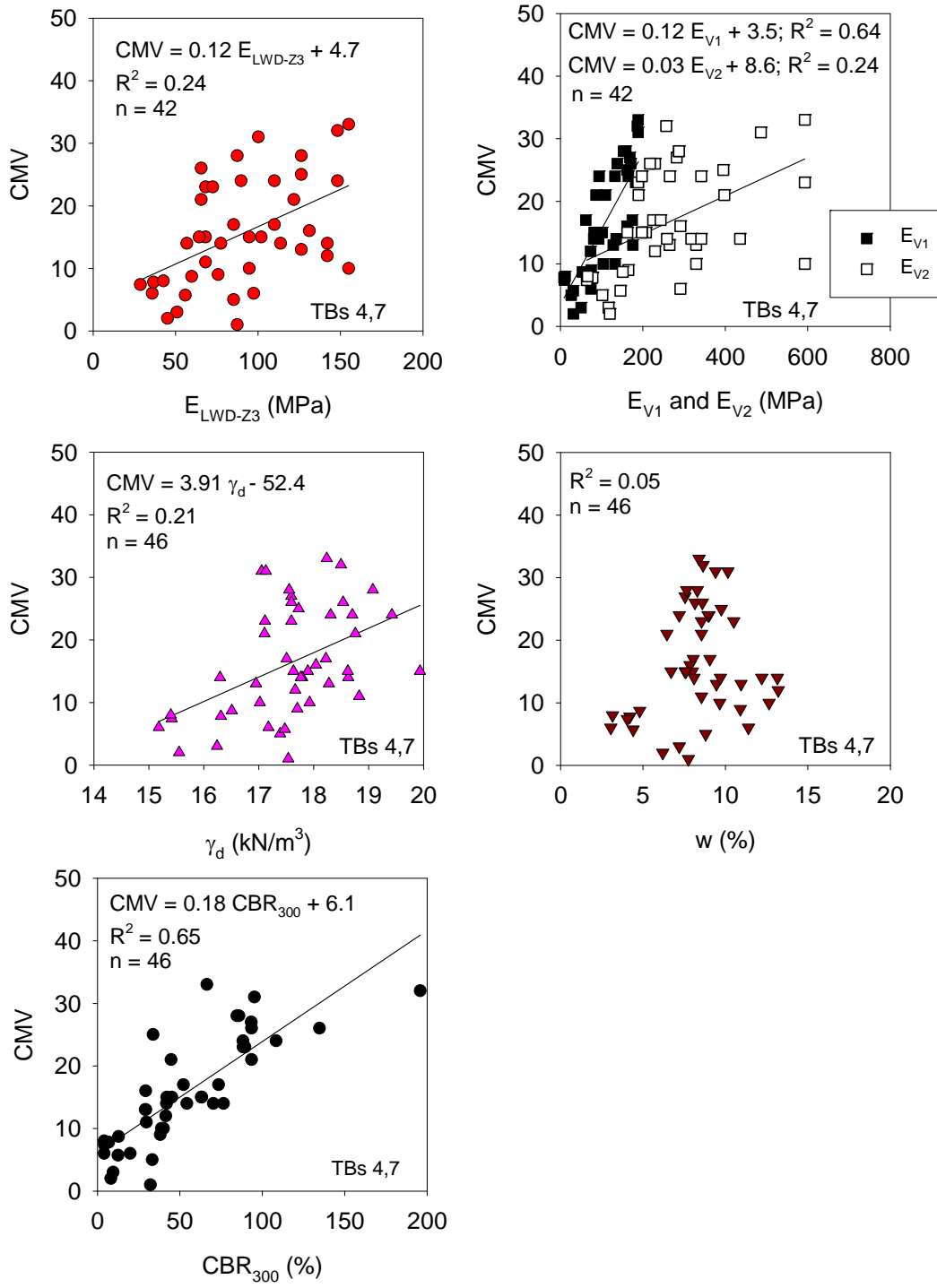
Figure 62. Regression analyses between CMV and in-situ point measurements – TBs 4 and 7
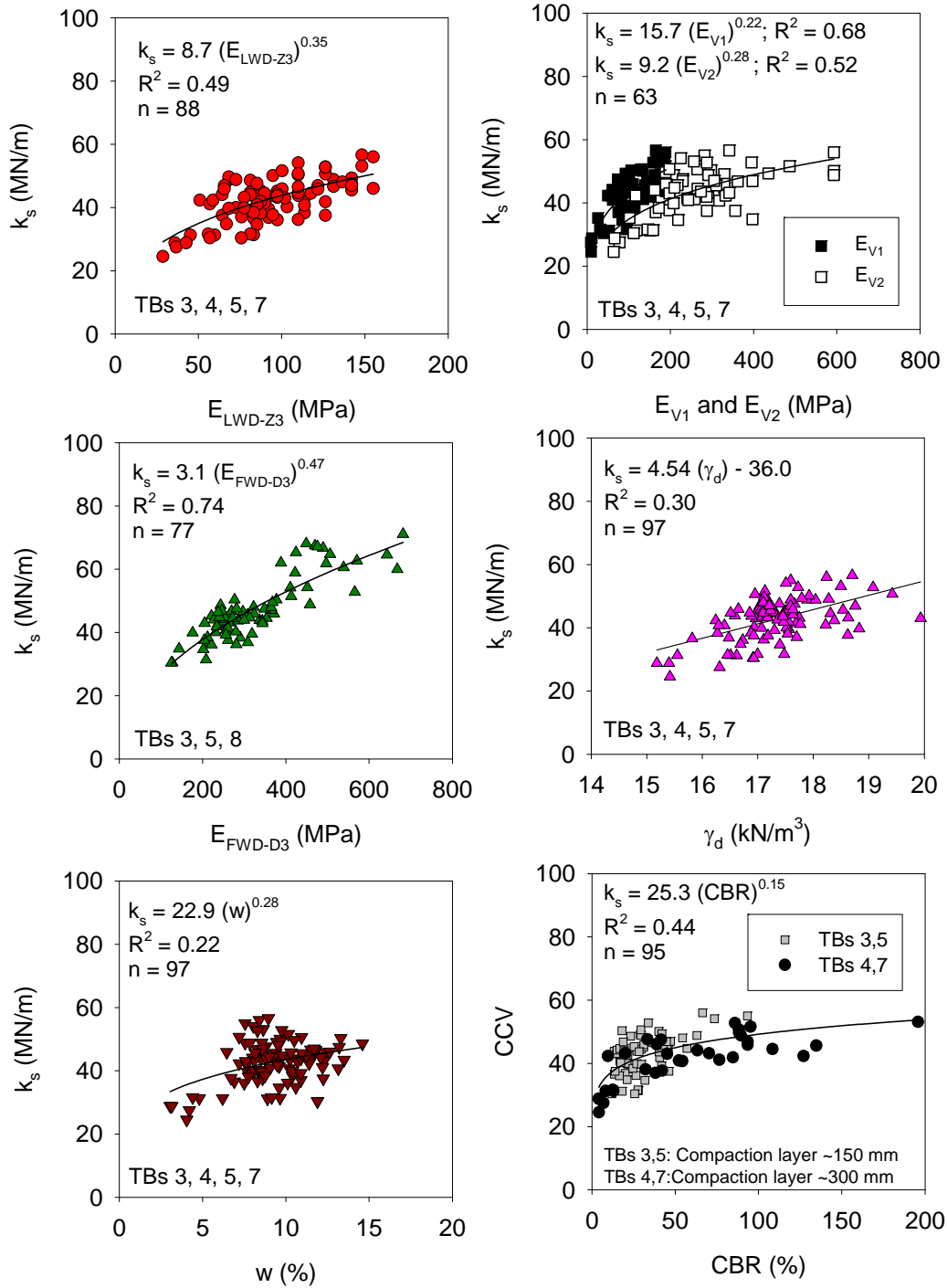
Figure 63. Regression analyses between k_s and in-situ point measurements – TBs 3, 4, 5, 7, and 8

FIELD DEMONSTRATION – OPEN HOUSE

An open house was conducted on 05/21/2009 as part of this field investigation which included dissemination of results from previous IC field studies and results from the current field study as part of a presentation. Demonstration of the two IC rollers, a tour of the Iowa State University geotechnical mobile lab with several laboratory and in-situ testing methods followed the presentation and were conducted at the project location. About 50 people attended the open house including New York DOT, contractor, and roller manufacturer personnel. Photographs from the open house are presented in Figure 64. Some of the attendees operated the IC rollers and received hands-on-experience.

Figure 64. Photographs from open house on the project site

SUMMARY AND CONCLUSIONS

Results from a field study conducted on the US84 project in Waynesboro, MS from July 13–17, 2009 are presented in this report. The project involved evaluating Caterpillar CP-56 padfoot, Case/Ammann SV212 smooth drum, and Sakai SW880 dual drum IC rollers on cement-treated and untreated sandy subgrade and base materials. A total of 9 test beds involving calibration and production operations on treated and untreated subgrade and base materials were constructed by obtaining IC-MVs in conjunction with various in-situ point-MVs (i.e., LWD, FWD, PLT, DCP, and NG). IC-MVs maps on the on-board computer display unit were utilized in selecting field QA test locations in production areas.

Results obtained from various test beds contributed to developing empirical relationships between IC-MVs and various in-situ point-MVs. Empirical correlations between IC-MVs and different point-MVs sometimes showed weak correlations when evaluated independently for each test bed, because of the narrow measurement range. The correlations improved when data are combined for site-wide correlations with a wide measurement range. IC-MVs generally correlated better with modulus based in-situ point-MVs (i.e., E_{LWD-Z3}, E_{FWD-K3}, E_{V1}, and E_{V2}) and CBR point MVs than with dry density point-MVs. Correlations between IC-MVs and E_{FWD-K3}, and IC-MVs and E_{V1} showed strongest correlation coefficients.

IC-MV mapping operations were performed in AFC mode using low, medium, and high performance settings on TB8, TB7, and TB9, respectively. When operated in high performance setting, the vibration amplitude was decreased and the excitation frequency was increased with increase in k_s. When operated in low and medium performance settings, the vibration amplitude was decreased with increase and k_s while the frequency remained relatively constant. Data indicated that the response distance for altering the amplitude and/or frequency was about 1 to 2 m for a roller travel speed of about 4 km/h. Case/Ammann machine on this project reported IC-MVs every 1 m. Denser sampling rate is required to accurately evaluate the response distance.

Geostatistical analysis methods were utilized to analyze spatially referenced IC-MV data to assess spatial non-uniformity of the untreated and treated subgrade and base materials. Results indicated that the spatial non-uniformity is higher on the treated subgrade and base layers after two days of curing compared to shortly after compaction and untreated layers. A number of construction related factors likely contribute to this increased non-uniformity which includes non-uniform application of cement, water content, compaction delay time, and compaction energy across the test bed area. This is an important finding and has not been well documented in the technical literature. While the implications of this increased non-uniform support conditions on the performance of the pavements is not well understood, this finding is in contrary to the common presumption that stabilization creates a more "uniform" working platform. More research is warranted to further investigate this topic.

The results from this study provided new information with application of IC-MVs in conjunction with various QA test devices on cement treated subgrade and base materials, which to the authors' knowledge, has not been previously documented in the United States. The study demonstrated several potential advantages of implementing IC roller operations and various in-situ testing methods into earthwork construction QC/QA practice.

REFERENCES

Arman, a., and Saifan, F. (1967). "The effect of delayed compaction on stabilized soil-cement," *Highway Research Board* No. 198, Washington, D.C., 30-38.

ASTM D6951-03. (2003). "Standard test method for use of the dynamic cone penetrometer in shallow pavement application." American Standards for Testing Methods (ASTM), West Conshohocken, Pennsylvania.

ASTM D698-07e1. (2007). "Standard test method for laboratory compaction characteristics of soil using standard effort." American Standards for Testing Methods (ASTM), West Conshohocken, Pennsylvania.

ASTM D422-63. (2007). "Standard test method for particle-size analysis of soils." American Standards for Testing Methods (ASTM), West Conshohocken, Pennsylvania.

ASTM D4318-05 (2005). "Standard test methods for liquid limit, plastic limit, and plasticity index of soils." American Standards for Testing Methods (ASTM), West Conshohocken, Pennsylvania.

ASTM D3282-09. (2009). "Standard practice for classification of soils and soil-aggregate mixtures for high construction purposes." American Standards for Testing Methods (ASTM), West Conshohocken, Pennsylvania.

ASTM D2487-10. (2010). "Standard practice for classification of soils for engineering purposes (unified soil classification system)." American Standards for Testing Methods (ASTM), West Conshohocken, Pennsylvania.

Anderegg R., and Kaufmann, K. (2004). "Intelligent compaction with vibratory rollers - feedback control systems in automatic compaction and compaction control," *Transportation Research Record No. 1868, Journal of the Transportation Research Board*, National Academy Press, 124-134.

Anderegg, R., von Felten, D., and Kaufmann, K. (2006). "Compaction monitoring using intelligent soil compactors." *Proc., GeoCongress 2006: Geotechnical Engineering in the Information Technology Age,* February, Atlanta, CD-ROM.

Brandl, H., and Adam, D. (1997). "Sophisticated continuous compaction control of soils and granular materials." *Proc. 14th Intl. Conf. Soil Mech. and Found. Engrg.*, Hamburg, Germany, 1–6.

Chilès, J-P., and Delfiner, P. (1999). *Geostatistics – Modeling Spatial Uncertainty.* John Wiley & Sons, Inc., New York.

Clark, I., and Harper, W. (2002). *Practical geostatistics 2000.* 3rd reprint, Ecosse North America Llc, Columbus, Ohio.

Cowell, M.J., and Irwin, L.H. (1979). "Effects of compaction delays and multiple treatments on the strength of cement stabilized soil," *Transportation Research Record* No. 702, Washington, D.C., 191-198.

Floss, R., Gruber, N., Obermayer, J. (1983). "A dynamical test method for continuous compaction control." *Proc. 8th European Conf. on Soil Mech. and Found. Engg,* H.G. Rathmayer and K. Saari, eds., May, Helsinki, 25-30.

Hertz, H. (1895). *Über die Berührung fester elasticscher Körper*, Gesammelte Werke, Bd. 1. Leipzig.

Isaaks, E. H., and Srivastava, R. M. (1989). *An introduction to applied geostatistics*. Oxford University Press, New York.

Kröber, W. (1988). "Untersuchung der dynamischen Vorgänge bei der Vibrationsverdichtung von Böden," Ph.D. Dissertation, Schriftenreihe, Heft 11, Lehrstuhl und Prüfamt für Grundbau, Bodenmechanik und Felsmechanik der Technischen Universität München (in German).

Kröber, W., Floss, R., Wallrath, W., (2001). "Dynamic soil stiffness as quality criterion for soil compaction." *Geotechnics for Roads, Rail Tracks and Earth Structures*, A.A. Balkema Publishers, Lisse / Abingdon / Exton (Pa) / Tokyo.

Lundberg, G. (1939). *Elastische Berührung zweier Halbräume, Forschung, auf dem Gebiete des Ingenieurwesens*, Band 10, Göteborg, 201–211.

NCHRP 21-09. (2010). *Intelligent soil compaction systems – NCHRP 21-09*, National Cooperative Highway Research Program, Transportation Research Board, Washington, D.C. (in print).

Samaras, A.A., Lamm, R., Treiterer, J. (1991). "Application of continuous dynamic compaction control for earthworks in railroad construction." *Transp. Res. Rec.,* 1309, Journal of the Transportation Research Board, Washington, D.C., 42–46.

Sandström, Å. (1994). *Numerical simulation of a vibratory roller on cohesionless soil,* Internal Report, Geodynamik, Stockholm, Sweden.

Sandström Å., and Pettersson, C. B., (2004). "Intelligent systems for QA/QC in soil compaction", *Proc. TRB 2004 Annual Meeting* (CD-ROM), Transportation Research Board, Washington, D. C.

Thompson, M., and White, D. (2008). "Estimating compaction of cohesive soils from machine drive power." *J. of Geotech. and Geoenv. Engrg.,* ASCE, 134(12), 1771-1777.

Vennapusa, P., White, D.J., and Gieselman, H. (2009). "Influence of support conditions on roller-integrated machine drive power measurements for granular base.", *Intl. Found. Cong. and Equip. Expo (IFCEE) 2009*, 15-19 March, Orlando, Florida.

Vennapusa, P., and White, D. J. (2009). "Comparison of light weight deflectometer measurements for pavement foundation materials." *Geotech.Test. J.*, ASTM, 32(3), 239-251.

Vennapusa, P., White, D.J., Morris, M. (2010). "Geostatistical analysis for spatially referenced roller-integrated compaction measurements, *J. of Geotech. and Geoenv. Engrg.,* ASCE, (in print).

White, D. J., Jaselskis, E., Schaefer, V., Cackler, T. (2005). "Real-time compaction monitoring in cohesive soils from machine response." *Transp. Res. Rec., 1936*, Journal of the Transportation Research Board, Washington D.C., 173–180.

White, D.J., and Thompson, M. (2008). Relationships between in situ and roller-integrated compaction measurements for granular soils. *J. of Geotech. and Geoenv. Engrg.,* ASCE, 134(2), 1763-1770.

White, D., Thopmson, M., Vennapusa, P., and Siekmeier, J. (2008). "Implementing intelligent compaction specifications on Minnesota TH 64: Synopsis of measurement values, data management, and geostatistical analysis." *Transp. Res. Rec.,* 2045, Journal of the Transportation Research Board, Washington, D.C, 1-9.

White, D.J., Vennapusa, P., Gieselman, H., Johanson, L., Siekmeier, J. (2009). "Alternatives to heavy test rolling for cohesive subgrade assessment," *Eighth Intl. Conf. on the Bearing Capacity of Roads, Railways, and Airfields (BCR2A'09)*, June 29 – July 2, Champaign, Illinois.

Zorn, G. (2003). *Operating manual: Light drop-weight tester ZFG2000*, Zorn Stendal, Germany.

APPENDIX: TEST BED SUMMARY SHEETS AND EXPERIMENTAL PLAN

Accelerated Implementation of IC Technology for Embankment Subgrade Soils, Aggregate Base, and Asphalt Pavement Materials

Iowa State University Research Team Field Testing, US84, Waynesboro, MS

| Test Bed # 1 (07/13/2009) | Photos |

Description: The test bed consisted of mapping an existing compacted granular subbase layer (unstabilized) with the Sakai smooth dual drum IC roller for one roller pass and Caterpillar padfoot IC roller for six roller passes. Nominal machine settings during passes are provided below. In-situ point measurements (LWD, FWD, NG, PLT, and DCP) were performed at 6 test locations. LWD and FWD tests were conducted at the surface and about 50 to 75 mm below the surface. The objectives of testing on this test bed were to obtain correlations between IC measurement values (IC-MVs) MDP_{40}, CCV and in-situ point measurements.

Machine Nominal settings:
Sakai smooth SW880: Low amp – a = 0.30 mm, f = 50 Hz (3000vpm), v = 5 km/h
Caterpillar padfoot CP56: Low amp – a = 0.90 mm, f = 30 Hz, v = 4 km/h

Caterpillar CP-56 roller used on the test bed

Picture of Test Bed 1

Sakai SW880 roller used on the test bed
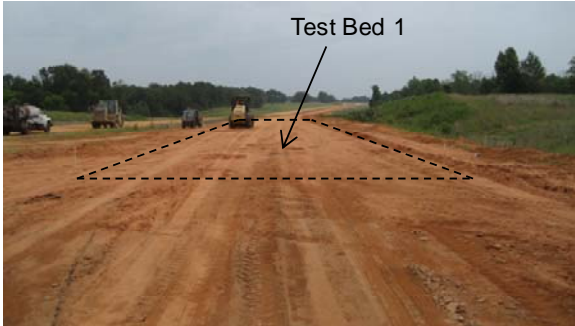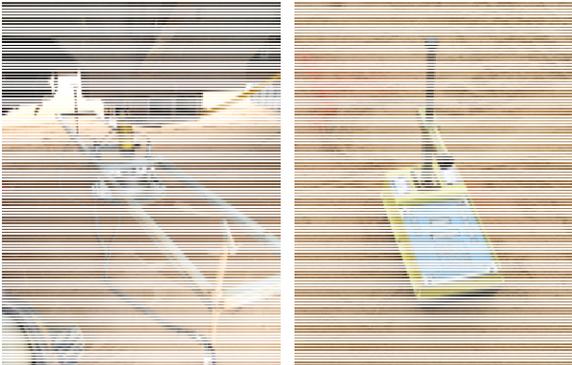
In-situ testing methods used on the test bed (left to right): Static plate load test (PLT), Nuclear moisture-density gauge (NG), Dynatest falling weight deflectometer (FWD), FWD measurements in excavation

Accelerated Implementation of IC Technology for Embankment Subgrade Soils, Aggregate Base, and Asphalt Pavement Materials
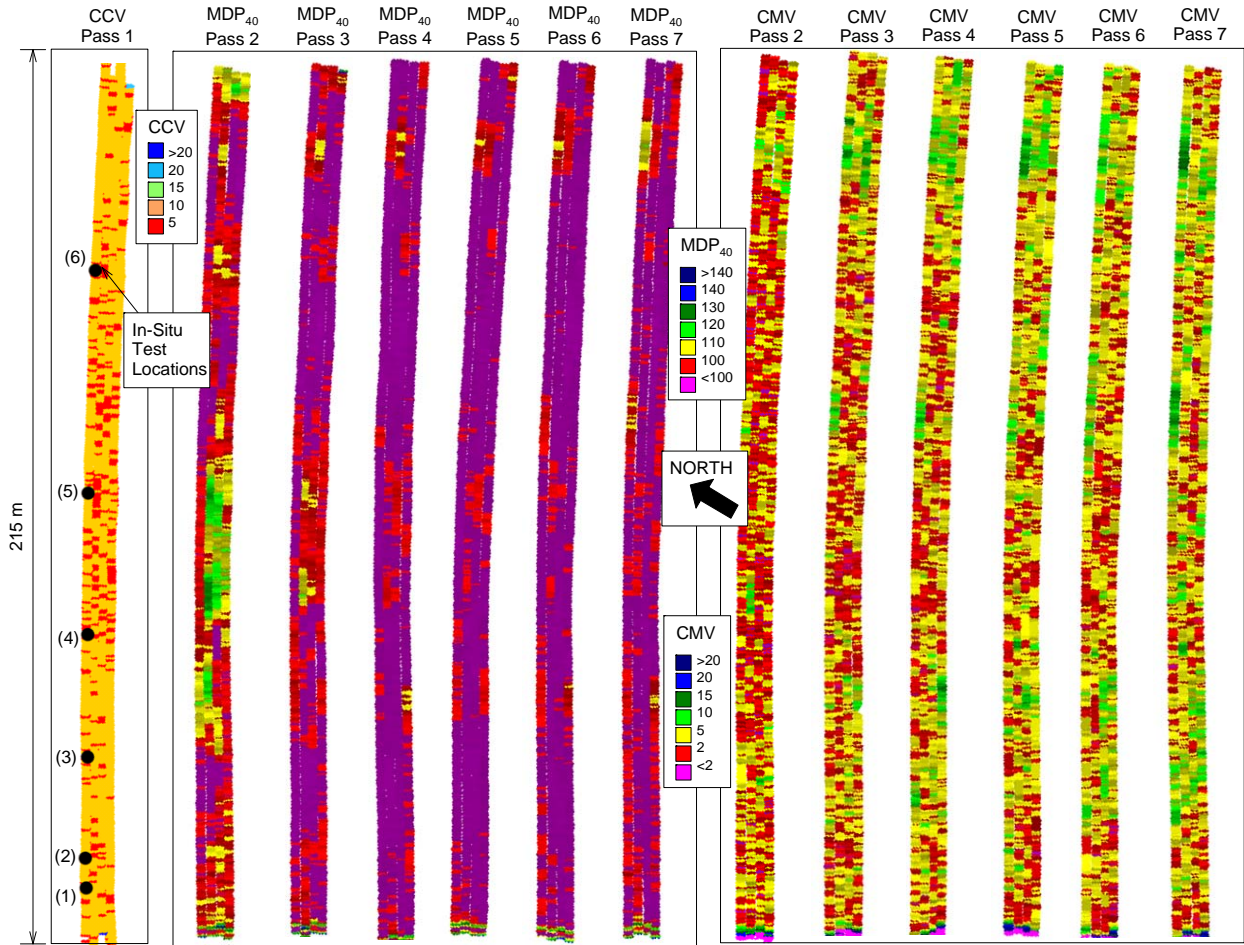
Iowa State University Research Team Field Testing, US84, Waynesboro, MS

Test Bed # 1 (07/13/2009): IC-MV (MDP$_{40}$ and CMV) Maps

CCV Pass 1

MDP$_{40}$ Pass 2

MDP$_{40}$ Pass 3

MDP$_{40}$ Pass 4

MDP$_{40}$ Pass 5

MDP$_{40}$ Pass 6

MDP$_{40}$ Pass 7

CMV Pass 2

CMV Pass 3

CMV Pass 4

CMV Pass 5

CMV Pass 6

CMV Pass 7

CCV
>20
20
15
10
5

In-Situ Test Locations

MDP$_{40}$
>140
140
130
120
110
100
<100

NORTH

CMV
>20
20
15
10
5
2
<2

215 m

(6)
(5)
(4)
(3)
(2)
(1)

After Pass 1

After Pass 3

North

A-2

Test Bed # 2 (07/13/2009)

Photos

Description: The test bed was located adjacent to test bed 1 and consisted of a 5-day cured cement stabilized granular subbase layer surfaced with an asphalt binder coat. The area was mapped with Sakai smooth dual drum IC roller. Nominal machine settings during passes are provided below. In-situ point measurements (LWD, FWD, NG, PLT, and DCP) were performed at 21 test locations selected based on the IC map. The asphalt binder coat was reportedly sprayed at the surface of the test bed after the stabilization work, to help retain moisture content in the stabilized material. The objectives of testing on this test bed were to obtain correlations between IC measurement values (IC-MVs) CCV and in-situ point measurements.

Machine Nominal settings:
Sakai SW880: Low amp – a = 0.30 mm, f = 50 Hz (3000vpm), v = 5 km/h

Sakai SW880 roller used on the test bed

Picture of Test Bed 2

In-situ testing methods used on the test bed (left to right): Dynatest falling weight deflectometer (FWD), Nuclear moisture-density gauge (NG), 300mm plate Zorn light weight deflectometer (LWD)
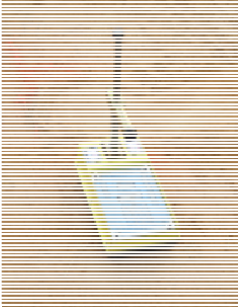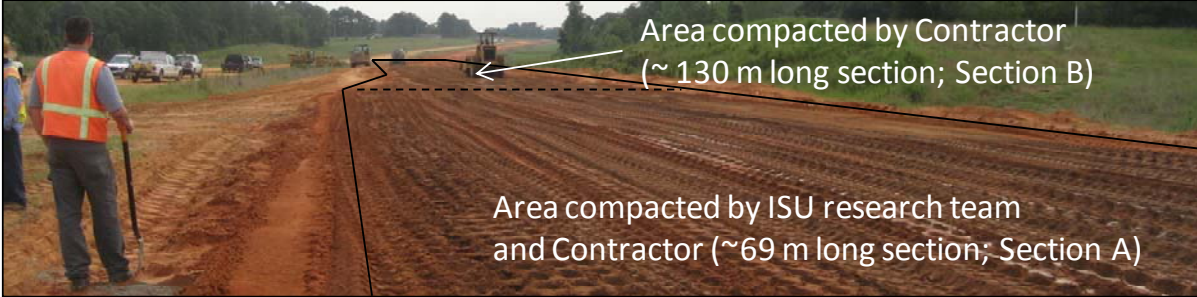
A-3

Test Bed # 3 (07/14/2009)

Photos

Description: The test bed involved stabilizing the TB1 granular subbase material with 5.5% (of dry weight of soil) of cement stabilizer. The stabilization process involved: (a) moisture-conditioning the subbase material to approximately $w = 10\%$, (b) spreading stabilizer on the test bed, (c) preparing the soil-cement mixture using a pulverizer (two passes), (d) compacting the area using padfoot roller (one pass) (e) moisture-conditioning the soil-cement mixture with a water truck, and (f) compacting the area. The test bed was divided in to a 69 m long section (Section A) and a 130 m long section (Section B). Section A was compacted using Caterpillar padfoot IC roller for five roller passes, and Case/Ammann smooth drum roller for five roller passes by the ISU research team. Roller measurements were continuously recorded during Caterpillar padfoot roller compaction. Following smooth drum roller compaction, Section A was trimmed using a motor grader to the design grade and the area was compacted using a rubber tire pneumatic roller for 6 to 8 passes by Contractor personnel. Compaction on Section B was performed by Contractor personnel. The area was compacted using a Caterpillar padfoot roller for eight roller passes and followed by a Sakai smooth drum roller for two passes. The area was trimmed to the design grade using a motor grader. Then, the area was compacted using Sakai smooth drum roller for two passes and a rubber tired pneumatic roller for six to eight passes. Following pneumatic roller compaction, the area was mapped using Case/Ammann smooth drum IC roller and in-situ point measurements (LWD, FWD, NG, PLT, and DCP) were performed at 30 test locations. The objectives of testing on this test bed were to obtain correlations between IC measurement values (IC-MVs) and in-situ point measurements, and obtain IC-MVs shortly after stabilization to compare with results after two-day curing (see TB8).

Machine Nominal settings (Section A):
Caterpillar padfoot CP56: low amp – $a = 0.90$ mm, $f = 30$ Hz, $v = 4$ km/h.
Case/Ammann smooth SV212: Ecc = 15% – $a \sim 0.9$ mm, $f = 27$ Hz, $v = 4$ km/h.
Caterpillar pneumatic tire PS360C: Static.
Machine Nominal settings (Section B):
Caterpillar padfoot CP563: Static.
Sakai smooth SV505T: Static.
Caterpillar pneumatic tire PS360C: Static.

Area compacted by Contractor
(~ 130 m long section; Section B)

Area compacted by ISU research team
and Contractor (~69 m long section; Section A)

In-situ testing methods used on the test bed (left to right): Dynatest falling weight deflectometer (FWD), Nuclear moisture-density gauge (NG), 300mm plate Zorn light weight deflectometer (LWD)

A-4

Accelerated Implementation of IC Technology for Embankment Subgrade Soils, Aggregate Base, and Asphalt Pavement Materials

Iowa State University Research Team Field Testing, US84, Waynesboro, MS

Test Bed # 3 (07/14/2009): Construction Photos

Scarified and moisture-conditioned subbase

Placement of cement stabilizer on subbase

Soil-cement mixing process using puliverzier

Moisture-conditioning the soil-cement mixture

Compaction using Caterpillar padfoot IC roller

Moisture-conditioning after first pass

Accelerated Implementation of IC Technology for Embankment Subgrade Soils, Aggregate Base, and Asphalt Pavement Materials

Iowa State University Research Team Field Testing, US84, Waynesboro, MS

Test Bed # 3 (07/14/2009): Construction Photos (Continued)

Compaction using Caterpillar padfoot roller

Compaction using Sakai smooth drum oller

Fine grading using motor grader

Final compaction passes using Caterpillar pneumatic tire roller

Test Bed # 3 (07/14/2009): IC-MV maps

IC-MV, Elevation, and Pass Count maps of Section A compacted by ISU research team

Test Bed # 3 (07/14/2009): IC-MV maps

IC-MV, Amplitude, Frequency, Pass Count, and Speed maps of Case/Ammann roller pass performed shortly after completion of pneumatic tire roller passes
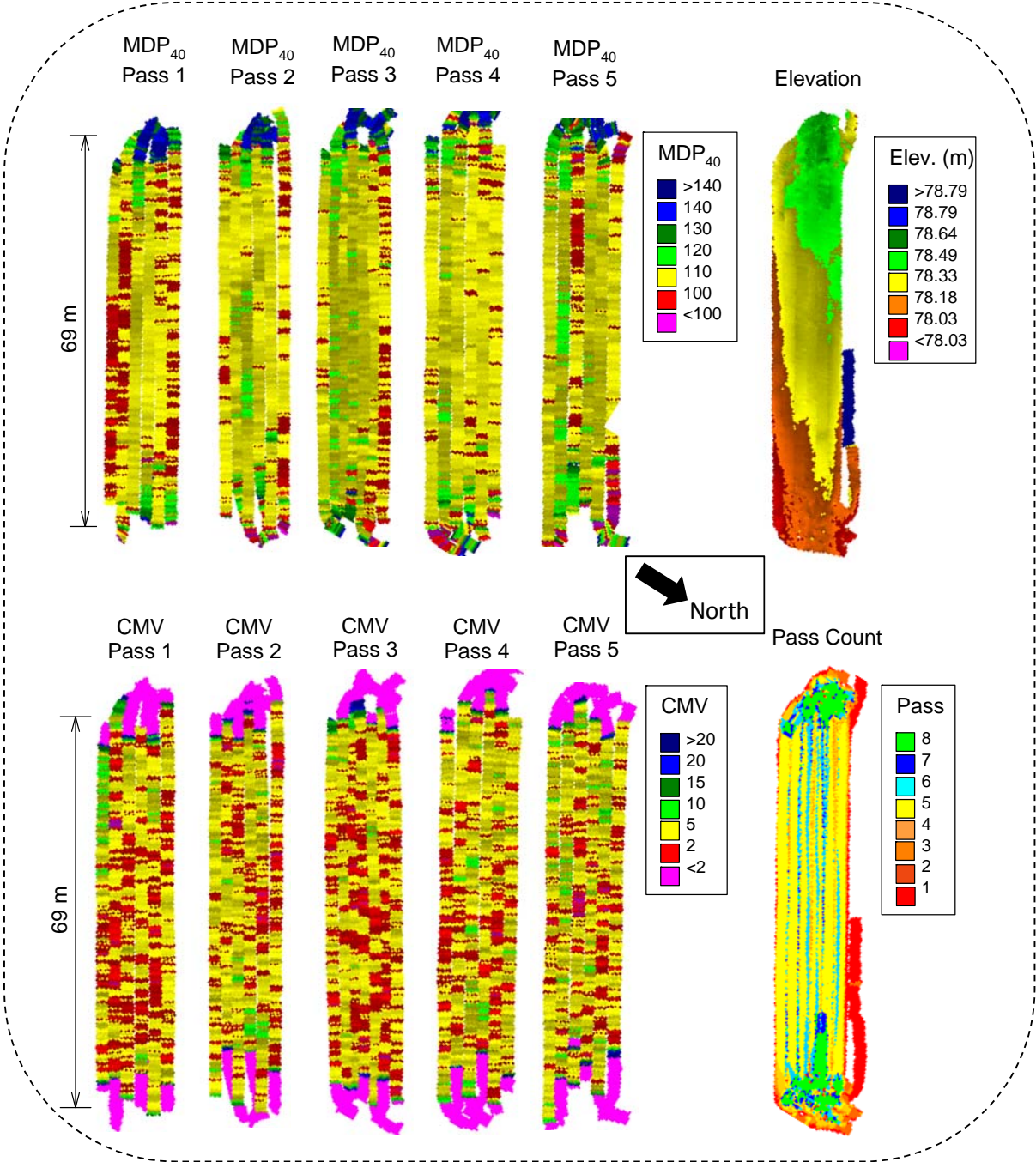
A-8

Accelerated Implementation of IC Technology for Embankment Subgrade Soils, Aggregate Base, and Asphalt Pavement Materials
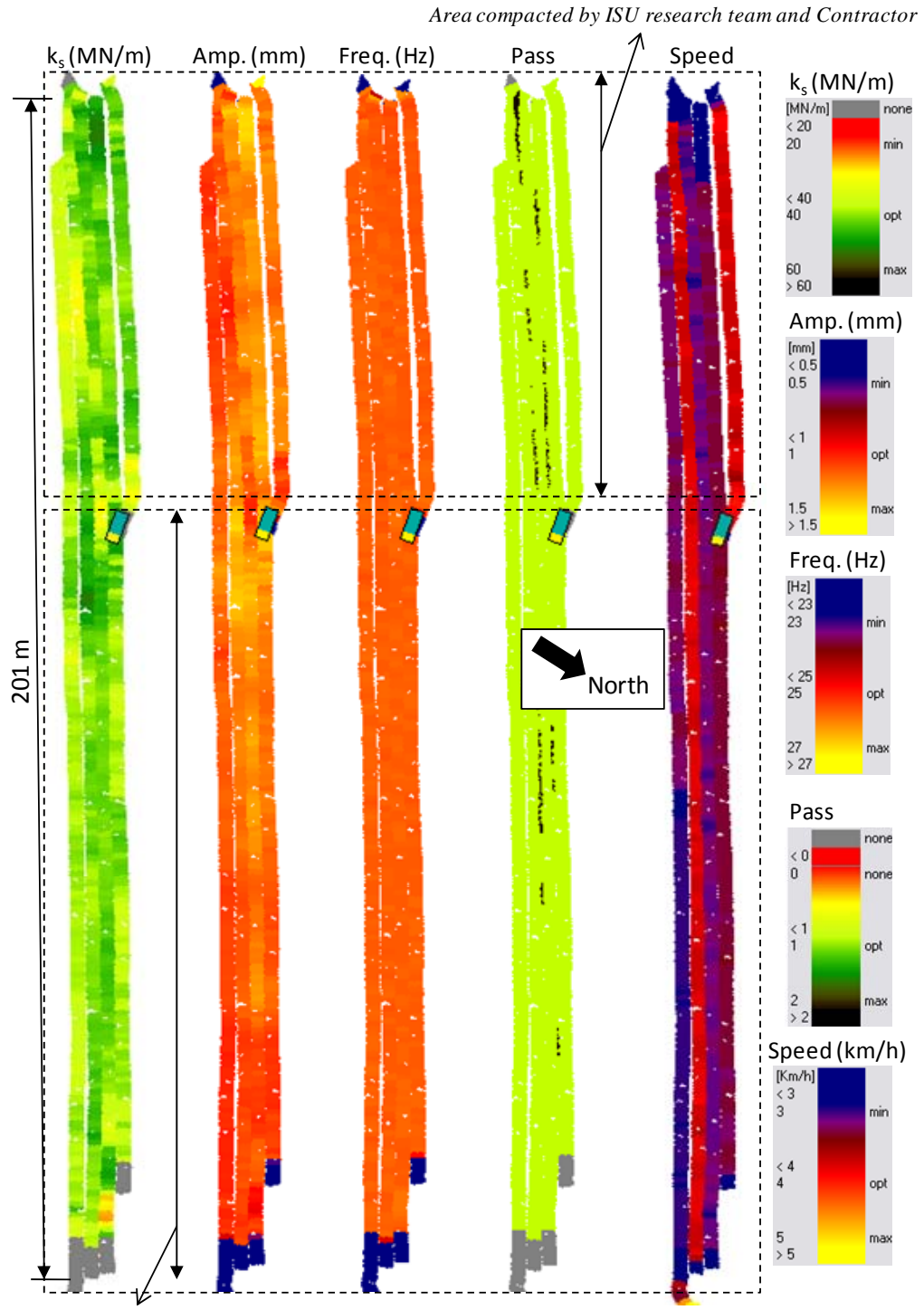Iowa State University Research Team Field Testing, US84, Waynesboro, MS

| Test Bed # 4 (07/14/2009) | Photos |

Description: The test bed consisted of mapping a 530 m long section of existing compacted granular subgrade layer (unstabilized) with Sakai smooth dual drum IC roller, Case/Ammann smooth drum IC roller, and Caterpillar padfoot IC roller for one roller pass each. Nominal machine settings during roller passes are provided below. In-situ point measurements (LWD, NG, PLT, and DCP) were performed at 39 test locations selected base on IC maps. The objectives of testing on this test bed were to obtain correlations between IC measurement values (IC-MVs) MDP_{40}, CCV, k_s and in-situ point measurements.

Machine Nominal settings:
Sakai smooth SW880: High amp – a = 0.60 mm, f = 50 Hz (3000vpm), v = 5 km/h
Case/Ammann smooth SV212: Ecc. = 15% - a ~ 0.90 mm, f = 27Hz, v = 4 km/h
Caterpillar padfoot CP56: Low amp – a = 0.90 mm, f = 30 Hz, v = 4 km/h

Picture of test bed

Sakai SW880, Case/Ammann SV212, and Caterpillar CP56 rollers (left to right) used for mapping

In-situ testing methods used on the test bed (left to right): 300mm plate Zorn light weight deflectometer (LWD), Dynamic Cone Penetrometer (DCP), Nuclear moisture-density gauge (NG), and Static Plate Load Test (PLT).

Accelerated Implementation of IC Technology for Embankment Subgrade Soils, Aggregate Base, and Asphalt Pavement Materials

Iowa State University Research Team Field Testing, US84, Waynesboro, MS

Test Bed # 4 (07/14/2009): IC-MV maps
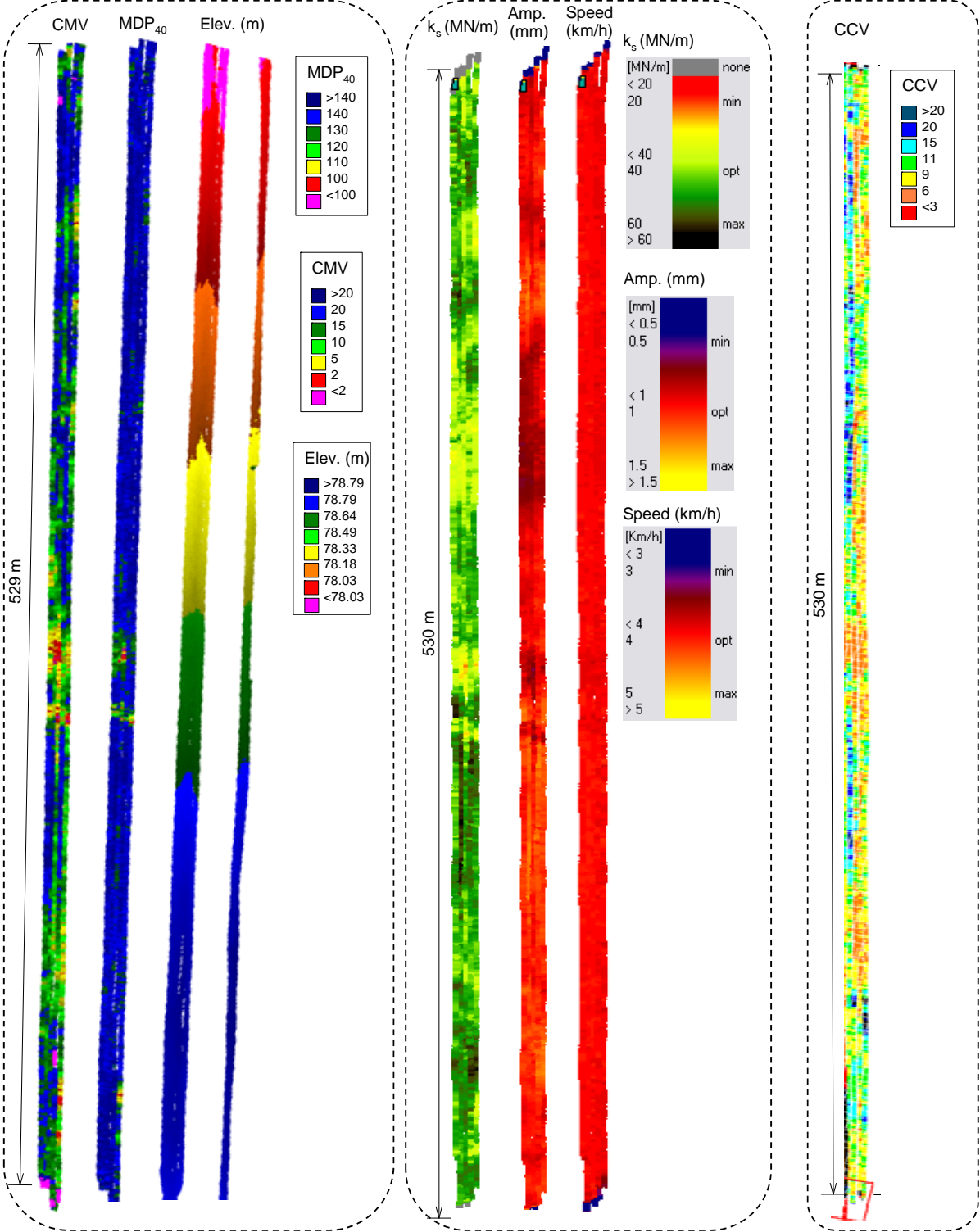
Accelerated Implementation of IC Technology for Embankment Subgrade Soils, Aggregate Base, and Asphalt Pavement Materials
Iowa State University Research Team Field Testing, US84, Waynesboro, MS

| Test Beds # 5 and 6 (07/15/2009) | Photos |

Description: Test beds 5 and 6 involved stabilizing a portion of TB4 granular subgrade material with 5.5% (of dry weight of soil) of cement stabilizer. The stabilization process involved: (a) moisture-conditioning the subgrade material to approximately w = 10%, (b) spreading stabilizer on the test bed, (c) preparing the soil-cement mixture using a pulverizer (two passes), (d) compacting the area using padfoot roller (one pass), (e) moisture-conditioning the soil-cement mixture, and (f) compacting the area. Test bed 5 was compacted by both ISU research team and Contractor personnel, while test bed 6 was compacted by Contractor personnel. Test bed 5 was compacted using Caterpillar padfoot IC roller for four roller passes, and Case/Ammann smooth drum roller for three roller passes by ISU research team. Roller measurements were recorded only during Caterpillar padfoot roller compaction. Then, the Contractor personnel used Sakai smooth drum roller for four roller passes. Following smooth drum roller compaction, the area was trimmed using a motor grader and then compacted using a rubber tire pneumatic roller for 6 to 8 passes. Compaction on test bed 6 was performed using a Caterpillar padfoot roller for four to six roller passes and followed by a Sakai smooth drum roller for four passes. The area was trimmed to the design grade using a motor grader in between the smooth drum roller passes. The area was then compacted using rubber tired pneumatic roller for six to eight passes. Following pneumatic roller compaction, test beds 5 and 6 were mapped using Case/Ammann smooth drum IC roller and in-situ point test measurements (LWD, FWD, NG, PLT, and DCP) were performed at 20 test locations selected based on the IC-map. The objectives of testing on this test bed were to obtain correlations between IC measurement values (IC-MVs) and in-situ point measurements, and obtain IC-MVs shortly after stabilization to compare with results after two-day curing (see TB9).

Machine Nominal settings (Section A):
Caterpillar padfoot CP56: low amp – $a = 0.90$ mm, $f = 30$ Hz, $v = 4$ km/h on lanes 1 to 3 and static, $v = 4$ km/h on lanes 4 to 6
Case/Ammann smooth SV212: Ecc = 15% – $a \sim 0.9$ mm, $f = 27$ Hz, $v = 4$ km/h.
Caterpillar pneumatic tire PS360C: Static.
Machine Nominal settings (Section B):
Caterpillar padfoot CP563: low amp.
Sakai smooth SV505T: low amp.
Caterpillar pneumatic tire PS360C : Static.

In-situ testing methods used on the test bed (left to right): Dynatest falling weight deflectometer (FWD), Nuclear moisture-density gauge (NG), 300mm plate Zorn light weight deflectometer (LWD)

A-11

Accelerated Implementation of IC Technology for Embankment Subgrade Soils, Aggregate Base, and Asphalt Pavement Materials

Iowa State University Research Team Field Testing, US84, Waynesboro, MS

Test Bed # 5 (07/15/2009): Construction Photos

Placement of cement stabilizer on subgrade

Pulverizing and moisture-conditioning process

Pulverizing and moisture-conditioning process

Moisture-conditioning process

Compaction using Caterpillar padfoot IC roller

Accelerated Implementation of IC Technology for Embankment Subgrade Soils, Aggregate Base, and Asphalt Pavement Materials

Iowa State University Research Team Field Testing, US84, Waynesboro, MS

Test Bed # 5 (07/15/2009): Construction Photos (continued)

Compaction using Sakai smooth drum roller

Trimming process using motor grader

Final compaction using Caterpillar pneumatic rubber tire roller

Test Bed # 6 (07/15/2009): Construction Photos

Soil-cement mixing process using pulverizer

Compaction using Caterpillar padfoot roller

Compaction using Caterpillar padfoot roller

Trimming process using motor grader

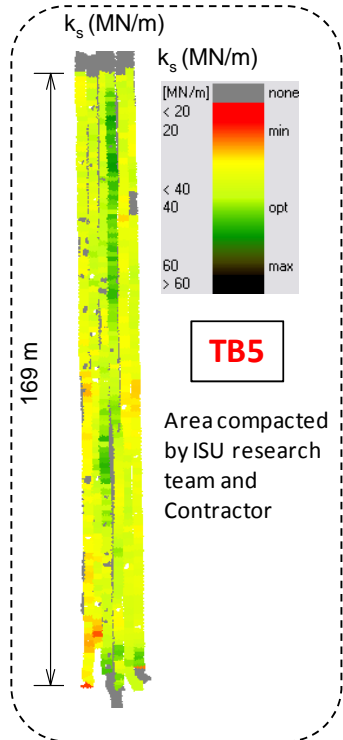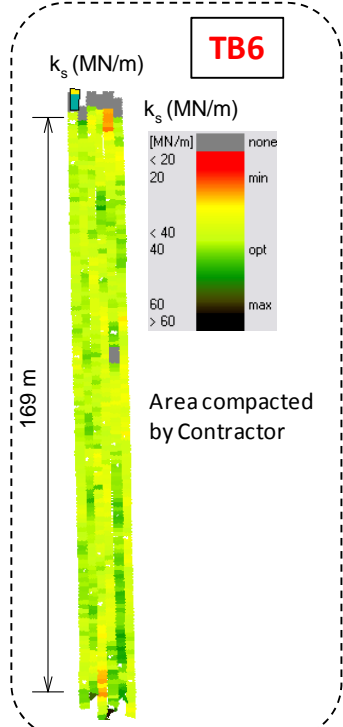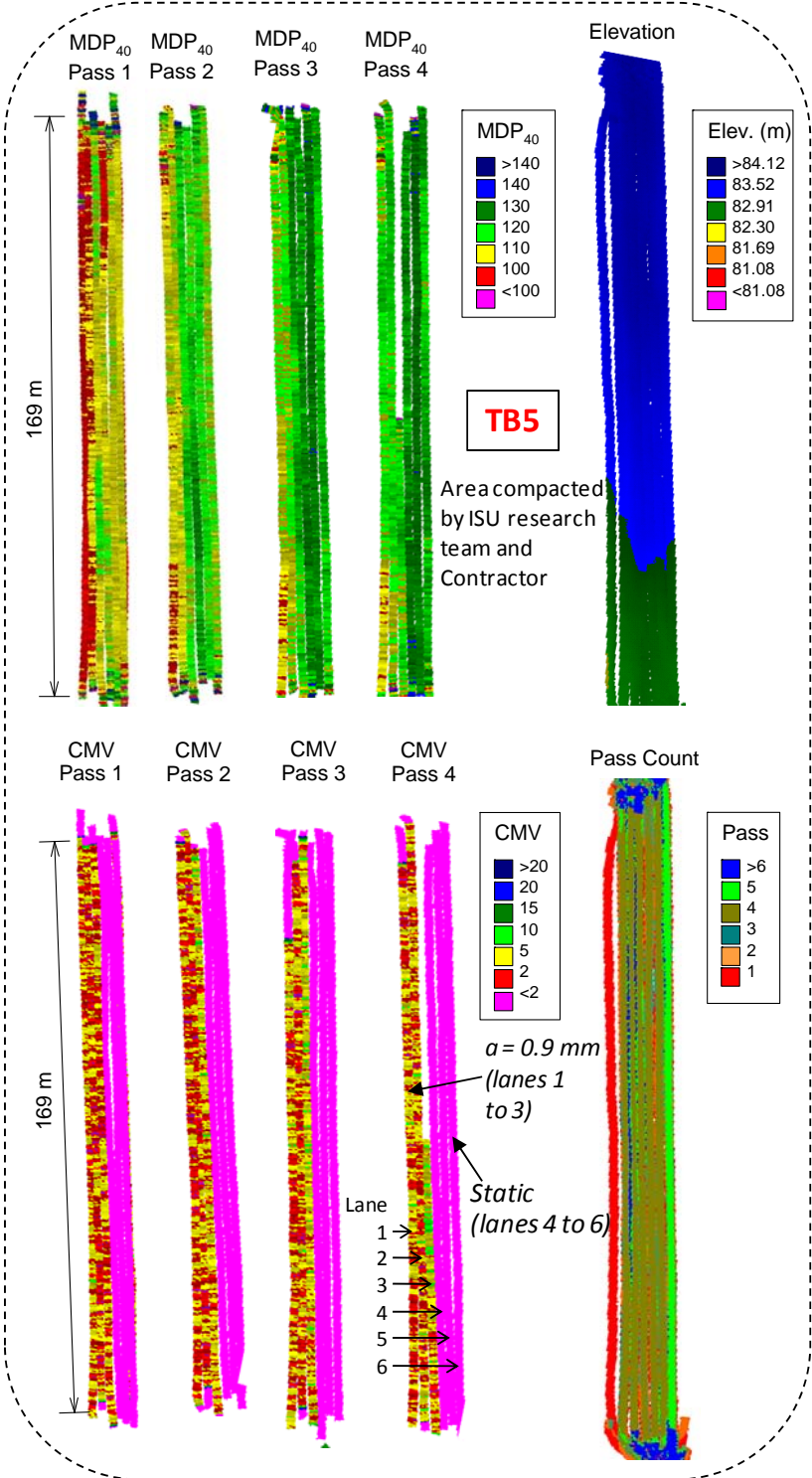Test Beds # 5 and 6 (07/15/2009): IC-MV maps

Accelerated Implementation of IC Technology for Embankment Subgrade Soils, Aggregate Base, and Asphalt Pavement Materials

Iowa State University Research Team Field Testing, US84, Waynesboro, MS

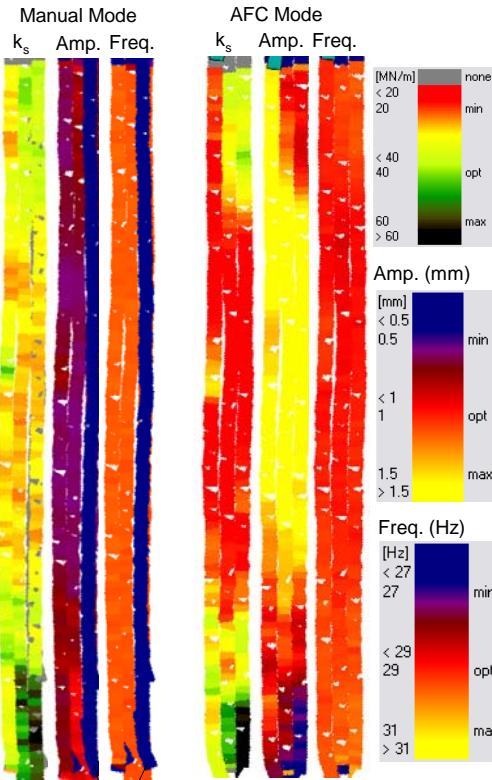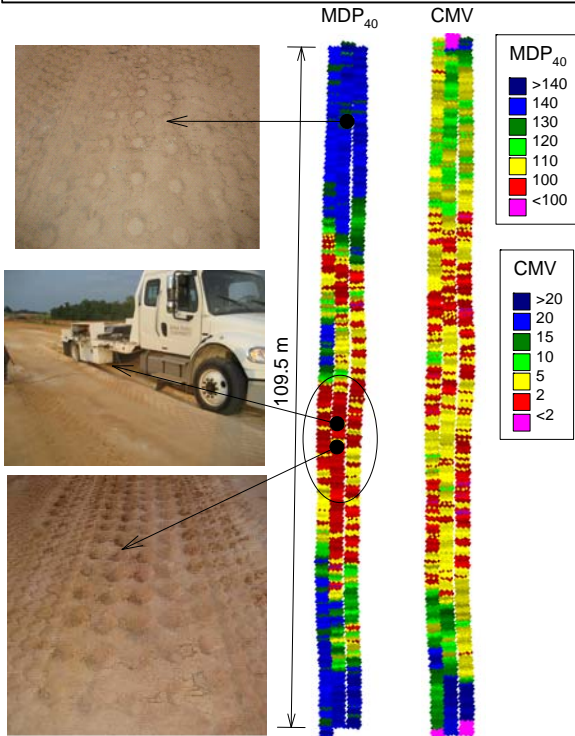Test Bed # 7 (07/15/2009)

Photos

<u>Description</u>: This test bed contained compacted existing granular subgrade material over a length of about 110 m. The subgrade material was variable across the test bed. Portion of the subgrade contained white poorly graded sand pocket that was unstable under traffic wheel loads. The area was mapped with Case/Ammann smooth drum roller for two passes (first pass in manual mode and second pass in AFC mode) and Caterpillar padfoot roller for one roller pass. In-situ testing (LWD, NG, PLT, and DCP) were performed at 10 test locations along middle lane of the test bed. The objectives of testing on this test bed were to evaluate the effectiveness of IC roller to indicate unstable/soft areas, correlate in-situ test measurements with IC-MVs, and to evaluate AFC mode compaction.

<u>Machine Nominal settings</u>:

Case/Ammann smooth SV212: Manual Ecc. = 15% - $a \sim 0.90$ mm, $f = 27$Hz, $v = 4$ km/h; AFC, $v = 4$ km/h.

Caterpillar padfoot CP56: Low amp – $a = 0.90$ mm, $f = 30$ Hz, $v = 4$ km/h

MDP_{40} CMV

MDP_{40}	
■	>140
■	140
■	130
■	120
■	110
■	100
■	<100

CMV	
■	>20
■	20
■	15
■	10
■	5
■	2
■	<2

109.5 m

Manual Mode   AFC Mode

k_s Amp. Freq. k_s Amp. Freq.

[MN/m]	
< 20	none
20	min
< 40	
40	opt
60	max
> 60	

Amp. (mm)

[mm]	
< 0.5	
0.5	min
< 1	
1	opt
1.5	
> 1.5	max

Freq. (Hz)

[Hz]	
< 27	
27	min
< 29	
29	opt
31	
> 31	max

Static pass after vibratory compaction pass

A-16

Accelerated Implementation of IC Technology for Embankment Subgrade Soils, Aggregate Base, and Asphalt Pavement Materials

Iowa State University Research Team Field Testing, US84, Waynesboro, MS

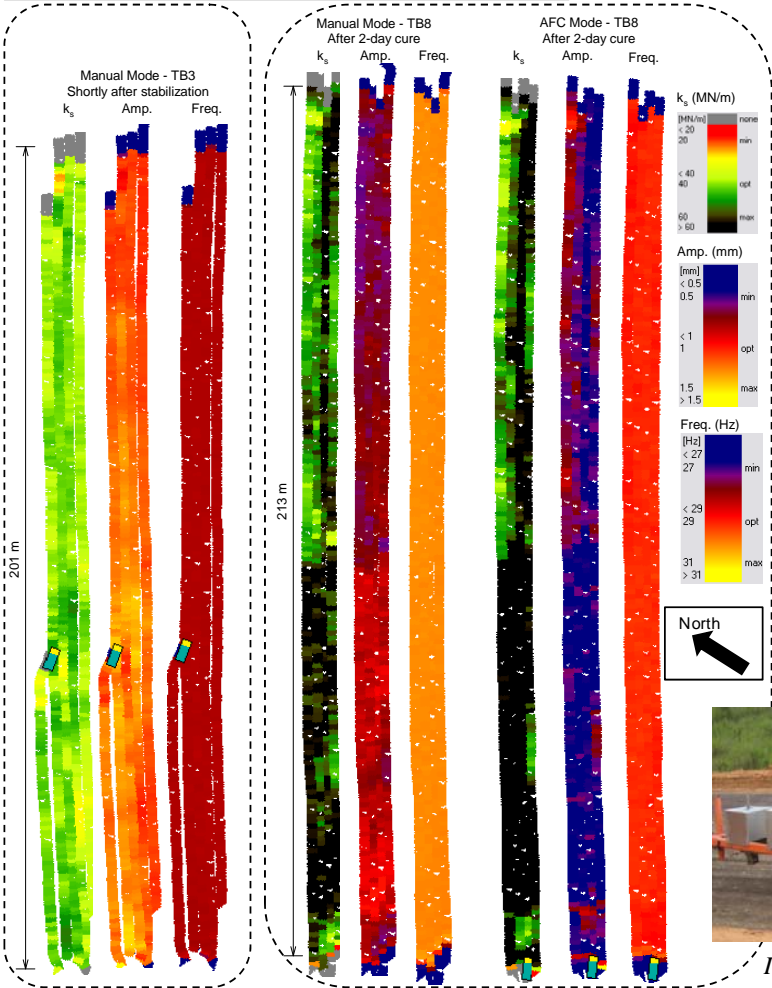Test Bed # 8 (07/16/2009)

Photos

<u>Description</u>: This test bed contained 2-day cured stabilized granular subbase material from TB3. The area was mapped with Case/Ammann smooth drum roller in manual and AFC modes and in-situ testing (LWD, FWD, NG, PLT, and DCP) was performed at 25 test locations selected using the IC-Map. The objectives of testing on this test bed were to evaluate strength gain in stabilized granular subbase layer by comparing IC-MVs obtained on TB3 shortly after stabilization and after 2-day curing, and to obtain correlations between in-situ test measurements and IC-MVs.

<u>Machine Nominal settings:</u>
Case/Ammann smooth SV212: Manual Ecc. = 10% - a ~ 0.90 mm, f = 27Hz, v = 4 km/h; AFC, v = 4 km/h.

Case/Ammann roller used for mapping

In-situ testing methods used on the test bed

Accelerated Implementation of IC Technology for Embankment Subgrade Soils, Aggregate Base, and Asphalt Pavement Materials

Iowa State University Research Team Field Testing, US84, Waynesboro, MS

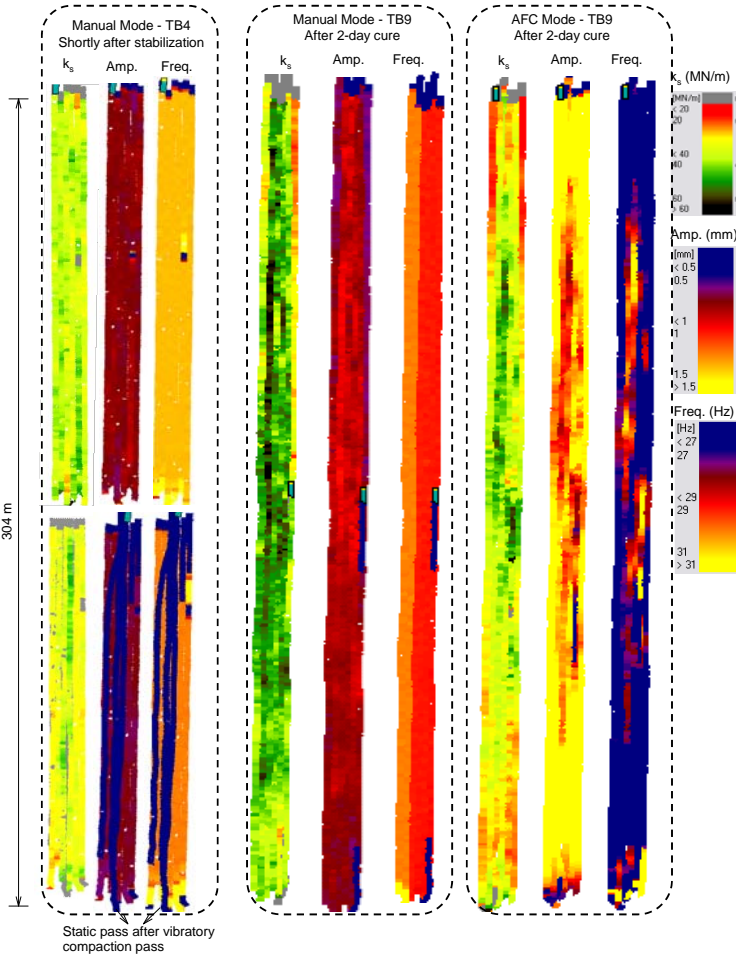Test Bed # 9 (07/17/2009)

Photos

Description: This test bed contained 2-day cured stabilized granular subgrade material from TBs 5 and 6. The area was mapped with Case/Ammann smooth drum IC roller in manual mode and AFC mode, and in-situ testing (LWD, FWD, NG, PLT, and DCP) were performed at 22 test locations selected using the IC-Map. The objectives of testing on this test bed were to evaluate strength gain in the stabilized granular subgrade layer by comparing IC-MVs obtained on TBs 5 and 6 shortly after stabilization and after 2-day curing, and to obtain correlations between in-situ test measurements and IC-MVs.

Machine Nominal settings:
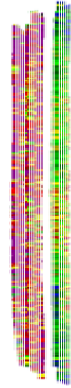Case/Ammann smooth SV212: Manual Ecc. = 15% - *a* ~ 0.90 mm, *f* = 27Hz, *v* = 4 km/h; AFC, *v* = 4 km/h.

Manual Mode - TB4
Shortly after stabilization
k_s   Amp.   Freq.

Manual Mode - TB9
After 2-day cure
k_s   Amp.   Freq.

AFC Mode - TB9
After 2-day cure
k_s   Amp.   Freq.

k_s (MN/m)

Amp. (mm)

Freq. (Hz)

304 m

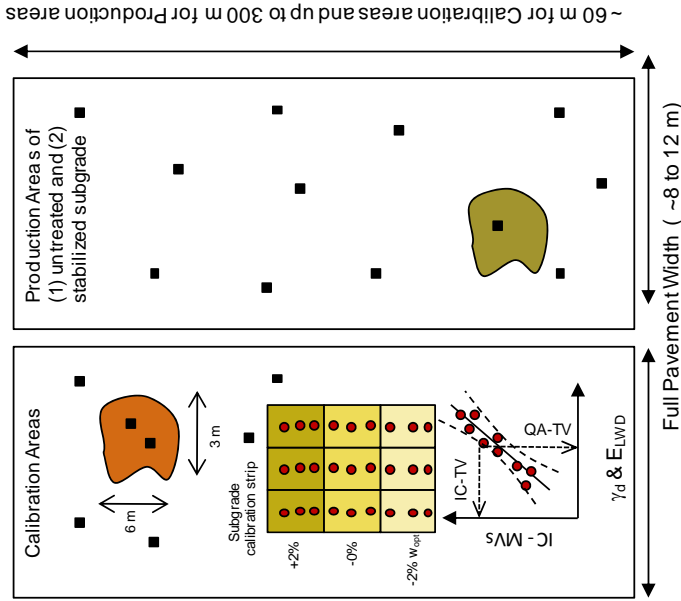Static pass after vibratory compaction pass

In-situ testing methods used on the test bed

Case/Ammann roller used for mapping

A-18

Accelerated Implementation of IC Technology for Embankment Subgrade Soils, Aggregate Base, and Asphalt Pavement Materials US 84, Wayne Co, MS – Mississippi Department of Transportation [June 1-June 5, 2009]

THE TRANSTEC GROUP
EERC EARTHWORKS ENGINEERING RESEARCH CENTER — TPF
IOWA STATE UNIVERSITY

Pavement Foundation Layers

- ❷ Stabilized Base (5% cement) — 6"
- ❶ Embankment/Subgrade (Stabilized) — ~8"

Date	TB	Machine	Amp (mm)	Spot Tests	Notes/Comments
06/01					ISU arrives at site to setup mobile lab (7 am) Meet with Contractor and identify potential test areas (7am) Setup CASE/CAT/SAKAI rollers and make trial runs with GPS (8 am) Collect material samples for on-site laboratory characterization (10 am)
06/01	1	CAT (padfoot)	Static, 0.9, 1.8	DCP, LWD, NG, and PLT	**8 m x 60 m calibration test area.** 1. Prepare then compact foundation layer with 8 roller passes and map for untreated subgrade. 2. Place one 200 to 300 mm loose lift of untreated subgrade. 3. Create variable moisture conditions. 4. Compact in three lanes using static, medium, and high amplitude @ 8-12 passes + 3 mapping passes 5. Develop compaction curves 6. Repeat compaction for **3 lifts** in same area
	2	Case (smooth)	TBD	DCP, LWD, NG, PLT, FWD	**Roller mapping in production areas** of (1) untreated and (2) stabilized subgrade. Monitor existing practice and perform in-situ tests for comparison. Use data for test run on IC QC/QA specification.
	3	Case (smooth)	Low, High, Feedback control	DCP, LWD, NG, PLT, FWD	**12 m x 60 m calibration test area.** 1. Compact foundation layer with 8 roller passes and map. 2. Place 150 mm lift of stabilized subgrade 3. Create variable moisture conditions. 4. Compact in three lanes using low, high, and feedback control @ 8-12 passes + 3 mapping passes 5. Develop compaction curves
06/02 - 06/03	4	CAT (padfoot)	Static, 0.9, 1.8	DCP, LWD, NG, PLT	
06/03 to 06/05	5/6	Case (smooth)/ CAT (padfoot)	TBD	DCP, LWD, NG, PLT, FWD	**Roller mapping in production areas** of (1) untreated and (2) stabilized subgrade. Monitor existing practice and perform in-situ tests for comparison. Use data for test run on IC QA specification.
06/04					Open House –presentation of preliminary results and roller demonstrations.

Notes:
A. Moisture condition calibration test strip areas ± 1.5% optimum except as noted.
B. MSDOT assistance requested for FWD testing and information on project QA testing requirements.
C. As time permits repeatability passes for roller will be performed on embankment and aggregate base.

ISU Research Team Contacts:
David J. White, Associate Professor, djwhite@iastate.edu, (515) 290-1080 (cell)
Heath Gieselman, Assistant Scientist, giese@iastate.edu (515) 450-1383 (cell)

~60 m for Calibration areas and up to 300 m for Production areas

Production Areas of (1) untreated and (2) stabilized subgrade

Calibration Areas

Subgrade calibration strip — 6 m, 3 m
+2%, -0%, -2% w_{opt}

QA-TV, IC-TV
IC-MVs
γ_d & E_{LWD}

Full Pavement Width (~8 to 12 m)

A-19

MSDOT - Project Goals

1. Document impact of variable feedback control on compaction uniformity
2. Document machine vibration amplitude influence on compaction efficiency
3. Study IC roller measurement influence depth
4. Develop correlations b/w IC roller values to traditional measurements
5. Compare IC results to tradition compaction operations
6. Study IC roller measurement values in production compaction operations
7. Evaluate IC measurement values in terms of alternative specification options